

FEDERAL UNIVERSITY OF PARAIBA
DEPARTMENT OF PHYSICS
DOCTORAL THESIS

Neutrino Masses in Two Higgs Doublet Models

Téssio Rogério Nóbrega Borja de Melo

JOÃO PESSOA

- February 2020 -

FEDERAL UNIVERSITY OF PARAIBA
DEPARTMENT OF PHYSICS
DOCTORAL THESIS

Neutrino Masses in Two Higgs Doublet Models

Téssio Rogério Nóbrega Borja de Melo

Thesis presented to the Graduate Program in
Physics of the Federal University of Paraíba,
as part of the requirements to obtain the
Degree of Doctor of Physics.

Research Field: Particle Physics.

Advisor: Prof. Dr. Farinaldo da Silva Queiroz.

JOÃO PESSOA

- February 2020 -

Catálogo na publicação
Seção de Catálogo e Classificação

M528n Melo, Tessio Rogerio Nobrega Borja de.
Neutrino Masses in Two Higgs Doublet Models / Tessio
Rogerio Nobrega Borja de Melo. - João Pessoa, 2020.
154 f. : il.

Orientação: Farinaldo da Silva Queiroz.
Tese (Doutorado) - UFPB/CCEN.

1. 2HDM. 2. Massa de neutrinos. 3. Mecanismo seesaw. 4.
Simetria U(1). 5. Bóson Z'. I. Queiroz, Farinaldo da
Silva. II. Título.

UFPB/BC



Universidade Federal da Paraíba
Centro de Ciências Exatas e da Natureza
Programa de Pós-Graduação *Stricto Sensu* em Física

CERTIDÃO DE TITULAÇÃO
Doutorado

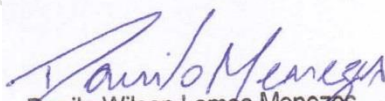
Certifico para os devidos fins de direito que, de acordo com os arquivos desta secretaria, **Téssio Rogério Nóbrega Borja de Melo**, Matrícula 20161002801, foi aluno de Doutorado deste Programa, na área Física das Partículas Elementares e Campos e defendeu sua tese intitulada: “*Neutrino Masses in Two Higgs Doublet Models*”, sendo aprovada no dia 28 de fevereiro de 2020, no Departamento de Física desta Universidade pela Banca Examinadora composta pelos professores:

Professores	IES
Prof. Dr. Farinaldo da Silva Queiroz (Orientador)	UFPB
Prof. Dr. --- (Coorientador)	---
Prof. Dr. Carlos Antônio de Sousa Pires	UFPB
Prof. Dr. Paulo Sérgio Rodrigues da Silva	UFPB
Prof. Dr. Celso Nishi	UFABC
Prof. Dr. Dimiter Hadjimichef	UFGRS

O aluno já requereu o diploma, cuja emissão se encontra em andamento.

Declaramos ainda que, em nossos registros, NADA CONSTA de pendências do aluno em relação ao término do seu curso.

João Pessoa, 2 de março de 2020.


Danilo Wilson Lemos Menezes
Técnico em Assuntos Educacionais
Mat. SIAPE 2647774

Ata da Sessão Pública da Defesa de Tese de
Doutorado do aluno **Téssio Rogério Nóbrega
Borja de Melo**, candidato ao Título de Doutor
em Física na Área de Concentração Física das
Partículas Elementares e Campos.

Aos vinte e oito dias do mês de fevereiro do ano de dois mil e vinte, às 14:00, no Auditório da Pós-Graduação em Física do Centro de Ciências Exatas e da Natureza da Universidade Federal da Paraíba, reuniram-se os membros da Banca Examinadora constituída para examinar o candidato ao grau de Doutor em Física na área de Física das Partículas Elementares e Campos, **Téssio Rogério Nóbrega Borja de Melo**. A comissão examinadora foi composta pelos professores doutores: *Farinaldo da Silva Queiroz* (UFPB), orientador e presidente da banca examinadora, *Carlos Antônio de Sousa Pires* (UFPB), *Paulo Sérgio Rodrigues da Silva* (UFPB), *Celso Nishi* (UFABC) e *Dimiter Hadjimichef* (UFGRS). Dando início aos trabalhos, o Prof. Farinaldo da Silva Queiroz comunicou aos presentes a finalidade da reunião. A seguir, passou a palavra para que o candidato fizesse, oralmente, a exposição do trabalho de tese intitulado “*Modelos para massas de neutrinos e matéria escura*”. Concluída a exposição, o candidato foi arguido pela Banca Examinadora, que emitiu o seguinte parecer: “**aprovado**”. Assim sendo, deve a Universidade Federal da Paraíba expedir o respectivo diploma de Doutor em Física na forma da lei. E para constar, eu, Danilo Wilson Lemos Menezes, redigi esta ata que vai assinada por mim e pelos membros da Banca Examinadora. João Pessoa, Paraíba, **28 de fevereiro de 2020**.

Prof. Dr. Farinaldo da Silva Queiroz
Orientador – PPGF/UFPB

Prof. Dr. Carlos Antônio de Sousa Pires
PPGF/UFPB

Prof. Dr. Paulo Sérgio Rodrigues da Silva
PPGF/UFPB

Prof. Dr. Celso Nishi
UFABC

Prof. Dr. Dimiter Hadjimichef
UFGRS

Farinaldo da S. Queiroz
Carlos Pires
Paulo Sérgio
Celso Nishi
Dimiter Hadjimichef

*“All our science, measured
against reality, is primitive and
childlike - and yet it is the most
precious thing we have.”*

Albert Einstein

Acknowledgements

I would like firstly to thank my family for all the support and affection. I am also very grateful to my cherished wife Ana Cláudia for standing by me throughout this journey with great fondness and patience.

I would like to express my deepest thanks to my advisor Prof. Farinaldo Queiroz for receiving me so well at the IIP and for conducting this work with commitment and enthusiasm. Thanks for all the opportunities and for being source of motivation and inspiration.

I also would like to thank Prof. Paulo Sérgio and Prof. Carlos Pires for the encouragement and for the important contributions to my formation along my graduate studies at UFPB. Thanks also to Prof. Diego Cogollo for the collaboration and for motivating me since the very beginning.

To professors Alex Dias and Diego Restrepo my special thanks for the invaluable assistance during the time as visitors at the IIP and after that by continuously helping me every time I needed.

I would like to thank my fellow colleagues from the UFPB and IIP: Pablo, Messias, Antônio, Clarissa, Yoxara, Álvaro and Arcênio.

Thanks to everyone who directly or indirectly contributed to this work.

Finally, thanks to CAPES for the financial support.

List of Publications

1. **Doubly Charged Scalar at the High-Luminosity and High-Energy LHC**, *International Journal of Modern Physics A*, 34 (2019) 27, 1950157; Tessio B. de Melo, Farinaldo S. Queiroz, Yoxara Villamizar.
2. **Lepton Flavor Violation and Collider Searches in a Type I + II Seesaw Model**, *European Physical Journal C*, 79 (2019) 11, 955; Manoel M. Ferreira, Tessio B. de Melo, Sergey Kovalenko, Paulo R. Pinheiro, Farinaldo S. Queiroz.
3. **Type I + II Seesaw in a Two Higgs Doublet Model**, *Physics Letters B* 797 (2019) 134813; D. Cogollo, Ricardo D. Matheus, T  ssio B. de Melo, Farinaldo S. Queiroz.
4. **A Two Higgs Doublet Model for Dark Matter and Neutrino Masses**, *Physics Letters B* 795 (2019) 319-326; Daniel A. Camargo, Miguel D. Campos, Tessio B. de Melo, Farinaldo S. Queiroz.
5. **Neutrino Masses in a Two Higgs Doublet Model with a U(1) Gauge Symmetry**, *Journal of High Energy Physics*, 1904 (2019) 129; Daniel A. Camargo, Alex G. Dias, T  ssio B. de Melo, Farinaldo S. Queiroz.
6. **Neutrino Masses and Absence of Flavor Changing Interactions in the 2HDM from Gauge Principles**, *Journal of High Energy Physics*, 1708 (2017) 092; Miguel Campos, D. Cogollo, Manfred Lindner, T. Melo, Farinaldo S. Queiroz, Werner Rodejohann.

List of Figures

1.1	Representation of neutrino mixing and mass differences in normal and inverted orderings. Figure taken from the Ref. [1].	12
3.1	Triangle diagram of the chiral anomaly.	27
3.2	Branching ratios as a function of the Z' mass for several $U(1)_X$ models under study. . .	36
3.3	Higgs associated production at LEP followed by its invisible decay, illustrated by $h \rightarrow XX$	40
3.4	Upper limits from invisible Higgs decay searches translated to the light Higgs mass m_h . . .	40
3.5	Ratio of the light Higgs decay width for different values of $\tan \beta$. In the left panel we set $\delta = 10^{-2}$, while in the right one $\delta = 10^{-3}$. One can see that if the product $\delta \tan \beta$ is sufficiently large, the light Higgs decays dominantly into $Z'Z'$. In this regime, the limits presented in the Fig. 3.4 can be directly applied.	41
3.6	Lower mass bound on the light Higgs stemming from the LEP precision measurement on the Z width.	44
3.7	Upper limits on the kinetic mixing as a function of the Z' mass for different values of the mass mixing parameter δ according to the first line of Table 3.5.	46
3.8	Feynman diagrams relevant for neutrino-electron scattering.	51
3.9	Constraints on the $B - L$ model based on measurements of neutrino-electron scattering. . .	53
3.10	Summary of constraints from neutrino-electron scattering on $U(1)_X$ models with very light Z' gauge bosons. These constraints have been interpreted from dark photon searches. . .	54
3.11	Summary of bounds from low energy accelerators constraints on the dark photon model [2]. After proper rescaling these constraints are also applicable to the $U(1)_X$ models in this work. In particular, the BaBar limits can be recast using the relation $\epsilon_{\text{DP}}^2 \rightarrow (g_v^l)^2 BR(Z' \rightarrow l^+ l^-)$. See text for details.	55

4.1	Region of parameter space that leads to a 125 GeV SM-like Higgs boson for $v_2 = 200$ GeV, $v_t = 1$ MeV and $\lambda_1 = 0.6$. In the left panel $\mu_{t2} = 100$ GeV and in the right panel, $\mu_{t2} = 100$ TeV.	62
4.2	Summary of experimental limits applicable to the model $U(1)_N$ and to the model $U(1)_{Y'}$ assuming $g_X \ll \epsilon$. Current limits are in gray while projected ones in color.	73

List of Tables

1.1	SM fermionic quantum numbers.	3
2.1	The four 2HDM types that satisfy the NFC criterion. Each type is defined according to which scalar couples to which right-handed fermion.	19
2.2	Parity assignment for fermions and scalars under the Z_2 symmetry in the different types of 2HDM.	20
2.3	Yukawa couplings for the physical scalars to fermions in the different types of 2HDM.	21
3.1	The first block of models is capable of explaining neutrino masses and the absence of flavor changing interactions in the 2HDM type I, whereas the second block refers to models where only the flavor problem is addressed. The first block accounts for type I 2HDM in which right-handed neutrinos are introduced without spoiling the NFC criterion ($Q_{X1} \neq Q_{X2}$). This is possible when $u \neq -2d$ (see Eq. (3.9) and Eq. (3.19)). Conversely, the second block shows Type I 2HDM with $u = -2d$. To preserve the NFC criterion, right-handed neutrinos can not be introduced while at the same time Q_{X1} is kept as a free parameter. The $U(1)_N$ model leads to a fermiophobic Z' setup [3]. The $U(1)_Y$ yields a "right-handed-neutrino-phobic" Z' boson. The $U(1)_{B-L}$ is the well-known model in which the accidental baryon and lepton global symmetries are gauged. The $U(1)_{C,G}$ models feature null couplings to right-handed charged leptons, whereas the $U(1)_{A,B}$ models have vanishing couplings to left-handed leptons. The $U(1)_D$ has null couplings to right-handed down-quarks. The $U(1)_{E,F}$ models induce Z' interactions to all fermions, but have rather exotic $U(1)_X$ charges.	30
3.2	Summary of constraints on the model from meson decays.	38

3.3	Higgs and light scalar interactions in the 2HDM type I. The coupling constants in the second column are the overall multiplicative factor in front of the SM couplings. In other words, when $\alpha = \beta$ the Higgs in the 2HDM type I interacts with fermions and gauge bosons identically to the SM Higgs.	39
3.4	List of experimental limits on the branching ratio of the SM Higgs. The channel $ZZ^* \rightarrow 2\ell 2\nu$ was obtained using the relation $BR(H \rightarrow ZZ^* \rightarrow 2\ell 2\nu) = BR(H \rightarrow ZZ^*)BR(Z \rightarrow 2\ell)BR(Z \rightarrow 2\nu)^2$	42
3.5	Existing (Cesium, E158) and projected constraints on the kinetic mixing parameter as a function of the mass mixing parameter δ and the Z' mass. All masses are in MeV, hence $m_Z = 91000$ MeV.	45
3.6	Summary of experiments that constrained $\nu - e$ scattering.	52
4.1	The table shows anomaly free Type I 2HDM where neutrino masses are generated via a type II seesaw mechanism. The first row shows the generic charges as functions of the d_R quark charge, d . Two particular cases are shown for $d = 0$ and $d = -2/3$, which correspond to sequential Z' and dark photon models, respectively. Notice that to prevent FCNI the scalar doublets have different charges under the $U(1)_X$ gauge symmetry.	59
4.2	Summary of collider bounds on the doubly charged scalar in our model using current and planned configurations. We used 13TeV of center-of-mass energy for the LHC configurations, whereas 27TeV for the high-energy upgrade. We can see that LHC and its upgrade will be paramount to probe the model up to the TeV scale.	70
5.1	Summary of the six general benchmark cases in this work where we investigate neutrino mass generation with and without the presence of right-handed neutrinos, a scalar triplet, and scalar singlet. Each scenario yields different scalar potentials and neutrino masses. See text for details.	77
5.2	Physical neutrino masses in different limits of the type I + II seesaw mechanism in 2HDM (benchmark scenario BM 1).	81
5.3	Physical neutrino masses in different limits of type II seesaw mechanism of benchmark scenario BM 3 in 2HDM.	83

Contents

Acknowledgements	iv
List of Publications	v
List of Figures	vii
List of Tables	ix
Contents	xii
Resumo	xiii
Abstract	xiv
Introduction	xv
1 The Standard Model of Particle Physics	1
1.1 The Standard Model Lagrangian	2
1.1.1 The Gauge Sector	2
1.1.2 The Matter Sector	2
1.1.3 The Scalar Sector and Higgs Mechanism	4
1.1.4 The Yukawa Sector	7
1.2 Some Problems in the Standard Model	8
1.2.1 Neutrino Masses	10
2 Two Higgs Doublet Models	13
2.1 The Scalar Sector with Two Higgs Doublets	14
2.2 The Yukawa Sector and FCNI	18
2.3 The Alignment Limit	21

3	Neutrino Masses and Absence of Flavor Changing Interactions in the 2HDM from Gauge Principles	23
3.1	2HDM with $U(1)_X$ Symmetries	24
3.1.1	Realizing NFC criterion with $U(1)_X$ Symmetries	25
3.1.2	Anomaly Cancellation	26
3.1.3	Neutrino Masses	28
3.1.4	Physical Gauge Bosons and Neutral Currents	31
3.1.5	Z' Decays	34
3.2	Phenomenological Constraints	35
3.2.1	Meson Decays	37
3.2.2	Higgs Physics	39
3.2.3	Z Decays	43
3.2.4	Charged Higgs Searches	44
3.2.5	Atomic Parity Violation	45
3.2.6	Muon Anomalous Magnetic Moment	49
3.2.7	Neutrino-Electron Scattering	50
3.2.8	Low Energy Accelerators	53
3.3	Discussion	55
4	Neutrino Masses in a Two Higgs Doublet Model with a $U(1)$ Gauge Symmetry	57
4.1	Type II seesaw in the 2HDM- $U(1)$	57
4.1.1	Mass Spectrum - Scalars	60
4.1.2	Mass Spectrum - Gauge Bosons	66
4.2	Phenomenological constraints	69
4.2.1	Electroweak Precision	69
4.2.2	Collider Bounds	69
4.2.3	LHC- Higgs	71
4.2.4	Accelerators	72
4.2.5	Low Energy Probes	73
4.2.6	Dark Matter Possibility	73
4.3	Discussion	74

5	Type I + II Seesaw in the Two Higgs Doublet Model	76
5.1	Seesaw realizations in the 2HDM-U(1)	76
5.1.1	Type I + II seesaw mechanism (BM 1)	78
5.1.2	Scalar singlet absent (BM 3)	82
5.1.3	Scalar triplet absent - Type I seesaw (BM 2)	84
5.1.4	Scalar singlet and triplet absent - Dirac neutrinos (BM 4)	84
5.1.5	Right-handed neutrinos and scalar singlet absent - type II seesaw (BM 6)	85
5.1.6	Right-handed neutrinos absent - Type II seesaw + singlet (BM 5)	86
5.2	Discussion	86
6	Conclusions and Perspectives	89
A	Appendix A	91
A.1	Conditions for Anomaly Freedom	91
A.2	Gauge bosons	92
A.3	δ Parameter	98
A.4	Currents for Z and Z'	98
A.5	Comparison with the 2HDM with Gauged $U(1)_N$	101
A.6	Higgs Interactions to Vector Bosons	101
B	Appendix B	103
C	Appendix C	111

Resumo

O Modelo Padrão (SM) da Física de Partículas fornece a descrição mais precisa do comportamento da matéria nas menores escalas de distância acessíveis. No entanto, como o SM não explica a massa não-nula dos neutrinos, a existência da matéria escura e também sofre com diversos problemas teóricos, é amplamente aceito que ele deve ser estendido. A parte menos compreendida do SM, o seu setor escalar, começou a ser investigada apenas recentemente e a questão de o bóson de massa 125 GeV encontrado no CERN Large Hadron Collider (LHC) ser o bóson de Higgs do SM ou apenas um de muitos escalares de um modelo além do SM ainda está em aberto. Uma das extensões do SM mais populares é o modelo de dois dubletos de Higgs (2HDM), que apresenta dois dubletos escalares, ao invés de apenas um como no SM. Os modelos 2HDM em geral sofrem de troca de sabor na corrente neutra (FCNI) devido à presença de escalares neutros extras. Além disso, a geração da massa dos neutrinos é tipicamente ignorada nas discussões sobre o 2HDM. Nesta Tese estudamos uma classe de 2HDM livre de FCNI por meio de uma simetria abeliana de gauge, que também permite acomodar massa para os neutrinos. Discutimos várias realizações do mecanismo seesaw nesse contexto, destacando as implicações fenomenológicas em cada caso. Em particular, estudamos em detalhes o novo bóson de gauge Z' , investigamos a fenomenologia das misturas cinética e de massa que engloba vários vínculos provenientes da violação de paridade atômica, momento magnético anômalo do múon, decaimentos raros de mésons, física do Higgs, dados de precisão do LEP, espalhamento neutrino-elétrons, aceleradores de baixa energia e dados do LHC.

Palavras-chave: 2HDM, Massa de neutrinos, Mecanismo seesaw, simetria $U(1)$, bóson Z' .

Abstract

The Standard Model (SM) of Particle Physics provides the most accurate description of the behaviour of matter in the smallest accessible distance scales. However, since the SM does not account for the nonzero neutrino masses, dark matter and also is plagued with a number of theoretical issues, it is widely accepted that the SM must be extended. The least understood part of the SM, the scalar sector, have just begun to be probed and the question whether the 125 GeV boson found in the CERN Large Hadron Collider (LHC) is the SM Higgs boson or just one of many scalars from a more complex model is still open. One of the most popular SM extension is the Two Higgs Doublet Model (2HDM), which features two scalar doublets, instead of only one, as in the SM. General 2HDM suffer from excessive Flavor Changing Neutral Interactions (FCNI) due to the presence of extra neutral scalars. Also, the generation of neutrino masses is typically neglected in 2HDM investigations. In this Thesis we study a class of 2HDM which is free from FCNI by means of an Abelian gauge symmetry, which also allows the accommodation of neutrino masses. We discuss several realizations of the seesaw mechanism in this framework, highlighting the phenomenological implications in each case. In particular we study in detail the new Z' gauge boson, investigate the kinetic and mass mixing phenomenology which encompass several constraints coming from atomic parity violation, muon anomalous magnetic moment, rare meson decays, Higgs physics, LEP precision data, neutrino-electron scattering, low energy accelerators and LHC probes.

Keywords: 2HDM, Neutrino masses, Seesaw mechanism, $U(1)$ symmetry, Z' boson.

Introduction

The branch of Physics devoted to unveil the elementary building blocks of matter in the Universe and the fundamental interactions that rule their behaviour is the field of Particle Physics. Over the past century, the effort expended both on theory and experimental sides to achieve this goal, culminated in the formulation of the Standard Model (SM) [4, 5], the theory which underlies the Particle Physics nowadays. This theory is based on the principles of Relativity and Quantum Mechanics and describes with enormous success three of the four known fundamental interactions ¹. In the SM framework, there are three types of fields: gauge bosons, fermions and scalars. The fermions are the fundamental constituents of matter and the gauge bosons are the force carriers, which mediate the fundamental interactions. The rationale that underlies the description of these interactions is the gauge principle, which relates each fundamental force with an internal local symmetry: the strong interaction is related to the symmetry of the group $SU(3)_C$; whereas the weak and electromagnetic interactions are related to the $SU(2)_L \otimes U(1)_Y$ group.

As the gauge symmetries forbid mass terms for the fermions and gauge bosons in the Lagrangian, a crucial idea for the SM consistency is the Higgs mechanism, which is responsible for reconciling the gauge principle with the existence of mass for the particles. The consequence of this mechanism is one of the most important SM predictions: the existence of the Higgs boson, the elementary scalar field remnant of the process of electroweak symmetry breaking. The announcement in 2012 by the ATLAS and CMS collaborations [6, 7] of the discovery of a spin-0 particle compatible with the SM Higgs boson, ended a search which lasted for decades, finally completing the missing piece in the SM puzzle.

¹The gravitational interaction is outside the scope of the SM and will not be subject of further discussion in this Thesis.

The discovery of the Higgs boson, however, raises a natural question: is this scalar found in the LHC the only kind of scalar field in Nature? Differently from the gauge bosons, whose number is fixed by the number of generators of the gauge symmetries, there is no theoretical constraint on the number of fermions and scalars; they need to be determined experimentally. The number of fermion families below half the Z boson mass was determined by the LEP as being 3. Thus, it remains to be known how many fundamental scalars there are in Nature. Looking at the fermion and gauge sectors, which display a rich structure, it is reasonable to expect the existence of many more scalars besides the SM Higgs, which motivates the study of models with extended scalar sector. One of the most popular of these extensions is the Two Higgs Doublet Model (2HDM), which features four new scalars and presents a rich phenomenology [8].

Despite the enormous success of the SM, the predominant view in the Particle Physics community is that the SM cannot be the ultimate theory about the fundamental interactions. Beyond the reasonable expectation of the existence of more scalars, there are several other reasons that strongly suggest that the SM is still an incomplete description of Nature. One of the most clear indications of that is the fact that neutrinos have mass. Looking at the SM spectrum, we see that the absence of right-handed neutrino fields in the theory forbids the neutrinos from interacting with the Higgs field and, thus, from acquiring a Dirac mass after the spontaneous symmetry breaking. Therefore, the simplest way of incorporating neutrino masses to the SM would be adding the missing right-handed neutrino fields, N_R . Nevertheless, this minimal fermionic extension rises a further question: why are the neutrino masses so much smaller than the other fermion masses?

A particular feature of the N_R fields is that they are singlets under the full SM gauge group and, therefore, nothing forbids them from having a Majorana mass. These two different masses, Dirac and Majorana, are the basic ingredients of the well known type I seesaw mechanism, which elegantly explains the smallness of the observed light neutrino masses as the ratio of two very distinct mass scales. In this scenario, the physical neutrino spectrum consists of one heavy and one light Majorana neutrino per generation. An interesting variation of this mechanism is the type II seesaw, in which the light neutrinos also have Majorana nature but the high energy scale is associated with new scalar degrees of freedom, and right-handed neutrinos are not required at all.

In this Thesis we study scalar and gauge extensions of the SM in connection with the generation of neutrino masses via seesaw mechanism. We focus mostly on the 2HDM, which is one of the most well studied SM extensions in the literature and have been used as a benchmark model by experimental collaborations [9]. This Thesis is organized as follows:

- In Chapter 1 we review the SM, emphasizing its key features, such as its symmetries and physical content, the generation of mass for the elementary particles through the Higgs mechanism, and the Higgs boson interactions. In the last section of the Chapter we comment about some of its main problems, which motivate the search for new physics beyond the SM, with emphasis on neutrino masses.
- In Chapter 2 we go beyond the SM and introduce the 2HDM, stressing the new features it adds as compared to the SM. We present the main phenomenological issue with this kind of scalar extension, which is the appearance of Flavor Changing Neutral Interactions (FCNI) at tree level, and the usual solution by means of a discrete Z_2 symmetry, which allows the realization of the Natural Flavor Conservation (NFC) criterion. We also discuss the so called alignment limit in which one of the scalars of the model behaves like the SM Higgs boson, as required by the recent LHC results.
- In Chapter 3 we start to present our original contributions. In this Chapter we discuss a gauge solution to the FCNI problem in the 2HDM, which in addition allows the generation of Majorana neutrino masses naturally. The idea is to substitute the ad-hoc Z_2 symmetry by a more fundamental Abelian $U(1)_X$ gauge symmetry. We discuss the effect of the presence of right-handed neutrinos on the anomaly cancellation conditions, and show how a whole class of models arises from this idea. Then we confront the models with various phenomenological constraints, specially the ones related to the new gauge boson Z' that has mass and kinetic-mixing with the SM Z boson, including a limit in which it resembles the so called dark photon.
- In the Chapter 4 we study a new model, still within the scope of 2HDM- $U(1)$, in which neutrino masses are generated via type II seesaw mechanism, without the need of right-handed neutrinos. We investigate the phenomenology of the light Z' and also discuss the possibility of inclusion of a dark matter candidate in the model.

- In Chapter 5 we extend the results of the models from the previous chapters and consider general realizations of type I + II seesaw mechanism in the 2HDM- $U(1)$ framework, highlighting the general phenomenological features in each scenario.

The Chapter 6 is reserved for our final considerations and perspectives. We also included three Appendices at the end of this document to cover in more detail some specific parts of the text.

Chapter 1

The Standard Model of Particle Physics

The Standard Model (SM) offers the best description of the strong, weak and electromagnetic interactions in nature. It is a quantum field theory formulated according to the gauge principle under the symmetry group,

$$G_{SM} \equiv SU(3)_C \otimes SU(2)_L \otimes U(1)_Y, \quad (1.1)$$

where the $SU(3)_C$ group corresponds to the strong color sector and the $SU(2)_L \otimes U(1)_Y$ group encompass the weak and electromagnetic sectors in an unified way. This unification is not apparent at low energies due to the spontaneous symmetry breaking phenomenon, which is crucial to explain the origin of mass of the elementary particles in the theory. The discovery of a scalar particle in 2012 in the LHC [6, 7], with properties consistent with those of the Higgs boson, corroborated this mechanism and completed the last piece in the SM puzzle, crowning decades of phenomenological success.

This Chapter is divided in two parts. The purpose of the first part is to make a short review of this theory which is the basis of particle physics, presenting briefly its main features and fundamental ideas. In the second part of the Chapter, we will point out some of its main problems to emphasize the need to go beyond the SM. This Chapter will also serve to fix the notation used throughout the Thesis.

1.1 The Standard Model Lagrangian

The Lagrangian of the SM is the most general Lagrangian which is Lorentz invariant, renormalizable and gauge invariant under the G_{SM} group. We can write it compactly as,

$$\mathcal{L}_{SM} = \mathcal{L}_{\text{gauge}} + \mathcal{L}_{\text{matter}} + \mathcal{L}_{\text{scalar}} + \mathcal{L}_{\text{yukawa}}. \quad (1.2)$$

In the following sections we will explain each one of the terms in this expression.

1.1.1 The Gauge Sector

The first piece in the expression (1.2), $\mathcal{L}_{\text{gauge}}$, is the term corresponding to the kinetic terms for the gauge bosons, which are fixed by the symmetry group G_{SM} . It contains eight gluons G_μ^a ($a = 1, \dots, 8$), one for each $SU(3)_C$ generator; three weak bosons W_μ^a ($a = 1, \dots, 3$) corresponding to the three $SU(2)_L$ generators; and one boson B_μ from the $U(1)_Y$ group. Explicitly, $\mathcal{L}_{\text{gauge}}$ reads,

$$\mathcal{L}_{\text{gauge}} = -\frac{1}{4}G_{\mu\nu}^a G^{a\mu\nu} - \frac{1}{4}W_{\mu\nu}^a W^{a\mu\nu} - \frac{1}{4}B_{\mu\nu}B^{\mu\nu}, \quad (1.3)$$

where the field strength tensors are given by,

$$G_{\mu\nu}^a = \partial_\mu G_\nu^a - \partial_\nu G_\mu^a + g_s f^{abc} G_\mu^b G_\nu^c \quad (1.4)$$

$$W_{\mu\nu}^a = \partial_\mu W_\nu^a - \partial_\nu W_\mu^a + g \epsilon^{abc} W_\mu^b W_\nu^c \quad (1.5)$$

$$B_{\mu\nu} = \partial_\mu B_\nu - \partial_\nu B_\mu, \quad (1.6)$$

with g_s and g the strong and weak coupling constants (the $U(1)_Y$ gauge coupling constant, g' , does not appear in these expressions), f^{abc} and ϵ^{abc} being the $SU(3)$ and $SU(2)$ structure constants. Notice that $\mathcal{L}_{\text{gauge}}$ does not contain any mass term for the gauge bosons because they are forbidden by the G_{SM} symmetries, but they will surface after spontaneous symmetry breaking.

1.1.2 The Matter Sector

The fermionic sector in the SM is composed by leptons and quarks. Leptons are fermions that do not possess strong interactions. There are six different flavors: electron,

muon, tau and their respective neutrinos. The left-handed leptons transform as doublets under the $SU(2)_L$ group, while the right-handed ones are singlets,

$$\begin{pmatrix} \nu_e \\ e \end{pmatrix}_L, \begin{pmatrix} \nu_\mu \\ \mu \end{pmatrix}_L, \begin{pmatrix} \nu_\tau \\ \tau \end{pmatrix}_L, e_R, \mu_R, \tau_R.$$

Notice that in the SM there are no right-handed neutrinos.

As for the quarks, which are the fermions that participate in all the fundamental interactions, come in six flavors as well, and they correspond to color triplets. They are named up, down, charm, strange, top and bottom. The left-handed quarks transform as doublets, whereas the right-handed ones transform as singlets under $SU(2)_L$,

$$\begin{pmatrix} u \\ d \end{pmatrix}_L, \begin{pmatrix} c \\ s \end{pmatrix}_L, \begin{pmatrix} t \\ b \end{pmatrix}_L, u_R, d_R, c_R, s_R, t_R, b_R.$$

The quantum numbers for the SM fermion fields are summarized in the Table 1.1, where T_3 is the third component of the weak isospin, Y is the hypercharge and Q is the electric charge.

Fermion	T_3	Y	Q
e_L	-1/2	-1	-1
e_R	0	-2	-1
ν_L	1/2	-1	0
d_L	-1/2	1/3	-1/3
d_R	0	-2/3	-1/3
u_L	1/2	1/3	2/3
u_R	0	4/3	2/3

Table 1.1: SM fermionic quantum numbers.

Once the fermion content and their respective representations are fixed, the Lagrangian $\mathcal{L}_{\text{matter}}$ is uniquely determined by gauge invariance,

$$\mathcal{L}_{\text{matter}} = \sum_{\text{fermions}} (\bar{\Psi}^L i \gamma^\mu D_\mu \Psi^L + \bar{\Psi}^R i \gamma^\mu D_\mu \Psi^R), \quad (1.7)$$

where the sum extends to all fermions. Similarly to what happens to the gauge bosons, gauge invariance forbids mass terms to the fermions. Their masses will be generated by the Yukawa interaction only after the Electroweak Symmetry Breaking (EWSB).

1.1.3 The Scalar Sector and Higgs Mechanism

As mentioned in the previous sections, mass terms for the fermions and gauge bosons explicitly violate the symmetry of the group $SU(2)_L \otimes U(1)_Y$. However, these terms may be generated without spoiling the symmetry of the theory through the Higgs mechanism [10, 11]. The main idea behind this mechanism is the spontaneous symmetry breaking, which occurs when the vacuum state of the theory is not invariant by the same symmetry transformations respected by the Lagrangian.

The implementation of the Higgs mechanism requires that one or more fields acquire a nonzero vacuum expectation value (VEV). In order to not spontaneously break the Lorentz symmetry as well, this field must be a scalar. The minimum scalar content capable of generating the masses for the SM fermions and gauge bosons is a scalar doublet Φ with hypercharge $Y = 1$, parameterized as,

$$\Phi = \begin{pmatrix} \phi^+ \\ \phi^0 \end{pmatrix}, \quad (1.8)$$

where ϕ^+ and ϕ^0 are complex scalar fields. In the SM, this minimum content comprises the whole scalar sector.

The most general renormalizable Lagrangian for the scalar Φ reads,

$$\mathcal{L}_{\text{scalar}} = (D^\mu \Phi)^\dagger D_\mu \Phi - \mu^2 \Phi^\dagger \Phi - \lambda (\Phi^\dagger \Phi)^2, \quad (1.9)$$

where μ^2 and λ are free parameters, with the restriction on the quartic coupling $\lambda > 0$, in order to ensure the stability of the potential. The covariant derivative for the doublet is,

$$D_\mu \Phi = \left[\partial_\mu + ig T^a W_\mu^a + ig' \frac{Y}{2} B_\mu \right] \Phi, \quad (1.10)$$

where T^a are the $SU(2)_L$ generators,

$$T^a = \frac{\sigma^a}{2}, \quad (1.11)$$

with σ^a the Pauli matrices.

The spontaneous symmetry breaking occurs when $\mu^2 < 0$, in which case the potential is minimized by a nontrivial value of the scalar field,

$$\langle \Phi \rangle = \begin{pmatrix} 0 \\ v/\sqrt{2} \end{pmatrix}, \quad (1.12)$$

where $v^2 = -\mu^2/\lambda$. In this case, the generators of the group $SU(2)_L \otimes U(1)_Y$ are broken and only the particular linear combination $T_3 + Y/2$ maintains the vacuum invariant. This combination is the generator of the remaining symmetry $U(1)_{\text{em}}$ from the Quantum Electrodynamics (QED). Thus, it is identified as the electric charge,

$$Q = T_3 + \frac{Y}{2}. \quad (1.13)$$

This is the Gell-Mann - Nishijima relation. Using this relation we can fix the weak hypercharges of the particles knowing their electric charges (this is how the values of Y were determined for the fermions in Table 1.1).

Since only one generator of the group $SU(2)_L \otimes U(1)_Y$ remained unbroken out of the initial four, Goldstone theorem would imply the existence of three Goldstone bosons. In the Higgs mechanism, however, these would-be Goldstone bosons are absorbed by the gauge bosons as longitudinal components, making them massive. Therefore, from the four scalar fields in the doublet Φ , only one is physical, which can be made explicit in the unitary gauge, in which the scalar doublet is brought to the form,

$$\Phi = \frac{1}{\sqrt{2}} \begin{pmatrix} 0 \\ v + H \end{pmatrix}. \quad (1.14)$$

The physical field H is the Higgs field. Its mass, in terms of the parameters of the potential, is given by,

$$m_H = \sqrt{2\lambda v^2} = \sqrt{-2\mu^2},$$

and the experimental value obtained in the LHC is $m_H = 125.09(24)$ GeV [12]. As the low energy phenomenology requires that the electroweak VEV v be related to the Fermi constant G_F by,

$$v^2 = \frac{1}{\sqrt{2}G_F}, \quad (1.15)$$

which in turn is precisely measured through the muon lifetime, $G_F = 1.1663787(6) \times 10^{-5}$ GeV⁻² [13], the value of v is fixed as $v \simeq 246$ GeV, which in turn also fix the quartic coupling of the potential as $\lambda = m_H^2/(2v^2) \simeq 0.13$.

The mass terms for the gauge bosons come from the kinetic term $(D^\mu \Phi)^\dagger D_\mu \Phi$ in the Lagrangian (1.9). Expanding it with Φ in the unitary gauge (1.14) and ignoring the derivative and interaction terms, we have,

$$(D_\mu \Phi)^\dagger (D^\mu \Phi) = \frac{1}{4}g^2 v^2 W_\mu^- W^{+\mu} + \frac{1}{8}v^2 \left[g^2 W_\mu^3 W^{3\mu} + g'^2 B_\mu B^\mu - 2gg' W_\mu^3 B^\mu \right], \quad (1.16)$$

where the physical W^\pm bosons were defined,

$$W_\mu^\pm = \frac{1}{\sqrt{2}} (W_\mu^1 \mp iW_\mu^2). \quad (1.17)$$

The other physical gauge bosons, Z and the photon A_μ , are obtained from B_μ and W^3_μ after the electroweak rotation,

$$\begin{pmatrix} A_\mu \\ Z_\mu \end{pmatrix} = \begin{pmatrix} \cos \theta_W & \sin \theta_W \\ -\sin \theta_W & \cos \theta_W \end{pmatrix} \begin{pmatrix} B_\mu \\ W_\mu^3 \end{pmatrix}, \quad (1.18)$$

where the electroweak angle θ_W is given by,

$$\tan \theta_W = \frac{g'}{g}, \quad (1.19)$$

and relates to the electric charge as,

$$e = g \sin \theta_W = g' \cos \theta_W. \quad (1.20)$$

After this rotation the mass of the photon is identified as being zero, and the masses of W^\pm and Z bosons as,

$$m_W = \frac{1}{2}gv \quad , \quad m_Z = \frac{1}{2} \frac{gv}{\cos \theta_W}. \quad (1.21)$$

The current experimental values of these masses, as verified at different experiments such as LEP, Tevatron and LHC, are $m_W = 80.385(15)$ GeV and $m_Z = 91.1876(21)$ GeV [13]. The relations among the couplings and masses of the electroweak gauge bosons is one of the most important predictions of the SM. The ρ parameter,

$$\rho = \frac{m_W^2}{m_Z^2 \cos^2 \theta_W}, \quad (1.22)$$

which measures the relative intensity between the neutral and charged currents, is predicted to be $\rho = 1$ at tree level in the SM, as can be seen from the mass expressions (1.21). Its experimental value is indeed very close to $\rho = 1$, in excellent accord with the SM. At 1σ level [13],

$$\rho = 1.00039 \pm 0.00019. \quad (1.23)$$

The small deviation from the unity can be accounted for when radiative corrections are included.

1.1.4 The Yukawa Sector

The last piece in the SM Lagrangian (1.2), $\mathcal{L}_{\text{yukawa}}$, describes the interaction among the scalars and fermions. Through this interaction the fermions acquire mass terms without spoiling any of the SM gauge symmetries. It reads,

$$\mathcal{L}_{\text{yukawa}} = -y_{ij}^l \bar{L}_i \Phi e_{Rj} - y_{ij}^d \bar{Q}_i \Phi d_{Rj} - y_{ij}^u \bar{Q}_i \tilde{\Phi} u_{Rj} + h.c., \quad (1.24)$$

where L and Q are the left-handed lepton and quark weak doublets, $\tilde{\Phi} = i\sigma^2 \Phi^*$ is the conjugate scalar doublet, and the Yukawa couplings $y^{l,u,d}$ are 3×3 complex matrices in flavor space. Notice that in the Lagrangian (1.24) a term like $y_{ij}^\nu \bar{L}_i \tilde{\Phi} \nu_{Rj}$ would be possible if right-handed neutrinos were included in the particle content. However, as the SM was constructed without right-handed neutrinos, this term is absent and the neutrinos remain massless, differently of the other fermions, as explained below.

After the EWSB in the unitary gauge, $\mathcal{L}_{\text{yukawa}}$ becomes,

$$\mathcal{L}_{\text{yukawa}} = -\frac{v+H}{\sqrt{2}} [y_{ij}^l \bar{e}_{Li} e_{Rj} + y_{ij}^d \bar{d}_{Li} d_{Rj} + y_{ij}^u \bar{u}_{Li} u_{Rj} + h.c.], \quad (1.25)$$

from where the mass matrices for the fermions can be identified as,

$$M^{l,u,d} = \frac{v}{\sqrt{2}} y^{l,u,d}. \quad (1.26)$$

These matrices can be diagonalized by biunitary transformations on the flavor eigenstates ψ_L and ψ_R (here ψ denotes generically the several fermion fields), leading to the basis of the mass eigenstates ψ'_L and ψ'_R ,

$$\begin{aligned} \psi'_L &= V_L^\dagger \psi_L \\ \psi'_R &= V_R^\dagger \psi_R, \end{aligned} \quad (1.27)$$

where $V_L^{l,u,d}$ e $V_R^{l,u,d}$ are such that,

$$V_L^{l,u,d\dagger} M^{l,u,d} V_R^{l,u,d} = M_{\text{diag}}^{l,u,d}. \quad (1.28)$$

After the diagonalization, $\mathcal{L}_{\text{yukawa}}$ can be rewritten as,

$$\mathcal{L}_{\text{yukawa}} = -(m_i^{l,u,d} + \frac{m_i^{l,u,d}}{v} H) [\bar{e}_i e_i + \bar{d}_i d_i + \bar{u}_i u_i]. \quad (1.29)$$

which makes clear that in the SM the strength of the Higgs boson interactions is proportional to the mass of the respective particle.

After this short review of the main features of the SM, in the next section we will discuss some of its problems.

1.2 Some Problems in the Standard Model

Despite the SM enormous success in explaining the observed physical phenomena from low energies all the way up to the highest energies available in the current experiments, there are several unanswered questions that strongly indicates that the SM cannot be the final theory of the fundamental interactions. The current understanding is that the SM is an effective theory valid up to some energy scale Λ_{NP} , where new physics effects become relevant. We list below some import SM issues that have motivated the search of physics beyond the SM and have been active research topics in the field of particle physics in the last decades:

- **Hierarchy problem:** Since scalar field masses are not protected by any symmetry (differently from fermion masses, e. g., which are protected by chiral symmetry), they become very sensitive to ultraviolet physics and their values are naturally pushed to be of order of the energy cutoff Λ of the theory (perturbatively this is reflected by the fact that loop corrections to the scalar masses are quadratically divergent with Λ). In the SM, the quantum corrections to the Higgs mass comes mostly from the top and gauge boson loops, giving,

$$\delta m_H^2 \sim \frac{\Lambda_{NP}^2}{v^2} \left[4m_t^2 - 2m_W^2 - m_Z^2 - m_H^2 + O\left(\log \frac{\Lambda_{NP}}{m_H}\right) \right]. \quad (1.30)$$

If one assumes that new physics effects appear only at the Planck scale, $\Lambda_{NP} \sim M_{\text{planck}} \sim 10^{19}$ GeV, it is apparent that the bare Higgs mass and its counter term must be tuned to an enormous accuracy in order to result in $m_H = 125$ GeV. This fine tuning generated by the large hierarchy between the electroweak and Planck scales, $m_H \ll M_{\text{planck}}$, is referred to as the hierarchy problem.

The main attempts to solve this problem, such as supersymmetry [14], extra dimensions [15] and Little Higgs models [16], requires $\Lambda_{NP} \sim \text{TeV}$, which is in tension with the LHC null results. One recent proposal which does not require new physics at the TeV scale is the cosmic relaxation mechanism [17].

- **Strong CP problem:** The SM gauge symmetries allows a CP-violating term in the QCD Lagrangian,

$$\mathcal{L} = \frac{\bar{\theta}}{32\pi^2} \epsilon^{\mu\nu\rho\sigma} G_{\mu\nu}^a G_{\rho\sigma}^a, \quad (1.31)$$

where $\bar{\theta} = \theta + \arg(\det(m_Q))$ and m_Q is the quark mass matrix. This CP-violating term leads in principle to a measurable electric dipole moment for the neutron, $d_n \approx \bar{\theta} \times 10^{-16}$ e-cm. However, current upper bounds on d_n constrain the $\bar{\theta}$ angle to be extremely small, $|\bar{\theta}| < 10^{-11}$. As the quark masses and the bare θ parameter come from completely unrelated sources, it is very unnatural that they cancel so perfectly to give a $\bar{\theta}$ so close to zero. This is the strong CP problem.

The most popular solution is based on the so called Peccei-Quinn symmetry and its very light pseudo-Goldstone boson, the axion, which can also account for the DM in the Universe if the Peccei-Quinn symmetry is broken at energies $< 10^{12}$ GeV [18].

- **Matter-antimatter asymmetry:** There is no indication of large concentrations of antimatter in any part of the observable Universe, so that the notorious predominance of matter over antimatter seems to hold everywhere. A successful model of baryogenesis, in which the matter-antimatter asymmetry in the Universe is generated dynamically, must fulfill the three Sakharov conditions: violation of baryon number; violation of CP symmetry; and departure from thermal equilibrium (to prevent the washout of the asymmetry once it be generated). It turns out that the SM meets all these requirements, but not with a sufficient amount of CP-violation to account for the observed baryon asymmetry, $\eta = (n_B - n_{\bar{B}})/n_\gamma = 6.1 \times 10^{-10}$. The most studied beyond SM scenarios for baryogenesis include: GUT baryogenesis [19]; strong first order electroweak phase transition [20] and leptogenesis [21].
- **Dark Matter:** Current astrophysical and cosmological data suggest that approximately 85% of the total amount of matter in the Universe is constituted by dark matter, i. e., a form of non-baryonic matter which does not interact appreciably with photons. The existence of dark matter is required at several different distance scales, from observations in the CMB power spectrum to the dynamics of clusters of galaxies. The formation process of structures in the Universe favors the so called cold dark matter candidates, i. e., particles which were non-relativistic in the epoch of recombination. For this reason, the SM neutrinos, which otherwise seemed to be perfectly good dark matter candidates, are actually ruled out, since their extremely small masses make them behave as hot dark matter. Therefore, the SM is not capable of explaining the existence of dark matter in the Universe.

The most popular dark matter candidates are the WIMPs (Weakly Interacting Massive Particles), which are well motivated by the fact that their thermal production in the early Universe through interaction cross sections of order of the weak interaction, leads to the correct relic abundance (the so called “WIMP miracle”). However, there are several other proposals, such as: QCD axions and axion like particles (not related to the strong CP problem); FIMPs (Feebly Interacting Massive Particles); and even primordial black holes, just to cite a few.

In this short list we did not include the problem which is perhaps the most convincing evidence of physics beyond the SM, which is the experimental fact that neutrinos have mass. We reserved the last section of this Chapter to discuss this subject in more detail. We will come back to this theme in the following chapters, when models for generation of neutrino masses will be discussed.

1.2.1 Neutrino Masses

In the epoch the SM was built there was not any evidence that neutrinos could be massive particles. They had been discovered in the fifties by Cowan and Reines [22] and quite soon was demonstrated in subsequent experiments [23, 24] that the neutrinos produced in charged weak interactions are always left-handed. The picture of left-handed massless neutrinos fitted well the experimental data available at the time and, therefore, the introduction of right-handed neutrino fields in the SM seemed to be unnecessary. This picture remained the same for almost half of a century, until the late nineties, when the phenomenon of neutrino oscillations was first observed [25, 26, 27].

The simplest explanation for this phenomenon, and the only one that survives to all the data from oscillation experiments, is that the neutrino flavor eigenstates ν_e, ν_μ and ν_τ , do not correspond to physical massless neutrinos. Rather, the actual mass eigenstates, denoted as ν_1, ν_2 and ν_3 , have nonzero masses and mix according to,

$$\nu_\alpha = \sum_{i=1}^3 (U_{\text{PMNS}})_{\alpha i} \nu_i, \quad (1.32)$$

where $\alpha = e, \mu, \tau$, and the mixing matrix U_{PMNS} is the so-called PMNS matrix, after Bruno Pontecorvo, who first proposed neutrino oscillations [28], and Maki-Nakagawa-Sakata, who introduced the mixing matrix [29]. This matrix is analogous to the quark

CKM matrix, and is usually parameterized as,

$$U_{\text{PMNS}} = \begin{pmatrix} c_{12}c_{13} & s_{12}c_{13} & s_{13}e^{-i\delta} \\ -s_{12}c_{23} - c_{12}s_{23}s_{13}e^{i\delta} & c_{12}c_{23} - s_{12}s_{23}s_{13}e^{i\delta} & s_{23}c_{13} \\ s_{12}s_{23} - c_{12}c_{23}s_{13}e^{i\delta} & -c_{12}s_{23} - s_{12}c_{23}s_{13}e^{i\delta} & c_{23}c_{13} \end{pmatrix} \cdot P, \quad (1.33)$$

where $c_{ij} = \cos \theta_{ij}$, $s_{ij} = \sin \theta_{ij}$, θ_{ij} are the neutrino mixing angles, δ is the CP-violating Dirac phase and the matrix $P = \text{diag}(1, e^{-i\alpha_1}, e^{-i\alpha_2})$ bears additional CP-violating Majorana phases.

The oscillation occurs because neutrinos are produced by the weak interaction as flavor eigenstates, i. e., as a quantum superposition of the mass eigenstates. Assuming the physical neutrinos have different masses m_1 , m_2 and m_3 , as the flavor neutrino propagates, the phases of the superposition (which are dependent on the masses) will evolve differently for each mass eigenstate, changing the neutrino flavor over time. Therefore, there is a nonzero probability that a neutrino produced as a specific flavor eigenstate ν_α , be later detected as another flavor eigenstate ν_β . It can be shown [30] that the probability of oscillation in vacuum depends on the U_{PMNS} matrix and on the squared mass differences $\Delta m_{ij}^2 = m_i^2 - m_j^2$,

$$\mathcal{P}_{\nu_\alpha \rightarrow \nu_\beta} = \sum_{i,j=1}^3 U_{\alpha i}^* U_{\beta i} U_{\alpha j} U_{\beta j}^* \exp \left(-i \frac{\Delta m_{ij}^2 L}{2E} \right), \quad (1.34)$$

where L is the propagation distance and E is the neutrino energy. Therefore, oscillations occur if neutrinos have nonzero masses, and these masses are non-degenerate.

The accumulated data from neutrino oscillation experiments, allowed to determine the mixing angles and mass differences with great precision. However, they still leave open two possibilities for the neutrino mass ordering: normal ordering, where $m_1 < m_2 < m_3$; and inverted ordering, where $m_3 < m_1 < m_2$. Also, the CP-violating phases have not been measured yet. Besides this, the absolute values of the masses are still unknown. As neutrino oscillation experiments are not sensitive to the absolute masses, they are probed in beta decay experiments, through kinematic effects. The determination of all these parameters are target of ongoing and future experiments [31, 32, 33, 34]. The current values of the available parameters at 1σ level are given below [35]. Assuming the masses follow the normal ordering:

$$\Delta m_{21}^2 = 7.50_{-0.17}^{+0.19} \times 10^{-5} \text{eV}^2, \quad \Delta m_{31}^2 = 2.524_{-0.040}^{+0.039} \times 10^{-3} \text{eV}^2, \quad \delta = 261_{-59}^{+51}^\circ$$

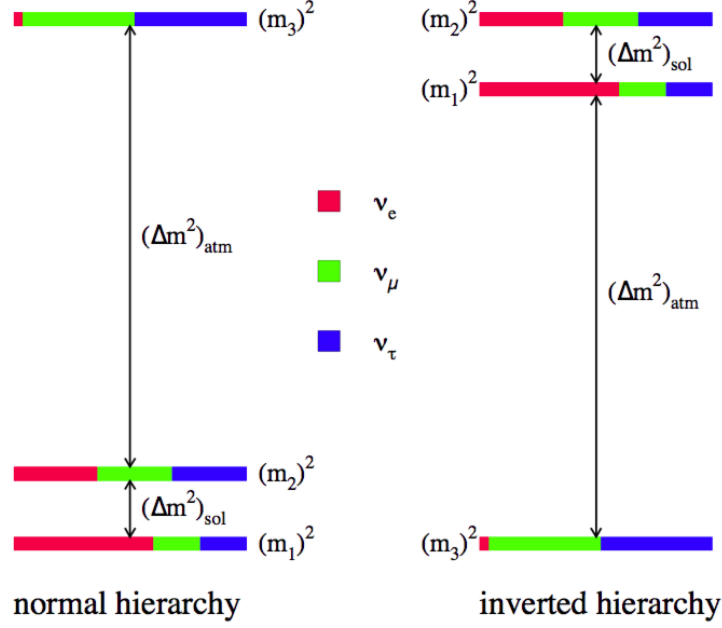


Figure 1.1: Representation of neutrino mixing and mass differences in normal and inverted orderings. Figure taken from the Ref. [1].

$$\sin^2 \theta_{12} = 0.306^{+0.012}_{-0.012} \quad , \quad \sin^2 \theta_{23} = 0.441^{+0.027}_{-0.021} \quad , \quad \sin^2 \theta_{13} = 0.02166^{+0.00075}_{-0.00075}.$$

Whereas for the inverted ordering:

$$\Delta m_{21}^2 = 7.50^{+0.19}_{-0.17} \times 10^{-5} \text{eV}^2 \quad , \quad \Delta m_{32}^2 = -2.514^{+0.038}_{-0.041} \times 10^{-3} \text{eV}^2 \quad , \quad \delta = 277^\circ_{-46^\circ}$$

$$\sin^2 \theta_{12} = 0.306^{+0.012}_{-0.012} \quad , \quad \sin^2 \theta_{23} = 0.587^{+0.024}_{-0.020} \quad , \quad \sin^2 \theta_{13} = 0.02179^{+0.00076}_{-0.00076}.$$

These numbers are also nicely illustrated compactly in Fig. 1.1.

As we saw in the previous sections of this Chapter, the SM symmetries and particle content does not allow neutrino mass terms in the Lagrangian. On the other hand, the evidence for the existence of neutrino masses is overwhelming. Therefore, the solution of this problem definitely lies beyond the SM. Although it may appear trivial to generate neutrino masses simply by introducing right-handed neutrinos and proceeding in the same way as for the other fermions, there is more than one way to do that, since it is not known whether right-handed neutrinos (if they do exist in first place) are Dirac or Majorana particles. Moreover, there are ways to generate neutrinos masses without the need of right-handed neutrinos at all. Therefore, it is important to explore the different possibilities. In the following chapters, starting in Chapter 3, we will study some SM extensions capable of accommodating massive neutrinos.

Chapter 2

Two Higgs Doublet Models

The fermion and gauge sectors of the SM have been experimentally tested in the last decades with great precision, confirming with enormous success the predictions of this theory. However, the scalar sector began to be explored directly only in the last years with the LHC, and remains as the part of the theory with the largest experimental uncertainties. In the SM, it is assumed that the structure of this sector is the simplest possible, with only one $SU(2)$ doublet, which suffices to generate the masses for the fermions and gauge bosons, as discussed in the Chapter 1. As there is no fundamental reason for the existence of only one Higgs doublet, and the other sectors show a rich structure with several different particles, it is reasonable to consider the possibility of the existence of more scalar particles besides the SM Higgs.

As mentioned in Chapter 1, the experimental value of the ρ parameter,

$$\rho = \frac{m_W^2}{m_Z^2 \cos^2 \theta_W}, \quad (2.1)$$

is in very good agreement with the SM prediction $\rho \simeq 1$. This precise agreement, however, can be spoiled in new physics models which add extra scalars to the particle content, if they contribute to the W and Z boson masses. It can be shown that in a gauge theory with scalar multiplets of weak isospin T_i , weak hypercharge Y_i and neutral component VEVs v_i , the ρ parameter at tree level is generally given by [36],

$$\rho = \frac{\sum_i^n [T_i(T_i + 1) - \frac{1}{4}Y_i^2] v_i^2}{\sum_i^n \frac{1}{2}Y_i^2 v_i^2}. \quad (2.2)$$

Therefore, a generic scalar sector with several multiplets will lead to a ρ value different from $\rho = 1$. However, according to this expression, $SU(2)$ doublets of hypercharge $Y = 1$

do not change the ρ value, so in this sense, they are natural candidates for building scalar extensions of the SM. One of the simplest extensions, the Two Higgs Doublet Model (2HDM), takes advantage of this fact and introduces two scalar doublets, Φ_1 and Φ_2 , while keeping the $\rho = 1$ value unchanged,

$$\Phi_i = \begin{pmatrix} \phi_i^+ \\ \phi_i^0 \end{pmatrix}, \quad i = 1, 2. \quad (2.3)$$

This kind of model has been extensively studied since the original proposal by T. D. Lee in 1973 [37].

One motivation to study 2HDMs is the supersymmetry. In supersymmetric models the scalar fields are written as components of chiral multiplets together with chiral spin-1/2 fields. Since the complex conjugate of such a chiral multiplet have opposite chirality and the supersymmetry forbids the coupling of fields of opposite chiralities in the Lagrangian, a single Higgs doublet is unable to generate mass for both the up and down quarks. Besides this, as the multiplets also contain chiral fermions, the anomaly cancellation is another reason for introducing a second doublet. Therefore, in the Minimal Supersymmetric Standard Model (MSSM), there are two Higgs doublets.

Another motivation is the fact that the SM is not able to produce the necessary amount of CP violation to explain the matter-antimatter asymmetry in the Universe. The 2HDM presents new possible sources of CP violation in its scalar sector and the baryogenesis in the 2HDM has been studied [38, 39, 40]. 2HDMs have also been studied in the context of axions [41, 42], and dark matter in the so called Inert Doublet Model (IDM) [43, 44].

In the following we present the main features of the most popular version of the 2HDM, which features a discrete Z_2 symmetry, stressing the novelties introduced by the presence of the second doublet as compared to the SM, specially in the scalar and Yukawa sectors.

2.1 The Scalar Sector with Two Higgs Doublets

The scalar sector in the 2HDM is described by the following Lagrangian,

$$\mathcal{L}_{\text{escalar}} = (D^\mu \Phi_1)^\dagger D_\mu \Phi_1 + (D^\mu \Phi_2)^\dagger D_\mu \Phi_2 - V(\Phi_1, \Phi_2), \quad (2.4)$$

where the covariant derivative is the same as in the SM, since the gauge symmetries are the same,

$$D_\mu = \partial_\mu + igT^a W_\mu^a + ig' \frac{Y}{2} B_\mu. \quad (2.5)$$

The most general renormalizable potential for two scalar doublets of hypercharge $Y = 1$ is given by,

$$\begin{aligned} V(\Phi_1, \Phi_2) = & m_1^2 \Phi_1^\dagger \Phi_1 + m_2^2 \Phi_2^\dagger \Phi_2 - \left(m_{12}^2 \Phi_1^\dagger \Phi_2 + h.c. \right) + \frac{\lambda_1}{2} \left(\Phi_1^\dagger \Phi_1 \right)^2 + \\ & + \frac{\lambda_2}{2} \left(\Phi_2^\dagger \Phi_2 \right)^2 + \lambda_3 \left(\Phi_1^\dagger \Phi_1 \right) \left(\Phi_2^\dagger \Phi_2 \right) + \lambda_4 \left(\Phi_1^\dagger \Phi_2 \right) \left(\Phi_2^\dagger \Phi_1 \right) + \\ & + \left[\frac{\lambda_5}{2} \left(\Phi_1^\dagger \Phi_2 \right)^2 + \lambda_6 \left(\Phi_1^\dagger \Phi_1 \right) \left(\Phi_1^\dagger \Phi_2 \right) + \lambda_7 \left(\Phi_2^\dagger \Phi_2 \right) \left(\Phi_1^\dagger \Phi_2 \right) + h.c. \right]. \end{aligned} \quad (2.6)$$

The requirement that the potential be hermitian implies that the parameters m_1^2 , m_2^2 , λ_1 , λ_2 , λ_3 and λ_4 are real, while m_{12}^2 , λ_5 , λ_6 and λ_7 are in general complex and can be sources of CP violation. From the 14 free parameters (6 real and 4 complex) only 11 are physical, since there is some freedom to redefine the fields Φ_1 and Φ_2 [8].

A general feature of 2HDMs is the existence of Flavor Changing Neutral Interactions (FCNI) at tree level, mediated by the extra neutral scalars, which imposes several constraints on the model since this kind of process is known to be very suppressed experimentally. For instance, the Yukawa coupling for the down quarks is (see Eq. 2.32),

$$- \mathcal{L}_{\text{Ydown}} = y_{ij}^{1d} \bar{Q}^i \Phi_1 d_R^j + y_{ij}^{2d} \bar{Q}^i \Phi_2 d_R^j + h.c. \quad (2.7)$$

where i, j are generation indices. The mass matrix after EWSB is,

$$M_{ij}^d = y_{ij}^{1d} \frac{v_1}{\sqrt{2}} + y_{ij}^{2d} \frac{v_2}{\sqrt{2}}. \quad (2.8)$$

FCNI will be present if the Yukawa interaction matrices y^1 and y^2 are non-diagonal. As y^1 and y^2 are generic complex matrices, the diagonalization of M^d does not imply the individual diagonalization of both y^1 and y^2 , thus leading to FCNI. In the SM this does not occur because the mass and Yukawa interaction matrices are proportional to each other so that in the physical basis the Yukawa interactions are diagonal.

In order to avoid these dangerous interactions, usually is implemented the Natural Flavor Conservation criterion, by imposing discrete or global symmetries in the Lagrangian. The most commonly adopted is the Z_2 discrete symmetry, under which the doublets transform as,

$$\begin{aligned} \Phi_1 &\rightarrow -\Phi_1 \\ \Phi_2 &\rightarrow \Phi_2. \end{aligned} \quad (2.9)$$

By imposing this symmetry in the potential, the Z_2 non-invariant terms m_{12} , λ_6 e λ_7 must be discarded. However, as is well known that the spontaneous breaking of an exact discrete symmetry leads to the domain wall problem [45], the m_{12} term is kept in the potential in order to explicitly break the Z_2 symmetry. Under these conditions, and assuming no CP violation, $V(\Phi_1, \Phi_2)$ reduces to,

$$\begin{aligned} V(\Phi_1, \Phi_2) = & m_1^2 \Phi_1^\dagger \Phi_1 + m_2^2 \Phi_2^\dagger \Phi_2 - m_{12}^2 (\Phi_1^\dagger \Phi_2 + \Phi_2^\dagger \Phi_1) + \frac{\lambda_1}{2} (\Phi_1^\dagger \Phi_1)^2 + \\ & + \frac{\lambda_2}{2} (\Phi_2^\dagger \Phi_2)^2 + \lambda_3 (\Phi_1^\dagger \Phi_1) (\Phi_2^\dagger \Phi_2) + \lambda_4 (\Phi_1^\dagger \Phi_2) (\Phi_2^\dagger \Phi_1) + \\ & + \frac{\lambda_5}{2} \left[(\Phi_1^\dagger \Phi_2)^2 + (\Phi_2^\dagger \Phi_1)^2 \right], \end{aligned} \quad (2.10)$$

where now all the parameters are real.

Parameterizing Φ_1 and Φ_2 as,

$$\Phi_i = \begin{pmatrix} \phi_i^+ \\ (v_i + \rho_i + i\eta_i)/\sqrt{2} \end{pmatrix}, \quad i = 1, 2 \quad (2.11)$$

we have in principle four charged and four neutral scalars. After the EWSB three of them become the longitudinal components of the gauge bosons W^+ , W^- and Z , leaving five physical scalars: two neutral H and h ; two charged H^+ and H^- and one pseudoscalar A .

The spontaneous symmetry breaking occurs when the doublets acquire nonzero VEVs. As the vacuum must be invariant under $U_{\text{em}}(1)$ transformations, only the neutral scalars can develop VEVs,

$$\langle \Phi_i \rangle_0 = \frac{1}{\sqrt{2}} \begin{pmatrix} 0 \\ v_i \end{pmatrix}, \quad i = 1, 2 \quad (2.12)$$

with v_1 and v_2 real. In order to this configuration correspond to a minimum of the potential,

$$\left(\frac{\partial V}{\partial \rho_i} \right)_{\Phi_i = \langle \Phi_i \rangle_0} = \left(\frac{\partial V}{\partial \eta_i} \right)_{\Phi_i = \langle \Phi_i \rangle_0} = \left(\frac{\partial V}{\partial \phi_i^\pm} \right)_{\Phi_i = \langle \Phi_i \rangle_0} = 0, \quad (2.13)$$

the following conditions must be satisfied,

$$\begin{aligned} m_1^2 v_1 - m_{12}^2 v_2 + \frac{1}{2} \lambda_1 v_1^3 + \frac{1}{2} (\lambda_3 + \lambda_4 + \lambda_5) v_1 v_2^2 &= 0 \\ m_2^2 v_2 - m_{12}^2 v_1 + \frac{1}{2} \lambda_2 v_2^3 + \frac{1}{2} (\lambda_3 + \lambda_4 + \lambda_5) v_1^2 v_2 &= 0. \end{aligned} \quad (2.14)$$

The neutral mixing matrix after using the minimum conditions (2.14) reads,

$$M_{H,h}^2 = \begin{pmatrix} m_{12}^2 \frac{v_2}{v_1} + \lambda_1 v_1^2 & -m_{12}^2 + \lambda_{345} v_1 v_2 \\ -m_{12}^2 + \lambda_{345} v_1 v_2 & m_{12}^2 \frac{v_1}{v_2} + \lambda_2 v_2^2 \end{pmatrix}, \quad (2.15)$$

where $\lambda_{345} = \lambda_3 + \lambda_4 + \lambda_5$ was defined. $M_{H,h}^2$ is diagonalized by the rotation,

$$\begin{pmatrix} h \\ H \end{pmatrix} = \begin{pmatrix} \cos \alpha & \sin \alpha \\ -\sin \alpha & \cos \alpha \end{pmatrix} \begin{pmatrix} \rho_1 \\ \rho_2 \end{pmatrix}, \quad (2.16)$$

with the angle α given by,

$$\tan 2\alpha = \frac{-2m_{12}^2 v_1 v_2 + 2\lambda_{345} v_1^2 v_2^2}{m_{12}^2 v_2^2 - m_{12}^2 v_1^2 + \lambda_1 v_1^3 v_2 - \lambda_2 v_1 v_2^3}. \quad (2.17)$$

The masses of the physical fields h and H are given by (notice that h is always lighter than H),

$$m_h^2 = \frac{1}{2} \left[\frac{m_{12}^2 v^2}{v_1 v_2} + \lambda_1 v_1^2 + \lambda_2 v_2^2 - \sqrt{\left(\frac{m_{12}^2 (v_1^2 - v_2^2)}{v_1 v_2} - \lambda_1 v_1^2 + \lambda_2 v_2^2 \right)^2 + 4(m_{12}^2 - \lambda_{345} v_1 v_2)^2} \right], \quad (2.18)$$

$$m_H^2 = \frac{1}{2} \left[\frac{m_{12}^2 v^2}{v_1 v_2} + \lambda_1 v_1^2 + \lambda_2 v_2^2 + \sqrt{\left(\frac{m_{12}^2 (v_1^2 - v_2^2)}{v_1 v_2} - \lambda_1 v_1^2 + \lambda_2 v_2^2 \right)^2 + 4(m_{12}^2 - \lambda_{345} v_1 v_2)^2} \right]. \quad (2.19)$$

In the same manner for the pseudo and charged scalars we have,

$$M_A^2 = [m_{12}^2 - \lambda_5 v_1 v_2] \begin{pmatrix} \frac{v_2}{v_1} & -1 \\ -1 & \frac{v_1}{v_2} \end{pmatrix}, \quad (2.20)$$

$$M_{H^\pm}^2 = [m_{12}^2 - \frac{1}{2}(\lambda_4 + \lambda_5) v_1 v_2] \begin{pmatrix} \frac{v_2}{v_1} & -1 \\ -1 & \frac{v_1}{v_2} \end{pmatrix}. \quad (2.21)$$

The mass matrices M_A^2 e $M_{H^\pm}^2$ are both diagonalized by the same angle β , given by,

$$\tan \beta = \frac{v_2}{v_1}, \quad (2.22)$$

such that,

$$\begin{pmatrix} G \\ A \end{pmatrix} = \begin{pmatrix} \cos \beta & \sin \beta \\ -\sin \beta & \cos \beta \end{pmatrix} \begin{pmatrix} \eta_1 \\ \eta_2 \end{pmatrix}, \quad (2.23)$$

and,

$$\begin{pmatrix} G^+ \\ H^+ \end{pmatrix} = \begin{pmatrix} \cos \beta & \sin \beta \\ -\sin \beta & \cos \beta \end{pmatrix} \begin{pmatrix} \phi_1^+ \\ \phi_2^+ \end{pmatrix}. \quad (2.24)$$

The pseudoscalar masses are,

$$m_G = 0 \quad (2.25)$$

$$m_A^2 = [m_{12}^2/v_1 v_2 - \lambda_5] (v_1^2 + v_2^2), \quad (2.26)$$

and for the charged scalars,

$$m_{G^+} = 0 \quad (2.27)$$

$$m_{H^+}^2 = \left[m_{12}^2/v_1 v_2 - \frac{1}{2}(\lambda_4 + \lambda_5) \right] (v_1^2 + v_2^2), \quad (2.28)$$

from which we can identify A , H^+ and H^- as the physical fields and G , G^+ and G^- as the Goldstone bosons absorbed by the Z , W^+ and W^- gauge bosons.

The doublet VEVs v_1 and v_2 are constrained in order to reproduce the correct EWSB pattern. Both VEVs contribute to the physical gauge boson masses, as can be seen from the kinetic term in the Eq. (2.4). With the additional doublet, the SM Lagrangian for the gauge boson masses (1.16) gets modified to,

$$\mathcal{L}_{\text{gauge mass}} = \frac{1}{4}g^2(v_1^2 + v_2^2)W_\mu^- W^{+\mu} + \frac{1}{8}(v_1^2 + v_2^2) \left[g^2 W_\mu^3 W^{3\mu} + g'^2 B_\mu B^\mu - 2gg' W_\mu^3 B^\mu \right]. \quad (2.29)$$

The mixing is eliminated by the same rotation (1.18) and the W and Z masses are,

$$m_W = \frac{1}{2}g\sqrt{v_1^2 + v_2^2}, \quad m_Z = \frac{1}{2}\frac{g\sqrt{v_1^2 + v_2^2}}{\cos\theta_W}. \quad (2.30)$$

Therefore, v_1 and v_2 must obey the constraint,

$$v \equiv \sqrt{v_1^2 + v_2^2} \simeq 246\text{GeV}. \quad (2.31)$$

The coupling of the neutral Higgs bosons h and H to the W and Z are as follows: the light Higgs h couples to either WW or ZZ in the same way as the SM Higgs, times the prefactor $\cos(\alpha - \beta)$; whereas the coupling of the heavier Higgs, H , is the same as the SM coupling times the prefactor $\sin(\beta - \alpha)$. Finally, the coupling of the pseudoscalar A to the vector bosons vanishes.

2.2 The Yukawa Sector and FCNI

The most general Yukawa coupling with two Higgs doublets is the following,

$$\begin{aligned} -\mathcal{L}_{Y_{2\text{HDM}}} = & y^{1d}\bar{Q}\Phi_1 d_R + y^{1u}\bar{Q}\tilde{\Phi}_1 u_R + y^{1e}\bar{L}\Phi_1 e_R + \\ & + y^{2d}\bar{Q}\Phi_2 d_R + y^{2u}\bar{Q}\tilde{\Phi}_2 u_R + y^{2e}\bar{L}\Phi_2 e_R + h.c. \end{aligned} \quad (2.32)$$

As already mentioned, this full Lagrangian leads to the appearance of FCNI at tree level. The imposition of the Z_2 symmetry, however, allows us to eliminate conveniently some

2HDM	u_R	d_R	e_R
Type I	Φ_2	Φ_2	Φ_2
Type II	Φ_2	Φ_1	Φ_1
Type X	Φ_2	Φ_2	Φ_1
Type Y	Φ_2	Φ_1	Φ_2

Table 2.1: The four 2HDM types that satisfy the NFC criterion. Each type is defined according to which scalar couples to which right-handed fermion.

terms in this expression. The specific terms which will be eliminated depend upon the parity assignment for the right-handed fermions under Z_2 (assuming that the left-handed fermions have always positive parity). We can, e. g., consider that all the right-handed fermions are even, i. e., they transform trivially. In this case, by the Eq. (2.9), the terms in $\mathcal{L}_{Y_{2\text{HDM}}}$ which contain Φ_1 change sign, violating the Z_2 symmetry, so that they must be discarded. Therefore $\mathcal{L}_{Y_{2\text{HDM}}}$ reduces to,

$$-\mathcal{L}_{Y_{2\text{HDM}}} = y_2^d \bar{Q} \Phi_2 d_R + y_2^u \bar{Q} \tilde{\Phi}_2 u_R + y_2^e \bar{L} \Phi_2 e_R + h.c. \quad (2.33)$$

and only Φ_2 couples to the fermions. Another possible choice is to consider that the leptons and down quarks have negative parity under Z_2 ,

$$\begin{aligned} d_R &\rightarrow -d_R \\ e_R &\rightarrow -e_R. \end{aligned} \quad (2.34)$$

In this case, $\mathcal{L}_{Y_{2\text{HDM}}}$ becomes,

$$-\mathcal{L}_{Y_{2\text{HDM}}} = y_1^d \bar{Q} \Phi_1 d_R + y_1^e \bar{L} \Phi_1 e_R + y_2^u \bar{Q} \tilde{\Phi}_2 u_R + h.c. \quad (2.35)$$

and we have that Φ_2 couples to up quarks only, while Φ_1 couples to leptons and down quarks. In this scenario, the up and down quark masses come from different sources, which could help to alleviate the mass hierarchy between these types of quarks.

In general, it is easy to see that if all the fermions which have the same quantum numbers (which in principle can mix one another) couples to the same Higgs multiplet, then FCNI are absent. This Natural Flavor Conservation (NFC) criterion was formalized by the Paschos-Glashow-Weinberg theorem [46, 47] which states that a necessary condition for the absence of FCNI at tree level is that all the fermions of the same charge and chirality receive contribution for their mass matrices from only one source. In the SM this theorem

Model	Φ_1	Φ_2	u_R	d_R	e_R	Q	L
Type I	—	+	+	+	+	+	+
Type II	—	+	+	—	—	+	+
Type X	—	+	+	+	—	+	+
Type Y	—	+	+	—	+	+	+

Table 2.2: Parity assignment for fermions and scalars under the Z_2 symmetry in the different types of 2HDM.

is trivially satisfied, preventing FCNI, as there is only one source for the fermion masses. Whereas in models in which there are several sources for the fermion masses, such as the 2HDM, the absence of FCNI can be guaranteed only by the introduction of symmetries.

There are only four different types of 2HDM which satisfy the NFC criterion, as shown in the Table 2.1. In order to realize this condition by means of the Z_2 symmetry, the required Z_2 parities of the fermions and scalars are as shown in the Table 2.2. The two examples discussed above related to the Yukawa Lagrangians in Eqs. (2.33) and (2.35) correspond to type I and type II 2HDMs, respectively. From the Table 2.1 it is straightforward to construct the Yukawa Lagrangians for the other two cases, the 2HDMs type X and type Y, which are also commonly referred as Lepton-specific and Flipped, respectively. The model in which there is not any symmetry and therefore have the most general Yukawa coupling of the Eq. (2.32) is called type III 2HDM.

Expanding the Yukawa Lagrangian for each 2HDM type in the physical basis after the rotations (2.24), (2.23) and (2.16), we obtain the interaction terms of the physical scalars h , H , H^+ and A with the fermions,

$$\begin{aligned}
-\mathcal{L}_{Y_{2\text{HDM}}} = & \sum_{f=u,d,\ell} \frac{m_f}{v} \left(\xi_h^f \bar{f} f h + \xi_H^f \bar{f} f H - i \xi_A^f \bar{f} \gamma_5 f A \right) \\
& + \left[\frac{\sqrt{2} V_{ud}}{v} \bar{u} (m_u \xi_A^u P_L + m_d \xi_A^d P_R) d H^+ + \frac{\sqrt{2} m_\ell \xi_A^\ell}{v} \bar{\nu}_L \ell_R H^+ + h.c. \right], \quad (2.36)
\end{aligned}$$

where $P_{L/R}$ are the projection operators for left-/right-handed fermions and the parameters $\xi_h^f, \xi_H^f, \xi_A^f$ were defined following the notation of Ref. [48]. This notation is convenient as it allows to express the Yukawa interactions for all the four 2HDM types in one single expression. The factors ξ are presented in Table 2.3.

One last thing that worth to be stressed is that the coupling of the scalars to the

	Type I	Type II	Lepton-specific	Flipped
ξ_h^u	$\sin \alpha / \sin \beta$	$\sin \alpha / \sin \beta$	$\sin \alpha / \sin \beta$	$\sin \alpha / \sin \beta$
ξ_h^d	$\sin \alpha / \sin \beta$	$\cos \alpha / \cos \beta$	$\sin \alpha / \sin \beta$	$\cos \alpha / \cos \beta$
ξ_h^ℓ	$\sin \alpha / \sin \beta$	$\cos \alpha / \cos \beta$	$\cos \alpha / \cos \beta$	$\sin \alpha / \sin \beta$
ξ_H^u	$\cos \alpha / \sin \beta$	$\cos \alpha / \sin \beta$	$\cos \alpha / \sin \beta$	$\cos \alpha / \sin \beta$
ξ_H^d	$\cos \alpha / \sin \beta$	$-\sin \alpha / \cos \beta$	$\cos \alpha / \sin \beta$	$-\sin \alpha / \cos \beta$
ξ_H^ℓ	$\cos \alpha / \sin \beta$	$-\sin \alpha / \cos \beta$	$-\sin \alpha / \cos \beta$	$\cos \alpha / \sin \beta$
ξ_A^u	$\cot \beta$	$\cot \beta$	$\cot \beta$	$\cot \beta$
ξ_A^d	$-\cot \beta$	$\tan \beta$	$-\cot \beta$	$\tan \beta$
ξ_A^ℓ	$-\cot \beta$	$\tan \beta$	$\tan \beta$	$-\cot \beta$

Table 2.3: Yukawa couplings for the physical scalars to fermions in the different types of 2HDM.

gauge bosons are same as described in the previous section, regardless of the 2HDM type.

2.3 The Alignment Limit

The LHC discovery of a scalar particle of mass 125 GeV which is compatible with the SM Higgs boson to the current precision limits, puts a strong constraint on the 2HDM scalar sector. One of the physical fields h or H must behave approximately in the same way as the SM Higgs, which means that their couplings to the other fields must mimic the SM Higgs couplings. This condition is satisfied in the so-called alignment limit [49, 50].

We can identify what would be the SM Higgs boson in the context of the 2HDM by working in a basis in which one of the doublets concentrates all of the VEV and the other is inert. The doublet that acquires the VEV behaves in the same manner as the SM doublet, since it is responsible to drive the EWSB. Therefore, its neutral component may be identified as the SM Higgs boson. This basis can be achieved by the following transformation on the original doublets Φ_1 and Φ_2 ,

$$\begin{aligned}
H_1 &= \cos \beta \Phi_1 + \sin \beta \Phi_2 \\
H_2 &= -\sin \beta \Phi_1 + \cos \beta \Phi_2,
\end{aligned}
\tag{2.37}$$

with β given by Eq. (2.22). After using (2.23) and (2.24), H_1 and H_2 read,

$$H_1 = \begin{pmatrix} G^+ \\ \frac{1}{\sqrt{2}}(v + H^{SM} + iG) \end{pmatrix}, \quad H_2 = \begin{pmatrix} H^+ \\ \frac{1}{\sqrt{2}}(\chi + iA) \end{pmatrix} \quad (2.38)$$

where $H^{SM} = \rho_1 \cos \beta + \rho_2 \sin \beta$ and $\chi = -\rho_1 \sin \beta + \rho_2 \cos \beta$. In this basis the physical fields H^+ and A and the Goldstone bosons G^+ and G are explicit, though the physical neutral scalars are not. By using Eq. (2.16), H^{SM} can be written in terms of h and H ,

$$H^{SM} = h \cos(\beta - \alpha) + H \sin(\beta - \alpha). \quad (2.39)$$

Thus we see that neither of the physical fields of the 2HDM correspond exactly to the SM Higgs boson for generic values of the mixing angles α and β . However, Eq. (2.39) reveals the condition that α and β must satisfy in order to obtain the alignment limit: when $\cos(\alpha - \beta) = 1$, h becomes SM-like Higgs; whereas if $\sin(\alpha - \beta) = 1$, then H is the SM-like Higgs.

This condition can be verified using the couplings of the Table 2.3. For instance, if we identify h as the SM-like Higgs, the alignment limit is $\alpha = \beta$. In this case, it is easy to see from the Table that the ξ factors become $\xi_h^u = \xi_h^d = \xi_h^\ell = 1$, confirming that h couples to fermions as the SM Higgs boson. It is interesting to notice that this happens regardless the type of 2HDM. The couplings with the gauge bosons also reduces to the SM ones, since the proportionality factor for these couplings is $\cos(\alpha - \beta)$.

Chapter 3

Neutrino Masses and Absence of Flavor Changing Interactions in the 2HDM from Gauge Principles

In the previous Chapter we presented the 2HDMs, which are attractive SM extensions due to, among other things, its simplicity and phenomenological richness. However, the 2HDM framework in its general form is plagued with FCNI and to cure this problem, an ad-hoc discrete symmetry is usually evoked. Furthermore, neutrino masses, one of the major observational evidences for physics beyond the SM, are typically not addressed in 2HDM.

In this Chapter we discuss a gauge solution to the FCNI problem which in addition naturally can incorporate Majorana neutrino masses. The idea is to add a gauged Abelian $U(1)_X$ symmetry to the 2HDM and find anomaly-free models that effectively lead to the usual 2HDM classes that have no FCNI. Anomaly-free models are also possible when right-handed neutrinos are added to the particle content. Their mass terms generate Majorana masses for the light neutrinos. Tracing the absence of dangerous flavor physics and the presence of neutrino masses to the same anomaly-free gauge origin is an attractive approach within 2HDM that deserves careful study. A whole class of models is generated by the idea. A new vector gauge boson that has mass and kinetic-mixing with the SM Z boson is present, and we investigate its phenomenology in a limit which resembles often studied dark photon models. In particular, we address several constraints coming from low energy as well as high energy probes, including atomic parity violation, the muon

anomalous magnetic moment, electron-neutrino scattering, and new physics searches at the LHC and several other MeV-GeV colliders such as BaBar.

This Chapter is structured as follows: in section 3.1 we introduce the 2HDM framework with gauged Abelian symmetries and study the constraints on the models from anomaly cancellation, including right-handed neutrinos. After that we explain how the neutrino masses are generated in this setup. In section 3.2 the models are confronted with various phenomenological constraints before we summarize our discussion in section 3.3. Some details of this Chapter are delegated to the Appendix A.

3.1 2HDM with $U(1)_X$ Symmetries

As discussed in the Chapter 2, the introduction of a Z_2 symmetry is sufficient to successfully implement the NFC criterion and avoid the problem of FCNI at the tree level in the 2HDM. Although effective to overcome this problem, the origin of this symmetry is not clear. Moreover, the ad-hoc introduction of the m_{12} term in the scalar potential to save the model from the cosmological domain wall problem does not seem natural.

However, the Z_2 symmetry is not the only way available to avoid the FCNI problem [51]. A fundamental solution to this flavor problem in the 2HDM could come from well-established gauge principles. The implementation of an Abelian gauge symmetry $U(1)_X$ can also be effective to eliminate conveniently terms in the Yukawa Lagrangian and generate all four 2HDM types free from FCNI, once suitable charges are assigned to the fields. In the next section we will explain how this can be achieved. The fundamental requirement, as we will see, is that the two Higgs doublets have different $U(1)_X$ charges. This requirement on Φ_1 and Φ_2 and the $U(1)_X$ invariance reduces the scalar potential to,

$$\begin{aligned}
 V(\Phi_1, \Phi_2) = & m_1^2 \Phi_1^\dagger \Phi_1 + m_2^2 \Phi_2^\dagger \Phi_2 + \frac{\lambda_1}{2} \left(\Phi_1^\dagger \Phi_1 \right)^2 + \frac{\lambda_2}{2} \left(\Phi_2^\dagger \Phi_2 \right)^2 \\
 & + \lambda_3 \left(\Phi_1^\dagger \Phi_1 \right) \left(\Phi_2^\dagger \Phi_2 \right) + \lambda_4 \left(\Phi_1^\dagger \Phi_2 \right) \left(\Phi_2^\dagger \Phi_1 \right).
 \end{aligned}
 \tag{3.1}$$

Generally speaking, a local Abelian transformation change the fields as follows,

$$\begin{aligned}
L_L &\rightarrow L'_L = e^{il\alpha(x)} L_L \\
Q_L &\rightarrow Q'_L = e^{iq\alpha(x)} Q_L \\
e_R &\rightarrow e'_R = e^{ie\alpha(x)} e_R \\
u_R &\rightarrow u'_R = e^{iu\alpha(x)} u_R \\
d_R &\rightarrow d'_R = e^{id\alpha(x)} d_R \\
\Phi_1 &\rightarrow \Phi'_1 = e^{iQ_{X1}\alpha(x)} \Phi_1 \\
\Phi_2 &\rightarrow \Phi'_2 = e^{iQ_{X2}\alpha(x)} \Phi_2,
\end{aligned} \tag{3.2}$$

where $l, q, e, u, d, Q_{X1}, Q_{X2}$ are the charges of the fields under $U(1)_X$. The fermion charges have also to obey certain conditions dictated by gauge invariance and anomaly cancellation. In what follows we will derive these conditions.

3.1.1 Realizing NFC criterion with $U(1)_X$ Symmetries

The requirement that the scalar doublets transform differently still leaves enough freedom to construct several models, based on the specific charge assignments for the SM particles. Once we write down a Yukawa Lagrangian and demand gauge invariance, the transformations in Eq. (3.2) are no longer arbitrary, and the charges under $U(1)_X$ will be interconnected. For instance, in the Type I 2HDM, where fermions couple only with Φ_2 , the following $U(1)_X$ transformations apply,

$$\begin{aligned}
-\mathcal{L}_{Y_{2\text{HDM}}} &\rightarrow -\mathcal{L}'_{Y_{2\text{HDM}}} = e^{i\alpha(-q+Q_{X2}+d)} y_2^d \bar{Q} \Phi_2 d_R + e^{i\alpha(-q-Q_{X2}+u)} y_2^u \bar{Q} \tilde{\Phi}_2 u_R \\
&\quad + e^{i\alpha(-l+Q_{X2}+e)} y_2^e \bar{L} \Phi_2 e_R + h.c.
\end{aligned} \tag{3.3}$$

The $U(1)_X$ invariance imposes the following conditions on the charges of the fields:

$$\begin{aligned}
d - q + Q_{X2} &= 0 \\
u - q - Q_{X2} &= 0 \\
e - l + Q_{X2} &= 0.
\end{aligned} \tag{3.4}$$

Notice that in this case couplings of fermions with Φ_1 are forbidden by the $U(1)_X$ symmetry. These couplings would be allowed only if Q_{X1} satisfies the same equations (3.4) as Q_{X2} , implying that $Q_{X1} = Q_{X2}$. However, since we require that $Q_{X1} \neq Q_{X2}$, there is no value of Q_{X1} satisfying these equations. Therefore, this charge assignment indeed implements the desired Yukawa coupling of the type I 2HDM.

We can proceed in the same way to obtain the other NFC types of 2HDM. We get type II 2HDM with the following condition,

$$d - q + Q_{X1} = u - q - Q_{X2} = e - l + Q_{X1} = 0, \quad (3.5)$$

whereas for the type X 2HDM,

$$d - q + Q_{X2} = u - q - Q_{X2} = e - l + Q_{X1} = 0, \quad (3.6)$$

and finally for the type Y 2HDM,

$$d - q + Q_{X1} = u - q - Q_{X2} = e - l + Q_{X2} = 0. \quad (3.7)$$

Besides the constraints on the charges from these equations, there are also the constraints from anomaly cancellation, which we now discuss.

3.1.2 Anomaly Cancellation

Anomalies occur when an apparent symmetry of the Lagrangian in a field theory is not actually a symmetry in the quantum theory. When this happens the symmetry is said to be anomalous. The anomaly manifests itself as a non-invariance of the measure in the path integral formulation (although the Lagrangian is invariant), or, in the canonical formalism, with the presence of a would-be conserved current with an anomalous nonzero divergence. Either way, anomalies must be avoided at all cost if the symmetry in question is a gauge symmetry, since in this case they lead to the violation of the Ward identities, which are responsible for the cancellation of non-physical gauge degrees of freedom and for the S matrix unitarity.

Chiral theories often have this issue, once the axial current acquire divergence through quantum corrections at the level of 1-loop, which couple this current to a pair of gauge bosons, as represented by the triangle diagram in Fig. 3.1. It can be shown that the anomalous term in the triangular diagram is proportional to

$$\mathcal{A}^{abc} = \text{Tr} [\{T_R^a, T_R^b\} T_R^c] - \text{Tr} [\{T_L^a, T_L^b\} T_L^c], \quad (3.8)$$

where T_R^a and T_L^a are the group generators in the right-handed and left-handed representations of the matter fields and Tr indicates the ordinary trace of the matrices involved and also the sum over all fermions that can participate in the loop. Demanding that $\mathcal{A}^{abc} = 0$

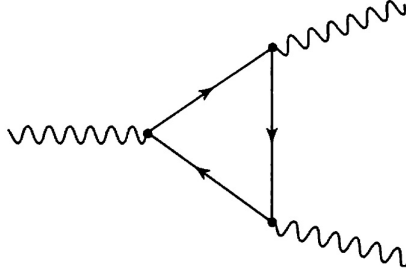


Figure 3.1: Triangle diagram of the chiral anomaly.

is a necessary condition to avoid the presence of anomalies. If a gauge theory satisfies this condition, it is said to be anomaly free.

Once the $U(1)_X$ symmetry in our model is a gauge chiral symmetry, we have to guarantee that it is anomaly free. The general constraints for the anomaly freedom of the $U(1)_X$ symmetry are shown in Appendix A.1. In the Type I 2HDM, in which we will focus our attention for the rest of this Chapter, the anomaly cancellation can be achieved by writing the charges of the fields as a function of u and d (to see this, combine Eq. (A.2) ($l = -3q$) with the constraints from (3.4)),

$$\begin{aligned}
 q &= \frac{(u+d)}{2}, \\
 l &= \frac{-3(u+d)}{2}, \\
 e &= -(2u+d), \\
 Q_{X2} &= \frac{(u-d)}{2}.
 \end{aligned} \tag{3.9}$$

It is then straightforward to prove that these charge assignments in Eq. (3.9) satisfy the anomaly conditions Eqs. (A.1)-(A.4). However, for the cancellation of the $[U(1)_X]^3$ term, Eq. (A.5), we find,

$$\begin{aligned}
 e^3 + 3u^3 + 3d^3 - 2l^3 - 6q^3 &= [-(2u+d)]^3 + 3u^3 + 3d^3 - 2 \left[\frac{-3(u+d)}{2} \right]^3 \\
 &\quad - 6 \left[\frac{(u+d)}{2} \right]^3 \\
 &= -(2u+d)^3 + 3u^3 + 3d^3 + 6(u+d)^3 \\
 &= u^3 + 8d^3 + 6u^2d + 12ud^2 \\
 &= (u+2d)^3.
 \end{aligned} \tag{3.10}$$

and this anomaly is not canceled for u and d arbitrary.

Here is the point at which neutrino physics can enter: if we decide to keep u and d arbitrary, the most straightforward possibility is to add right-handed neutrinos (one per generation). If their charge n is given by

$$n = -(u + 2d), \quad (3.11)$$

the $[U(1)_X]^3$ anomaly term is canceled because Eq. (A.5) becomes

$$n^3 + e^3 + 3u^3 + 3d^3 - 2l^3 - 6q^3 = -(u + 2d)^3 + (u + 2d)^3 = 0. \quad (3.12)$$

The presence of right-handed neutrinos is an essential ingredient to the implementation of the type I seesaw mechanism, as we will discuss in the next section. It is important to note, however, that this anomaly can also be canceled without right-handed neutrinos if $u = -2d$, but in this case the implementation of type I seesaw mechanism is not possible.

Concerning the Φ_1 charge under $U(1)_X$, we have only demanded so far that $Q_{X1} \neq Q_{X2}$ to respect the NFC criterion, and no relation between Q_{X1} and Q_{X2} exist. By adding a singlet scalar to generate a Majorana mass term for the neutrinos, also necessary for the implementation of the seesaw mechanism, the values of Q_{X1} and Q_{X2} are no longer independent, as we will see next.

3.1.3 Neutrino Masses

As aforementioned, in the conventional 2HDM neutrinos are massless. Similarly to the SM one can simply add right-handed neutrinos and generate Dirac masses to the neutrinos. However, a compelling explanation for tiny neutrino masses arises via the seesaw mechanism [52, 53, 54, 55, 56]. In order to realize the type I seesaw mechanism one needs Dirac and Majorana mass terms for the neutrinos. This can be realized in our 2HDM framework by proper assignments of the quantum numbers, as we will demonstrate in what follows.

Typically, a bare mass term is introduced for the right-handed neutrinos in the realization of the seesaw mechanism without explaining its origin. Here, we explain the neutrino masses by adding a scalar singlet Φ_s , with charge q_X under $U(1)_X$. The first consequence of introducing a new singlet scalar is the extension of the scalar potential which adds to Eq. (3.1) the potential

$$V_s = m_s^2 \Phi_s^\dagger \Phi_s + \frac{\lambda_s}{2} (\Phi_s^\dagger \Phi_s)^2 + \mu_1 \Phi_1^\dagger \Phi_1 \Phi_s^\dagger \Phi_s + \mu_2 \Phi_2^\dagger \Phi_2 \Phi_s^\dagger \Phi_s + \left(\mu \Phi_1^\dagger \Phi_2 \Phi_s + h.c. \right), \quad (3.13)$$

where

$$\Phi_s = \frac{1}{\sqrt{2}}(v_s + \rho_s + i\eta_s).$$

All these terms are straightforwardly invariant under $U(1)_X$ except for the last term which requires $q_X = Q_{X1} - Q_{X2}$. That said, the Yukawa Lagrangian involving the neutrinos reads

$$-\mathcal{L} \supset y_{ij}^D \bar{L}_{iL} \tilde{\Phi}_2 N_{jR} + Y_{ij}^M \overline{(N_{iR})^c} \Phi_s N_{Rj} + h.c.. \quad (3.14)$$

After the spontaneous symmetry breaking, picking up only the neutrino mass terms, we have the Lagrangian corresponding to the type I seesaw mechanism,

$$\begin{aligned} -\mathcal{L}_\nu &= \bar{\nu}_L m_D N_R + \frac{1}{2} \overline{N_R^c} M_R N_R + h.c. \\ &= (\overline{\nu}_L \overline{N_R^c}) \begin{pmatrix} 0 & m_D \\ m_D^T & M_R \end{pmatrix} \begin{pmatrix} \nu_L \\ N_R^c \end{pmatrix} + h.c. \end{aligned} \quad (3.15)$$

where $m_D = \frac{y^D v_2}{2\sqrt{2}}$ and $M_R = \frac{y^M v_s}{2\sqrt{2}}$. As long as $M_R \gg m_D$, the mass of the light neutrinos become suppressed by the large M_R , giving the seesaw relation,

$$m_\nu = -m_D^T \frac{1}{M_R} m_D, \quad (3.16)$$

whereas the masses of the heavy neutrinos are $m_N = M_R$. We take v_s to be at the TeV scale, and in this case $y^D \sim 10^{-4}$ and $y^M \sim 1$ lead to $m_\nu \sim 0.1$ eV in agreement with current data [57]. In this scenario right-handed neutrinos have masses at around 300 – 400 GeV, although smaller right-handed neutrino masses are also possible.

Let us now take a closer look at Eq. (3.14). Gauge invariance of the first term requires

$$-l - Q_{X2} + n = 0. \quad (3.17)$$

Using Eq. (3.9) and Eq. (3.11) we get

$$-l - Q_{X2} + n = -\left[\frac{-3(u+d)}{2}\right] - \left[\frac{(u-d)}{2}\right] - (u+2d) = 0. \quad (3.18)$$

Therefore, the condition in Eq. (3.17) is automatically fulfilled. However, the Majorana mass term in Eq. (3.14) is gauge invariant if $2n + q_X = 0$, which implies from Eq. (3.11) that $q_X = 2u + 4d$. Using that $q_X = Q_{X1} - Q_{X2}$ from the term $\mu \Phi_1^\dagger \Phi_2 \Phi_s$ in the scalar potential Eq. (3.13), we get

$$Q_{X1} = \frac{5u}{2} + \frac{7d}{2}. \quad (3.19)$$

Two Higgs Doublet Models free from FCNI

Fields	u_R	d_R	Q_L	L_L	e_R	N_R	Φ_2	Φ_1
Charges	u	d	$\frac{(u+d)}{2}$	$\frac{-3(u+d)}{2}$	$-(2u+d)$	$-(u+2d)$	$\frac{(u-d)}{2}$	$\frac{(5u+7d)}{2}$
$U(1)_A$	1	-1	0	0	-1	1	1	-1
$U(1)_B$	-1	1	0	0	1	-1	-1	1
$U(1)_C$	1/2	-1	-1/4	3/4	0	3/2	3/4	-9/4
$U(1)_D$	1	0	1/2	-3/2	-2	-1	1/2	5/2
$U(1)_E$	0	1	1/2	-3/2	-1	-2	-1/2	7/2
$U(1)_F$	4/3	2/3	1	-3	-10/3	-8/3	1/3	17/3
$U(1)_G$	-1/3	2/3	1/6	-1/2	0	-1	-1/2	3/2
$U(1)_{B-L}$	1/3	1/3	1/3	-1	-1	-1	0	2
$U(1)_Y$	4/3	-2/3	1/3	-1	-2		1	$\neq Q_{X2}$
$U(1)_N$	0	0	0	0	0		0	$\neq Q_{X2}$

Table 3.1: The first block of models is capable of explaining neutrino masses and the absence of flavor changing interactions in the 2HDM type I, whereas the second block refers to models where only the flavor problem is addressed. The first block accounts for type I 2HDM in which right-handed neutrinos are introduced without spoiling the NFC criterion ($Q_{X1} \neq Q_{X2}$). This is possible when $u \neq -2d$ (see Eq. (3.9) and Eq. (3.19)). Conversely, the second block shows Type I 2HDM with $u = -2d$. To preserve the NFC criterion, right-handed neutrinos can not be introduced while at the same time Q_{X1} is kept as a free parameter. The $U(1)_N$ model leads to a fermiophobic Z' setup [3]. The $U(1)_Y$ yields a "right-handed-neutrino-phobic" Z' boson. The $U(1)_{B-L}$ is the well-known model in which the accidental baryon and lepton global symmetries are gauged. The $U(1)_{C,G}$ models feature null couplings to right-handed charged leptons, whereas the $U(1)_{A,B}$ models have vanishing couplings to left-handed leptons. The $U(1)_D$ has null couplings to right-handed down-quarks. The $U(1)_{E,F}$ models induce Z' interactions to all fermions, but have rather exotic $U(1)_X$ charges.

Now the Φ_1 charge under $U(1)_X$ is generally determined so that neutrino masses are generated. If we happened to choose $u = d = 1/3$, then $q_X = Q_{X1} = 2$, $Q_{X2} = 0$, and the $U(1)_X$ symmetry is identified to be $U(1)_{B-L}$ symmetry, which is spontaneously broken when Φ_s gets a vacuum expectation value. Various other choices of the charges are possible, see Table 3.1 for a list. From the list, the $U(1)_{B-L}$, $U(1)_N$ have been previously investigated in the literature in different contexts [58, 59, 60, 61, 62, 63, 64, 65, 66, 67, 68, 69].

The spontaneous symmetry breaking pattern from high to low energy goes as follows: (i) the vev v_s sets the scale which the $U(1)_X$ symmetry is broken, say TeV; (ii) then v_2 breaks the $SU(2)_L \otimes U(1)_Y$ group to Quantum Electrodynamics. As for the v_1 scale, there is some freedom, but it should be either comparable to v_2 or smaller, as long as $v^2 = v_2^2 + v_1^2$, where $v = 246$ GeV, since $m_W^2 = g^2 v^2 / 4$ (see Appendix A.2). In the regime in which $v_s > v_2 > v_1$ one needs to tune down the g_X coupling in order to have a Z' boson that is lighter than the SM Z , which is the regime we will focus in here.

In summary, the introduction of a new gauge symmetry with the charge assignments as exhibited in Table 3.1 leads to a compelling solution to the flavor problem in the Type I 2HDM, while successfully generating fermion masses. In particular, neutrino masses are explained via the seesaw mechanism. A similar reasoning, respecting the NFC criterion ($Q_{X1} \neq Q_{X2}$), can be applied to other types of 2HDM preventing them of FCNI. Nevertheless, the addition of extra chiral fermions is required to preserve them free of anomalies. Therefore, we focus here on 2HDM of Type I, see Table 3.1.

Now that we have reviewed the theoretical motivations for introducing an Abelian symmetry to the framework of the 2HDM we discuss in more detail the spectrum of the gauge bosons and neutral currents.

3.1.4 Physical Gauge Bosons and Neutral Currents

We emphasize that we are including all renormalizable terms allowed guided by gauge invariance. Therefore, kinetic mixing between the two Abelian groups is present. To understand the impact of kinetic mixing in the determination of the physical gauge boson we should start off writing down the kinetic terms of the gauge bosons. Note that throughout, the kinetic mixing parameter should fulfill $\epsilon \ll 1$ to be consistent with precision electroweak constraints. That said, the most general gauge Lagrangian associated to these groups is [70, 71, 72]:

$$\mathcal{L}_{\text{gauge}} = -\frac{1}{4}\hat{B}_{\mu\nu}\hat{B}^{\mu\nu} + \frac{\epsilon}{2\cos\theta_W}\hat{X}_{\mu\nu}\hat{B}^{\mu\nu} - \frac{1}{4}\hat{X}_{\mu\nu}\hat{X}^{\mu\nu}, \quad (3.20)$$

with the following covariant derivative

$$D_\mu = \partial_\mu + igT^a W_\mu^a + ig'\frac{Q_Y}{2}\hat{B}_\mu + ig_X\frac{Q_X}{2}\hat{X}_\mu. \quad (3.21)$$

Here T^a , W_μ^a and g are the generators, gauge bosons and gauge coupling constant of $SU(2)_L$ respectively; \hat{X}_μ and \hat{B}_μ the $U(1)_X$ and $U(1)_Y$ gauge bosons, g_X (Q_X) is

the $U(1)_X$ coupling constant (charge) and $g' (Q_Y)$ is $U(1)_Y$ coupling constant (charge). The hats means that they are non-physical, i.e. yet to be diagonalized, fields. As usual $\hat{B}_{\mu\nu} = \partial_\mu \hat{B}_\nu - \partial_\nu \hat{B}_\mu$ and $\hat{X}_{\mu\nu} = \partial_\mu \hat{X}_\nu - \partial_\nu \hat{X}_\mu$.

One first performs a $GL(2, R)$ transformation in order to make the kinetic terms canonical,

$$\begin{pmatrix} X_\mu \\ B_\mu \end{pmatrix} = \begin{pmatrix} \sqrt{1 - (\epsilon/\cos\theta_W)^2} & 0 \\ -\epsilon/\cos\theta_W & 1 \end{pmatrix} \begin{pmatrix} \hat{X}_\mu \\ \hat{B}_\mu \end{pmatrix}. \quad (3.22)$$

Therefore $\hat{B}_\mu = \eta_X X_\mu + B_\mu$, and $\hat{X}_\mu = X_\mu$, where

$$\eta_X = \frac{\epsilon/\cos\theta_W}{\sqrt{1 - (\epsilon/\cos\theta_W)^2}} \simeq \epsilon/\cos\theta_W, \quad (3.23)$$

since we are taking $\epsilon/\cos\theta_W \ll 1$ throughout. Thus, the covariant derivative now reads,

$$D_\mu = \partial_\mu + igT^a W_\mu^a + ig' \frac{Q_Y}{2} B_\mu + \frac{i}{2} \left(g_X Q_X + g' \frac{\epsilon}{\cos\theta_W} Q_Y \right) X_\mu. \quad (3.24)$$

which is from where we derive the gauge boson masses.

The general formalism of diagonalizing the neutral gauge boson mass matrix is delegated to Appendix A.2. The gauge boson mixing is parametrized in terms of ϵ_Z and ϵ , coming from the contributions of the second Higgs doublet and the kinetic mixing between the $U(1)$ groups respectively (see below and (A.37)). In the regime in which the new vector boson is much lighter than the SM Z boson, we get two mass eigenstates; one identified as the SM Z boson, labeled Z^0 with, $m_{Z^0}^2 = \frac{g^2 v^2}{4 \cos^2 \theta_W}$ and the Z' boson with,

$$m_{Z'}^2 = \frac{v_s^2}{4} g_X^2 q_X^2 + \frac{g_X^2 v^2 \cos^2 \beta \sin^2 \beta}{4} (Q_{X1} - Q_{X2})^2, \quad (3.25)$$

where q_X , Q_{X1} , Q_{X2} are the charges under $U(1)_X$ of the singlet scalar, Higgs doublets Φ_1 and Φ_2 respectively, $\tan \beta = v_2/v_1$, $v = \sqrt{v_1^2 + v_2^2} = 246$ GeV, v_s sets the $U(1)_X$ scale of spontaneous symmetry breaking, and g_X is the coupling constant of the $U(1)_X$ symmetry.

It will be useful to write the Z' mass in a compact form as (see Appendix A.3) by defining $\tan \beta_d = \frac{v_s}{v_1}$ as follows,

$$m_{Z'} = \frac{g_X v \cos^2 \beta}{\delta}, \quad (3.26)$$

where

$$\delta = \frac{2 \cos \beta \cos \beta_d}{\sqrt{q_X^2 + \cos^2 \beta_d (\sin^2 \beta (Q_{X1} - Q_{X2})^2 - q_X^2)}}. \quad (3.27)$$

The mixing angle for the diagonalization of the gauge bosons, ξ , in this general setup can be parametrized as follows (see (A.34)),

$$\xi \equiv \epsilon_Z + \epsilon \tan \theta_W, \quad (3.28)$$

where,

$$\epsilon_Z \equiv \frac{g_X}{g_Z} (Q_{X1} \cos^2 \beta + Q_{X2} \sin^2 \beta). \quad (3.29)$$

For instance, in the $B - L$ model one has,

$$\epsilon_Z = 2 \frac{g_X}{g} \cos^2 \beta, \quad (3.30)$$

and with the use of Eq. (3.26) we get,

$$\delta = \frac{m_Z}{m_{Z'}} \epsilon_Z, \quad (3.31)$$

which agrees with [62], validating our findings.

Having obtained the physical fields we can rewrite the neutral current Lagrangian (see Appendices A.2 and A.4):

$$\begin{aligned} \mathcal{L}_{\text{NC}} = & -e J_{\text{em}}^\mu A_\mu - \frac{g}{2 \cos \theta_W} J_{\text{NC}}^\mu Z_\mu - \left(\epsilon e J_{\text{em}}^\mu + \epsilon_Z \frac{g}{2 \cos \theta_W} J_{\text{NC}}^\mu \right) Z'_\mu \\ & + \frac{1}{4} g_X \sin \xi \left[(Q_{Xf}^R + Q_{Xf}^L) \bar{\psi}_f \gamma^\mu \psi_f + (Q_{Xf}^R - Q_{Xf}^L) \bar{\psi}_f \gamma^\mu \gamma_5 \psi_f \right] Z_\mu \\ & - \frac{1}{4} g_X \cos \xi \left[(Q_{Xf}^R + Q_{Xf}^L) \bar{\psi}_f \gamma^\mu \psi_f - (Q_{Xf}^L - Q_{Xf}^R) \bar{\psi}_f \gamma^\mu \gamma_5 \psi_f \right] Z'_\mu, \end{aligned} \quad (3.32)$$

where Q_X^R (Q_X^L) are the left-handed (right-handed) fermion charges under $U(1)_X$. We emphasize that Eq. (3.32) is the general neutral current for 2HDM augmented by a $U(1)_X$ gauge symmetry.

Again, it is important to validate our results with the existing literature. For instance, in the $U(1)_{B-L}$ model we get

$$\begin{aligned} \mathcal{L}_{\text{NC}} = & -e J_{\text{em}}^\mu A_\mu - \frac{g}{2 \cos \theta_W} J_{\text{NC}}^\mu Z_\mu - \left(\epsilon e J_{\text{em}}^\mu + \epsilon_Z \frac{g}{2 \cos \theta_W} J_{\text{NC}}^\mu \right) Z'_\mu \\ & - \frac{g_X}{2} Q_{Xf} [\bar{\psi}_f \gamma^\mu \psi_f] Z'_\mu, \end{aligned} \quad (3.33)$$

where $Q_{Xf} = -1$ for charged leptons and $Q_{Xf} = 1/3$ for quarks, with g_X and ϵ_Z related by Eq. (3.30), in agreement with [73].

Now that we have obtained the neutral current for a generic $U(1)_X$ model in the context of the 2HDM we will address the relevant constraints these $U(1)_X$ models are subject to.

3.1.5 Z' Decays

We have introduced a multitude of Abelian gauge groups in the context of the 2HDM that address two major issues in the original 2HDM framework, namely the absence of neutrino masses and the presence of flavor changing interactions. Abelian groups generally give rise to neutral gauge bosons which are subject to a rich phenomenology that we plan to explore in what follows. Before doing so, some general remarks are in order:

- (i) The kinetic mixing (ϵ) as well as the mass mixing (ϵ_Z) parameters are required to be smaller than 10^{-3} to be consistent with a variety of constraints that we will discuss.
- (ii) We will focus on the regime $m_{Z'} \ll m_Z$, say $m_{Z'} = 1 \text{ MeV} - 10 \text{ GeV}$. Some comments on different regimes will nevertheless be made whenever relevant.
- (iii) A light Z' can be achieved at the expense of tuning the gauge coupling g_X .
- (iv) The phenomenology of our models will be dictated by either the kinetic mixing or the mass-mixing terms.

That said, some of the constraints we will investigate are based on dark photon searches. Notice that our models are a bit different than the dark photon model that has only the kinetic mixing term, due to the presence of mass-mixing and the non-vanishing $U(1)_X$ charges of the SM fermions. We remind the reader that only the models that simultaneously explain neutrino masses and free the 2HDM from flavor changing interactions are of interest throughout this work, as displayed in the first block of Table 3.1. With this in mind we discuss the Z' decays in each one of the models.

- It is important to first mention the dark photon model. In such models the coupling of the dark photon A' with SM fermions f goes as $\bar{f}\gamma^\mu f A'_\mu$. The corresponding branching ratios are shown in Fig. 3.2. It is important to have a clear picture of the dark photon model because some of the bounds discussed in this work have the dark photon model as benchmark as we shall see when we address neutrino-electron scattering and low energy accelerator constraints.
- In the $U(1)_A$ model, the charged leptons and light quarks charges under $U(1)_A$ are the same but due to color multiplicity the Z' decays mostly into light quarks as

shown in Fig. 3.2. As for the $U(1)_B$ model, the results are same. Notice that the label B has nothing to do with baryon number. No decays into active neutrinos exist since the lepton doublet is uncharged under the new gauge group.

- In the $U(1)_C$ model, the branching ratio into neutrinos is more relevant in comparison with previous models since now the lepton doublet has charge $3/4$ under the new gauge group. However, decays into light quarks are still the most relevant. The $U(1)_G$ model has a similar behavior.
- In the $U(1)_D$ model, the branching ratio into leptons prevails. A similar feature happens in the $U(1)_{B-L}$ model, where B and L account for the baryon and lepton numbers. In the former, the branching ratios into charged fermions and neutrinos are very similar, but as soon the decay into muons becomes kinematically accessible the branching ratio into charged leptons increases. In the latter, decays into neutrinos are always dominant in the mass region of interest, as a straightforward consequence of the baryon and lepton quantum numbers of the fermions.
- In the $U(1)_E$ model, decays into neutrinos are dominant until the Z' mass approximates the strange quark and muon kinematic thresholds.

Now that we have highlighted the properties of the Z' gauge boson for each $U(1)_X$ model we will discuss a variety of constraints going from mesons decays to low energy accelerators.

3.2 Phenomenological Constraints

In this section we will span over the existing limits on the $U(1)_X$ models proposed previously. Our main goal is to estimate limits on the parameter space of these models and assess how relevant they are. A more dedicated study will be conducted elsewhere. We start with meson decays.

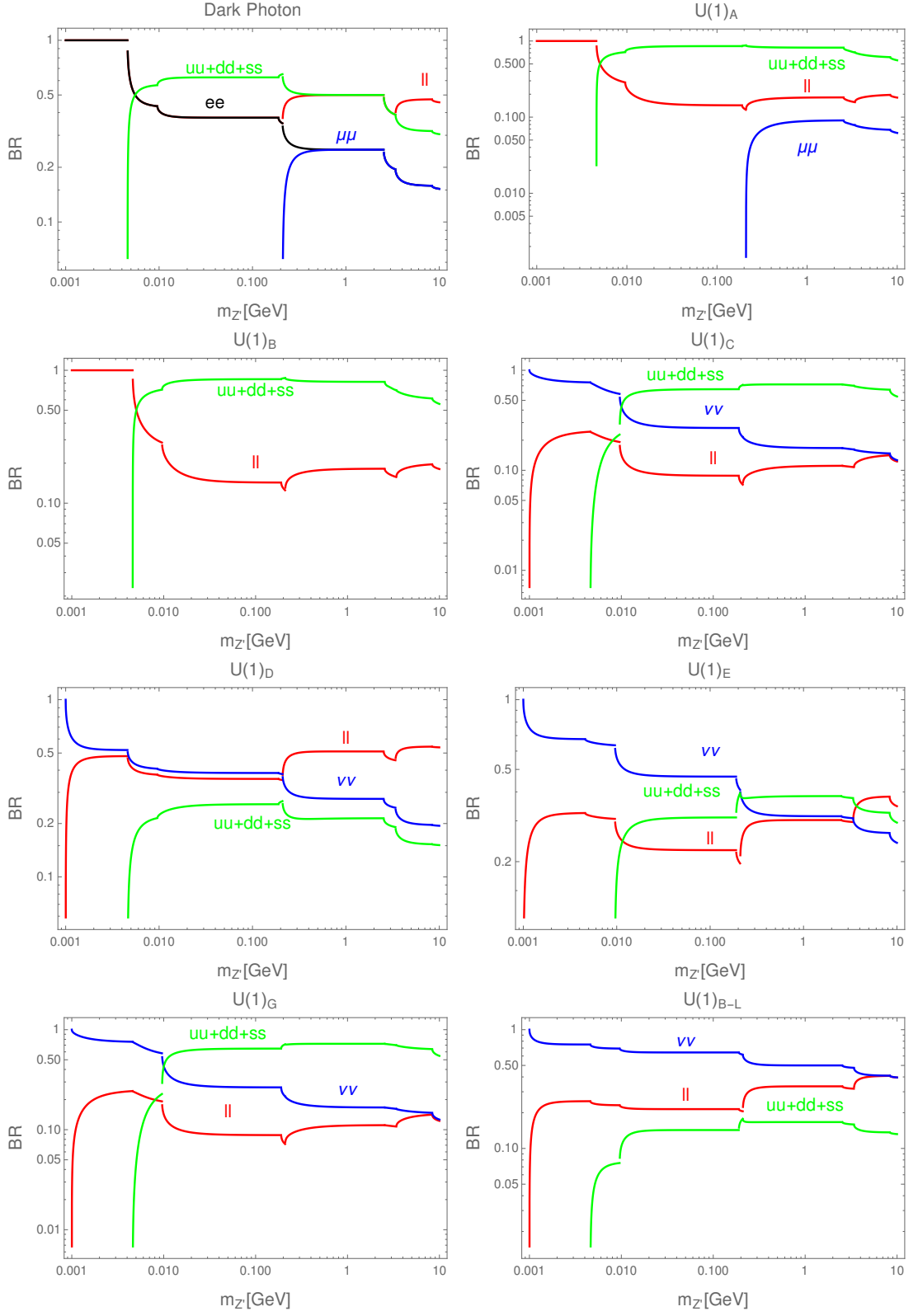


Figure 3.2: Branching ratios as a function of the Z' mass for several $U(1)_X$ models under study.

3.2.1 Meson Decays

Rare K Decays

The main decays modes of the charged Kaon are $\mu\nu_\mu$, $\pi^+\pi^0$ and $\pi^+\pi^+\pi^-$ with branching ratios of 64%, 21% and 6% respectively. Searches for rare meson decays such as $K^+ \rightarrow \pi^+ l^+ l^-$ have also been performed [74, 75], which led to the experimental constraints [76],

$$\text{BR}(K^+ \rightarrow \pi^+ e^+ e^-)_{\text{exp}} = (3.00 \pm 0.09) \times 10^{-7}, \quad (3.34)$$

$$\text{BR}(K^+ \rightarrow \pi^+ \mu^+ \mu^-)_{\text{exp}} = (9.4 \pm 0.6) \times 10^{-8}, \quad (3.35)$$

$$\text{BR}(K^+ \rightarrow \pi^+ \nu \bar{\nu})_{\text{exp}} = (1.7 \pm 1.1) \times 10^{-10}. \quad (3.36)$$

In a Two Higgs Doublet Model with $Z - Z'$ mass mixing the branching ratio of $K^+ \rightarrow \pi^+ Z'$ is estimated to be [77],

$$\text{BR}(K^+ \rightarrow \pi^+ Z') \simeq 4 \times 10^{-4} \delta^2, \quad (3.37)$$

where $\delta = \epsilon_Z m_Z / m_{Z'}$ (see Appendix A.3). Comparing Eq. (3.37) with Eqs. (3.34)-(3.36) we conservatively find that,

$$\delta \lesssim \frac{2 \times 10^{-2}}{\sqrt{\text{BR}(Z' \rightarrow l^+ l^-)}}, \quad (3.38)$$

$$\delta \lesssim \frac{7 \times 10^{-4}}{\sqrt{\text{BR}(Z' \rightarrow \text{missing energy})}}. \quad (3.39)$$

These bounds should be used with care since they are not applicable to any Z' mass. For instance, the bound obtained in Eq. (3.34) was obtained with a hard cut in the dilepton invariant mass, namely $m_{ee} > 140$ MeV [75]. Thus this limit is valid for $m_{Z'} > 140$ MeV.

In the $U(1)_{B-L}$ model, for instance, for $m'_Z < 2m_\mu$, the Z' decays with $\sim 75\%$ branching ratio into neutrinos and therefore Eq. (3.39) should be used, giving stronger constraints. In the $U(1)_N$ model, on other hand, the situation strongly depends on the ratio ϵ/ϵ_Z . In particular, for $\epsilon/\epsilon_Z \gg 1$, the Z' decays mostly into charged leptons with Eq. (3.38) yielding stronger limits, conversely for $\epsilon/\epsilon_Z < 1$, Eq. (3.39) is more restrictive in agreement with [59]. Either way it is clear that rare kaon decays introduce an interesting pathway to probe new physics, specially low mass Z' gauge bosons [78, 79, 80, 81, 82].

<i>K</i> Decays
$\delta \lesssim 2 \times 10^{-2} / \sqrt{BR(Z' \rightarrow l^+ l^-)}$
$\delta \lesssim 7 \times 10^{-4} / \sqrt{BR(Z' \rightarrow \text{missing energy})}$
<i>B</i> Decays
$\delta \lesssim 2 \times 10^{-3} / \sqrt{BR(Z' \rightarrow l^+ l^-)}$
$\delta \lesssim 1.2 \times 10^{-2} / \sqrt{BR(Z' \rightarrow \text{missing energy})}$

Table 3.2: Summary of constraints on the model from meson decays.

Rare *B* Decays

Similar to the *K* mesons discussed previously rare *B* decays offer a promising environment to probe new physics. In particular, the charged *B* meson with mass of 5.3 GeV, comprised of $u\bar{b}$, may possibly decay into $K^+ l^+ l^-$ [83, 84, 85] or $K^+ \nu \bar{\nu}$ [86, 87]. Such decays have been measured to be [76],

$$BR(B^+ \rightarrow K^+ \bar{l}^+ l^-)_{\text{exp}} < 4.5 \times 10^{-7}, \quad (3.40)$$

$$BR(B^+ \rightarrow K^+ \bar{\nu} \nu)_{\text{exp}} < 1.6 \times 10^{-5}. \quad (3.41)$$

Having in mind that the mass mixing in the 2HDM induces [77, 84, 59],

$$BR(B \rightarrow K Z') \simeq 0.1 \delta^2, \quad (3.42)$$

implying that,

$$\delta \lesssim \frac{2 \times 10^{-3}}{\sqrt{BR(Z' \rightarrow l^+ l^-)}}, \quad (3.43)$$

$$\delta \lesssim \frac{1.2 \times 10^{-2}}{\sqrt{BR(Z' \rightarrow \text{missing energy})}}. \quad (3.44)$$

Comparing Eqs. (3.43)–(3.44) with Eqs. (3.38)–(3.39) we can see the rare *B* decays give rise to more stringent limits on the parameter δ when the Z' decays mostly into charged leptons. We highlight that the large factor in Eq. (3.42) is result of the presence of the top quark in the Feynman diagram responsible for the $b \rightarrow s$ conversion, and consequently the $B \rightarrow K Z'$ decay.

As for Z' decays into neutrino pairs, then precise measurements on Kaon decays offer the leading constraints. The constraints from meson decays are summarized in Table 3.2. We will now move to Higgs physics.

vertex	coupling constant
$H t\bar{t}, H b\bar{b}, H \tau\bar{\tau}$	$\frac{\sin \alpha}{\sin \beta}$
$H WW, H ZZ$	$\cos(\beta - \alpha)$
$h t\bar{t}, h b\bar{b}, h \tau\bar{\tau}$	$\frac{\cos \alpha}{\sin \beta}$
$h WW, h ZZ$	$\sin(\beta - \alpha)$

Table 3.3: Higgs and light scalar interactions in the 2HDM type I. The coupling constants in the second column are the overall multiplicative factor in front of the SM couplings. In other words, when $\alpha = \beta$ the Higgs in the 2HDM type I interacts with fermions and gauge bosons identically to the SM Higgs.

3.2.2 Higgs Physics

Higgs Properties

Our models are comprised of two Higgs doublets and a singlet scalar. In the limit in which the scalar doublets do not mix with the singlet, i.e. the regime in which the parameters μ_1, μ_2, μ in the potential (3.13) are suppressed, one finds,

$$\begin{aligned}
m_s^2 &= \lambda_s v_s^2, \\
m_h^2 &= \frac{1}{2} \left(\lambda_1 v_1^2 + \lambda_2 v_2^2 - \sqrt{(\lambda_1 v_1^2 - \lambda_2 v_2^2)^2 + 4(\lambda_3 + \lambda_4)^2 v_1^2 v_2^2} \right), \\
m_H^2 &= \frac{1}{2} \left(\lambda_1 v_1^2 + \lambda_2 v_2^2 + \sqrt{(\lambda_1 v_1^2 - \lambda_2 v_2^2)^2 + 4(\lambda_3 + \lambda_4)^2 v_1^2 v_2^2} \right),
\end{aligned} \tag{3.45}$$

and the H - h mixing is given by,

$$\begin{pmatrix} H \\ h \end{pmatrix} = \begin{pmatrix} \cos \alpha & \sin \alpha \\ -\sin \alpha & \cos \alpha \end{pmatrix} \begin{pmatrix} \rho_1 \\ \rho_2 \end{pmatrix} \tag{3.46}$$

with

$$\tan 2\alpha = \frac{2(\lambda_3 + \lambda_4)v_1 v_2}{\lambda_1 v_1^2 - \lambda_2 v_2^2}. \tag{3.47}$$

We are considering here that the scalar H is the SM-like Higgs (notice from the Eqs. (3.45) that H is always heavier than h). Their interaction strengths with SM particles are summarized in Table 3.3. The coupling constants in the second column of the table are multiplicative factors appearing in front of the SM couplings. In other words, when $\alpha = \beta$ the Higgs in the 2HDM type I interacts with fermions and gauge bosons identically to the SM Higgs (the alignment limit). Furthermore, close to the alignment $\beta \sim \alpha$, the $h t\bar{t}, h b\bar{b}$ and $h \tau\bar{\tau}$ couplings are governed by $\cot \beta$, whereas the $h WW, h ZZ$ interactions are dwindled.

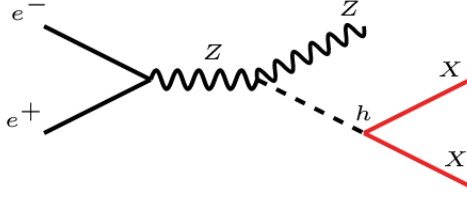


Figure 3.3: Higgs associated production at LEP followed by its invisible decay, illustrated by $h \rightarrow XX$.

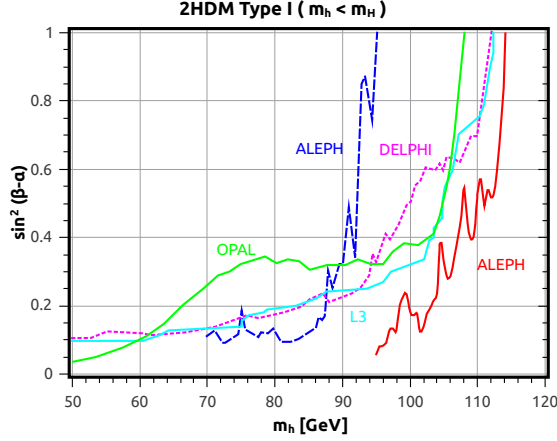


Figure 3.4: Upper limits from invisible Higgs decay searches translated to the light Higgs mass m_h .

Higgs Associated Production

Several experiments have searched for scalars with similar properties to the SM Higgs at LEP. They were particularly focused on the associated production with the Z boson, with the scalar decaying either into fermions or invisibly as displayed in Fig. 3.3. The light Higgs in the models under study, h , decays at tree-level into $Z'Z'$. Since the LEP searches did not cover fermions with very small invariant mass, i.e. stemming from a light Z' , one should use the results from the invisible decay search. That said, the Zh associated production search resulted into limits on the product of the production cross section strength and branching ratio, i.e. $\sigma(Zh)/\sigma(ZH_{SM})BR(h \rightarrow \text{inv})$.

Assuming $BR(h \rightarrow \text{inv}) \simeq 1$ throughout, one can reinterpret the results from [88, 89, 90] for the light Higgs h , having in mind that the hZZ coupling goes with $\sin(\beta - \alpha)$, to place a bound on $\sin^2(\beta - \alpha)$ as a function of the scalar mass as shown in the Fig. 3.4 [62]. From Fig. 3.4, one can conservatively conclude that $\sin^2(\beta - \alpha) \lesssim 0.1$, $\cos^2(\beta - \alpha) > 0.9$, independent of $\tan \beta$. Weaker limits are applicable depending on the light Higgs mass.

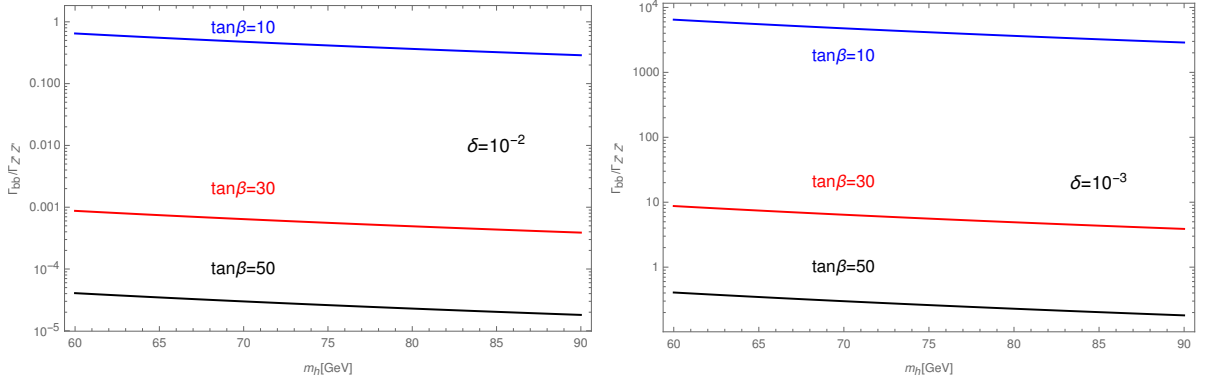


Figure 3.5: Ratio of the light Higgs decay width for different values of $\tan \beta$. In the left panel we set $\delta = 10^{-2}$, while in the right one $\delta = 10^{-3}$. One can see that if the product $\delta \tan \beta$ is sufficiently large, the light Higgs decays dominantly into $Z'Z'$. In this regime, the limits presented in the Fig. 3.4 can be directly applied.

However, the limit presented in Fig. 3.4 may be not robust because it relies on the assumption that $BR(h \rightarrow \text{inv}) \simeq 1$. A simple check can be done by comparing the decay into $Z'Z'$ with the usually dominant $b\bar{b}$ mode that lead to the following decay rates,

$$\Gamma_{h \rightarrow Z'Z'} = \frac{g_Z^2}{128\pi} \frac{m_h^3}{m_Z^2} (\delta \tan \beta)^4 \left(\frac{\cos^3 \beta \cos \alpha - \sin^3 \beta \sin \alpha}{\cos \beta \sin \beta} \right)^2, \quad (3.48)$$

$$\Gamma_{h \rightarrow b\bar{b}} = \frac{3m_b^2 m_h}{8\pi v^2} \left(\frac{\cos \alpha}{\sin \beta} \right)^2. \quad (3.49)$$

We thus conclude that the ratio reads

$$\frac{\Gamma_{h \rightarrow b\bar{b}}}{\Gamma_{h \rightarrow Z'Z'}} = \frac{12m_b^2}{m_h^2} \frac{1}{(\delta \tan \beta)^4} \left(\frac{\cos \beta \sin \beta}{\cos^3 \beta \cos \alpha - \sin^3 \beta \sin \alpha} \right)^2 \left(\frac{\cos \alpha}{\sin \beta} \right)^2, \quad (3.50)$$

which is displayed in Fig. 3.5, where we plot this ratio for different values of $\tan \beta$ as a function of the light Higgs mass. In the left panel we fix $\delta = 10^{-2}$, whereas in the right one $\delta = 10^{-3}$. One can see that if the product $\delta \tan \beta$ is sufficiently large, the light Higgs decays dominantly into $Z'Z'$, as predicted by Eq. (3.49), justifying our procedure in the derivation of Fig. 3.4. A more detailed study regarding the light Higgs properties has been conducted in the Ref. [62]. In this work, we are limited to discuss all relevant limits to the $U(1)_X$ models introduced above.

Higgs Decays

After the Higgs discovery the LHC has turned into a Higgs factory and today we have at our disposal much better measurements of the Higgs branching ratio (see Table

Higgs decay channel	branching ratio	error
$b\bar{b}$	5.84×10^{-1}	1.5%
$c\bar{c}$	2.89×10^{-2}	6.5%
$g g$	8.18×10^{-2}	4.5%
ZZ^*	2.62×10^{-2}	2%
WW^*	2.14×10^{-1}	2%
$\tau^+\tau^-$	6.27×10^{-2}	2%
$\mu^+\mu^-$	2.18×10^{-4}	2%
$\gamma\gamma$	2.27×10^{-3}	2.6%
$Z\gamma$	1.5×10^{-3}	6.7%
$ZZ^* \rightarrow 4\ell$	2.745×10^{-4}	2%
$ZZ^* \rightarrow 2\ell 2\nu$	1.05×10^{-4}	2%

Table 3.4: List of experimental limits on the branching ratio of the SM Higgs. The channel $ZZ^* \rightarrow 2\ell 2\nu$ was obtained using the relation $BR(H \rightarrow ZZ^* \rightarrow 2\ell 2\nu) = BR(H \rightarrow ZZ^*)BR(Z \rightarrow 2\ell)BR(Z \rightarrow 2\nu)^2$.

3.4). Since we are mostly interested in the regime in which the Z' is light enough for the Higgs to decay into, some channels are of great interest for our purposes, namely $H \rightarrow ZZ^* \rightarrow 4\ell$ and $H \rightarrow ZZ^* \rightarrow 2\ell 2\nu$. In the context of 2HDM it has been shown that in the limit in which the Z' gauge boson is much lighter than the Z boson we get [62],

$$\Gamma(H \rightarrow ZZ') = \frac{g_Z^2}{64\pi} \frac{(m_H^2 - m_Z^2)^3}{m_H^3 m_Z^2} \delta^2 \tan^2 \beta \sin^2(\beta - \alpha), \quad (3.51)$$

and

$$\Gamma(H \rightarrow Z'Z') = \frac{g_Z^2}{128\pi} \frac{m_H^3}{m_Z^2} \delta^4 \tan^4 \beta \left(\frac{\cos^3 \beta \sin \alpha + \sin^3 \beta \cos \alpha}{\cos \beta \sin \beta} \right)^2. \quad (3.52)$$

One can now use precision measurements on Higgs properties summarized in Table 3.4 to constrain the model. We will focus on the decay into ZZ' since δ is supposed to be small to obey meson decay constraints¹. Enforcing the branching ratio $\Gamma(H \rightarrow ZZ' \rightarrow 4\ell)/\Gamma_{\text{total}}$ with $\Gamma_{\text{total}} = 4.1 \text{ MeV}$, to match the measured value within the error bars as indicated in the Table 3.4 we obtain,

$$\delta^2 \leq \frac{4.6 \times 10^{-6}}{BR(Z' \rightarrow l^+ l^-) \sin^2(\beta - \alpha) \tan^2 \beta}. \quad (3.53)$$

¹In some regions of the parameter space with sufficiently large $\tan \beta$ the decay $Z'Z'$ might become relevant as discussed in [62].

To have an idea on how competitive this constraint is compared to previous discussions we shall plug in some numbers. Taking $\sin^2(\beta - \alpha) = 0.01$ and $\tan \beta = 10$, we get

$$\delta \leq \frac{0.002}{\sqrt{BR(Z' \rightarrow l^+ l^-)}}, \quad (3.54)$$

which is comparable to the bound stemming from Kaon decays. We emphasize that this bound is applicable to all $U(1)_X$ models under study here. One need now to simply choose a model and substitute the respective branching ratio into charged leptons as provided by Fig. 3.2.

3.2.3 Z Decays

In the models we are investigating both the light Higgs h and the Z' can be much lighter than the Z , kinematically allowing the decay $Z \rightarrow hZ'$. In the limit that the Z' mass is very small compared to the Z mass we find,

$$\Gamma(Z \rightarrow hZ') = (\mathcal{C}_{h-Z-Z'})^2 \frac{m_Z}{64\pi m_{Z'}^2} \left(1 - \frac{m_h^2}{m_Z^2}\right)^3. \quad (3.55)$$

where (see Appendix A.6)

$$\mathcal{C}_{h-Z-Z'} = g_Z g_X v \cos \beta \sin \beta \cos(\beta - \alpha). \quad (3.56)$$

Knowing that we can write down the Z' mass as a function of δ , as derived in Appendix A.3, we get

$$\Gamma(Z \rightarrow hZ') = \frac{g_Z^2 m_Z}{64\pi} (\delta \tan \beta)^2 \cos^2(\beta - \alpha) \left(1 - \frac{m_h^2}{m_Z^2}\right)^3. \quad (3.57)$$

We highlight that the exact expression for this decay depends on the Φ_1 charge under $U(1)_X$. Eq. (3.57) is valid for the $B - L$ model for instance, and it agrees with [62]. Anyways, knowing that the total decay width of the Z is $\Gamma_Z = 2.4952 \pm 0.0023$ GeV [91], one can conservatively enforce the new physics decay to be within the error bars of the measured value. One can use this to place a lower mass limit on m_h as a function of $\delta \tan \beta$ taking $\cos^2(\beta - \alpha) \sim 0.9 - 1$ as shown in Fig. 3.6.

One can conclude that for sufficiently small $\delta \tan \beta$ the bounds from LEP substantially weaken. We have seen in the previous sections that $\delta < 10^{-2} - 10^{-3}$, and since we are interested in the limit of large $\tan \beta$, say $\tan \beta \sim 10$, then the light Higgs in the $U(1)_X$ models under study can be arbitrarily light as long as a fine-tuning in Eq. (3.45) is

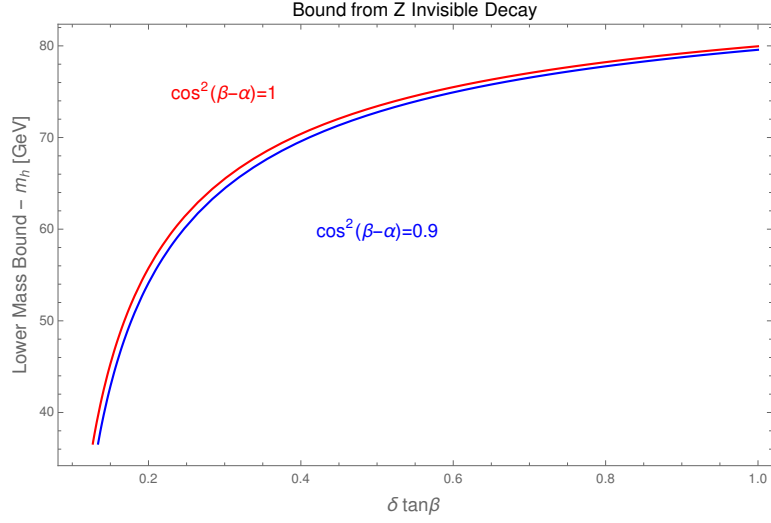


Figure 3.6: Lower mass bound on the light Higgs stemming from the LEP precision measurement on the Z width.

invoked. It has been noted that if $\sin \alpha$ is different from unity, m_h cannot be lighter than $m_H/2$, otherwise the heavy Higgs, i.e. the SM Higgs, would decay dominantly into hh in strong disagreement with data [92]. Thus this very light Higgs scenario is only possible in the limit $\sin \alpha = 1$.

3.2.4 Charged Higgs Searches

In 2HDM type I, the coupling of the charged Higgs to fermions is suppressed by a factor of $\tan \beta$. In the models under study, the charged Higgs mass is found to be $m_{H^\pm}^2 = \frac{\lambda_4}{2} v^2$. This mass determines which final state is dominant in its decays [93, 94, 8, 95, 96]. In this work we will adopt $\lambda_4 \sim 1$, and in this case the hW , HW and $t\bar{b}$ decays are the dominant ones and are found to be described by [97, 98]

$$\Gamma(H^\pm \rightarrow hW^\pm) = \frac{\cos^2(\beta - \alpha)}{16\pi v^2} \frac{1}{m_{H^\pm}^3} \lambda^{3/2}(m_{H^\pm}^2, m_h^2, m_W^2) \quad (3.58)$$

with $\lambda(x, y, z) \equiv x^2 + y^2 + z^2 - 2xy - 2yz - 2zx$,

$$\Gamma(H^\pm \rightarrow HW^\pm) = \frac{\sin^2(\beta - \alpha)}{16\pi v^2} \frac{1}{m_{H^\pm}^3} \lambda^{3/2}(m_{H^\pm}^2, m_H^2, m_W^2), \quad (3.59)$$

and the decay width into $t\bar{b}$ is given by

$$\Gamma(H^\pm \rightarrow t\bar{b}) \simeq \frac{3m_{H^\pm}}{8\pi v^2} \frac{m_t^2}{\tan^2 \beta} \left(1 - \frac{m_t^2}{m_{H^\pm}^2}\right)^2 \quad (3.60)$$

where we have taken $V_{tb} = 1$.

Experiment	$\langle Q \rangle$	$\sin^2 \theta_W(m_Z)$	Bound on dark Z (90% CL)
Cesium APV	2.4 MeV	0.2313(16)	$\varepsilon^2 < \frac{39 \times 10^{-6}}{\delta^2} \left(\frac{m_{Z'}}{m_Z} \right)^2 \frac{1}{K(m_{Z'})^2}$
E158 (SLAC)	160 MeV	0.2329(13)	$\varepsilon^2 < \frac{62 \times 10^{-6}}{\delta^2} \left(\frac{(160 \text{ MeV})^2 + m_{Z'}^2}{m_Z m_{Z'}} \right)^2$
Qweak (JLAB)	170 MeV	± 0.0007	$\varepsilon^2 < \frac{7.4 \times 10^{-6}}{\delta^2} \left(\frac{(170 \text{ MeV})^2 + m_{Z'}^2}{m_Z m_{Z'}} \right)^2$
Moller (JLAB)	75 MeV	± 0.00029	$\varepsilon^2 < \frac{1.3 \times 10^{-6}}{\delta^2} \left(\frac{(75 \text{ MeV})^2 + m_{Z'}^2}{m_Z m_{Z'}} \right)^2$
MESA (Mainz)	50 MeV	± 0.00037	$\varepsilon^2 < \frac{2.1 \times 10^{-6}}{\delta^2} \left(\frac{(50 \text{ MeV})^2 + m_{Z'}^2}{m_Z m_{Z'}} \right)^2$

Table 3.5: Existing (Cesium, E158) and projected constraints on the kinetic mixing parameter as a function of the mass mixing parameter δ and the Z' mass. All masses are in MeV, hence $m_Z = 91000$ MeV.

The constraints coming from charged Higgs bosons searches are not very restrictive and in the limit of large $\tan \beta$ as assumed in this work, charged Higgs searches do not yield competitive limits and thus ignored henceforth. For a detailed discussion see [99].

3.2.5 Atomic Parity Violation

The search for Atomic Parity Violation (APV) provides a promising pathway to probe new physics, especially the existence of neutral light bosons. It is known that for $m_{Z'} \sim 0.1 - 1$ GeV, existing limits exclude $\epsilon^2 > 10^{-6}$ [65]. As we shall see in what follows, APV offers an orthogonal and complementary probe for new physics depending on the parameter δ .

Anyways, this parity violation is two fold: (i) it can be induced via the non-zero SM fermion charges under the $U(1)_X$ symmetry; (ii) it can arise via the $Z' - Z$ mass mixing. That said, let us first review how one can constrain $U(1)_X$ models via atomic parity violation. Using effective field theory APV is parametrized as [100],

$$\begin{aligned}
-\mathcal{L}_{\text{eff}} = & \frac{1}{4} \frac{g^2 + g'^2}{m_Z^2} \bar{e} \gamma_\mu \gamma_5 e \left[\left(\frac{1}{4} - \frac{2}{3} \sin^2 \theta_W \right) \bar{u} \gamma^\mu u + \left(-\frac{1}{4} + \frac{1}{3} \sin^2 \theta_W \right) \bar{d} \gamma^\mu d \right] \\
& - \frac{f_{A_e}}{m_{Z'}^2} \bar{e} \gamma_\mu \gamma_5 e [f_{V_u} \bar{u} \gamma^\mu u + f_{V_d} \bar{d} \gamma^\mu d].
\end{aligned} \tag{3.61}$$

Here f_{xy} are effective couplings to be derived below for the different models.

The Lagrangian involves the product of the Z and Z' axial vector currents of the electron with the vector neutral currents of the quarks. Remembering that the vector part of the Z weak neutral current is associated with the Z weak charge, we get from Eq.

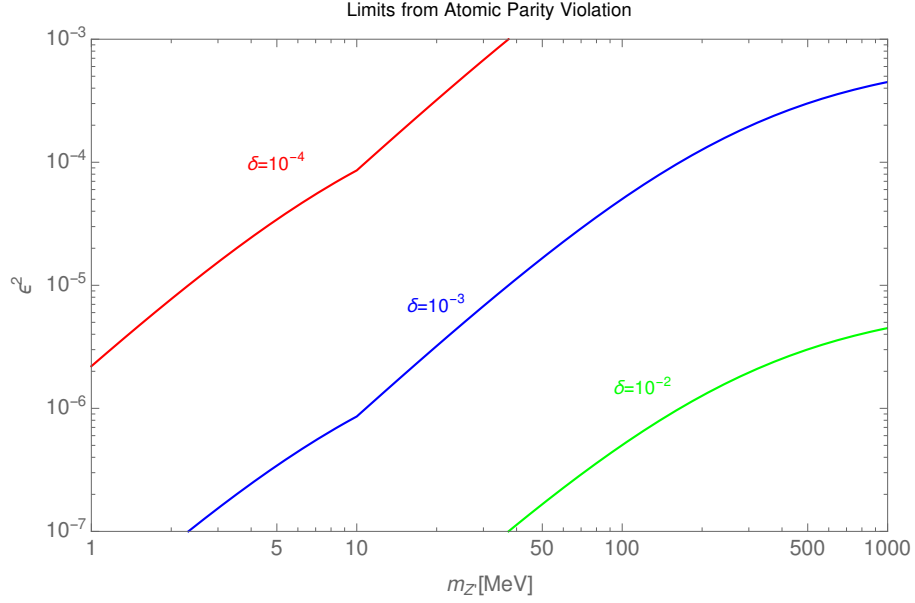


Figure 3.7: Upper limits on the kinetic mixing as a function of the Z' mass for different values of the mass mixing parameter δ according to the first line of Table 3.5.

(3.61)

$$\begin{aligned} Q_Z &= (2Z + N) \left(\frac{1}{4} - \frac{2}{3} \sin^2 \theta_W \right) + (Z + 2N) \left(-\frac{1}{4} + \frac{1}{3} \sin^2 \theta_W \right), \\ &= \frac{1}{4} [Z(1 - 4 \sin^2 \theta_W) - N] = \frac{1}{4} Q_W^{\text{SM}}(Z, N). \end{aligned} \quad (3.62)$$

The quantity Q_W^{SM} is usually referred to as weak charge of a nucleus of Z protons and N neutrons. Similarly, the quark contribution to the charge $Q_{Z'}$ associated with the vector part of the Z' current is found to be

$$Q_{Z'} = (2Z + N)f_{V_u} + (Z + 2N)f_{V_d} \quad (3.63)$$

$$= (2f_{V_u} + f_{V_d})Z + (f_{V_u} + 2f_{V_d})N. \quad (3.64)$$

The effective Lagrangian Eq. (3.61) implies the following parity violation Hamiltonian density for the electron field in the vicinity of the nucleus²

$$\begin{aligned} \mathcal{H}_{\text{eff}} &= e^\dagger(\vec{r}) \gamma_5 e(\vec{r}) \left[\frac{g^2 + g'^2}{4m_Z^2} \frac{1}{4} Q_W^{\text{SM}} - \frac{g^2 + g'^2}{4m_{Z'}^2} \epsilon_Z^2 \left(1 - \frac{l - e}{Q_{X1} \cos^2 \beta + Q_{X2} \sin^2 \beta} \right) Q_{Z'} \right] \delta(\vec{r}) \\ &= e^\dagger(\vec{r}) \gamma_5 e(\vec{r}) \frac{G_F}{2\sqrt{2}} Q_W^{\text{eff}}(Z, N) \delta(\vec{r}), \end{aligned} \quad (3.65)$$

² $\delta(\vec{r})$ can be replaced by the nuclear density $\rho(\vec{r})$ to take into account finite size effects of the nucleus. For a more detailed discussion about APV see reference [100].

where

$$Q_W^{\text{eff}} = Q_W^{\text{SM}} - 4\delta^2 Q_{Z'} \left(1 - \frac{l - e}{Q_{X1} \cos^2 \beta + Q_{X2} \sin^2 \beta} \right), \quad (3.66)$$

using that $\epsilon_Z = \frac{m_{Z'}}{m_Z} \delta$. We remind the reader that l and e are the charges of the left-handed and right-handed electron under $U(1)_X$.

Notice that the effective weak charge of the nucleus Q_W^{eff} includes in addition to the standard contribution Q_W^{SM} an additional Z' contribution. In order to know Q_W^{eff} , it is necessary to calculate $Q_{Z'}$. To do so, we need to specify from Eq. (3.32) f_{V_u} and f_{V_d} associated to the Z' boson,

$$f_{V_u} = \left[\frac{1}{4} - \frac{2}{3} \sin^2 \theta_W \left(1 - \frac{\epsilon \cos \theta_W}{\epsilon_Z \sin \theta_W} \right) + \frac{1}{4} \frac{q + u}{Q_{X1} \cos^2 \beta + Q_{X2} \sin^2 \beta} \right], \quad (3.67)$$

$$f_{V_d} = \left[-\frac{1}{4} + \frac{1}{3} \sin^2 \theta_W \left(1 - \frac{\epsilon \cos \theta_W}{\epsilon_Z \sin \theta_W} \right) + \frac{1}{4} \frac{q + d}{Q_{X1} \cos^2 \beta + Q_{X2} \sin^2 \beta} \right], \quad (3.68)$$

where $q(u)$ is the charge of the left-handed (right-handed) quark field under $U(1)_X$.

Substituting (3.67) and (3.68) into (3.66) we obtain the following general expression for $\Delta Q_W = Q_W^{\text{eff}} - Q_W^{\text{SM}}$,

$$\begin{aligned} \Delta Q_W = & -\delta^2 Q_W^{\text{SM}} - \delta^2 4Z \sin \theta_W \cos \theta_W \frac{\epsilon}{\epsilon_Z} - \delta^2 \frac{(q + u)(2Z + N)}{Q_{X1} \cos^2 \beta + Q_{X2} \sin^2 \beta} \\ & - \delta^2 \frac{(q + d)(Z + 2N)}{Q_{X1} \cos^2 \beta + Q_{X2} \sin^2 \beta} \left(1 - \frac{l - e}{Q_{X1} \cos^2 \beta + Q_{X2} \sin^2 \beta} \right). \end{aligned} \quad (3.69)$$

Currently, the SM prediction for the weak nuclear charge in the Cesium case is [101]

$$Q_W^{\text{SM}} = -73.16(5), \quad (3.70)$$

so that the general expression Eq. (3.69) becomes:

$$\begin{aligned} \Delta Q_W = & 73.16\delta^2 - 220\delta \left(\epsilon \frac{m_Z}{m_{Z'}} \right) \sin \theta_W \cos \theta_W - \delta^2 \frac{188(q + u)}{Q_{X1} \cos^2 \beta + Q_{X2} \sin^2 \beta} \\ & - \delta^2 \frac{211(q + d)}{Q_{X1} \cos^2 \beta + Q_{X2} \sin^2 \beta} \left(1 - \frac{l - e}{Q_{X1} \cos^2 \beta + Q_{X2} \sin^2 \beta} \right). \end{aligned} \quad (3.71)$$

On the other hand the experimental value for the weak nuclear charge in the Cesium case is [102, 103]

$$Q_W^{\text{exp}} = -73.16(35), \quad (3.72)$$

and the 90% CL bound on the difference is [58]

$$|\Delta Q_W(Cs)| = |Q_W^{\text{exp}} - Q_W^{\text{SM}}| < 0.6, \quad (3.73)$$

which yields the general APV expression for $U(1)_X$ models for the Cesium nucleus:

$$\left| 73.16\delta^2 - 220\delta \left(\epsilon \frac{m_Z}{m_{Z'}} \right) \sin \theta_W \cos \theta_W - \delta^2 \frac{188(q+u)}{Q_{X1} \cos^2 \beta + Q_{X2} \sin^2 \beta} - \delta^2 \frac{211(q+d)}{Q_{X1} \cos^2 \beta + Q_{X2} \sin^2 \beta} \left(1 - \frac{l-e}{Q_{X1} \cos^2 \beta + Q_{X2} \sin^2 \beta} \right) \right| \times K(Cs) < 0.6. \quad (3.74)$$

The correction factor $K(Cs)$ is introduced for low values of $m_{Z'}$ where the local limit approximation is not valid. Different values for this correction factor are listed in Table I of reference [100]. At first order, one can drop the terms proportional to δ^2 in Eq. (3.74) and then solve it for ϵ in terms of δ , using $220\delta \left(\epsilon \frac{m_Z}{m_{Z'}} \right) \sin \theta_W \cos \theta_W = 0.6$.

Doing so, we find the bound shown in the first line of Table 3.5. The numerical upper limit on the kinetic mixing as a function of the Z' mass for different values of δ taking into account the energy dependence on $K(Cs)$ is displayed in Fig. 3.7.

It is useful again to apply our procedure to a well known model in the literature such as the $B-L$ model. In this case $q = u = d = 1/3$, $Q_{X2} = 0$, $Q_{X1} = 2$, $\ell = e$. With these values the expression (3.71) becomes

$$\Delta Q_W = -59.84\delta^2 - 220\delta \left(\epsilon \frac{m_Z}{m_{Z'}} \right) \sin \theta_W \cos \theta_W - 133\delta^2 \tan^2 \beta, \quad (3.75)$$

which coincides with the expressions obtained in [59, 58], except for the last term, that arises due to the non-zero $U(1)_{B-L}$ charges of the fermions. Applying the 90% CL bound in Eq. (3.74) we get

$$\left| -59.84\delta^2 - 220\delta \left(\epsilon \frac{m_Z}{m_{Z'}} \right) \sin \theta_W \cos \theta_W - 133\delta^2 \tan^2 \beta \right| \times K(Cs) < 0.6. \quad (3.76)$$

From Eq. (3.76) we can see the term proportional to δ^2 can not always be dropped as we did before to obtain the limit in the first line of Table 3.5. For sufficiently large $\tan \beta$ the last term in Eq. (3.76) might become relevant yielding changes for the upper limits on the kinetic mixing. Since the importance of this last term is rather model dependent we will not devote time to discuss its impact here.

Regardless, the conclusion that Cesium nucleus provides an interesting and orthogonal test for new physics stands, and depending on the $U(1)_X$ model under study it gives rise to restrictive limits on the kinetic mixing parameter following Table 3.5.

Another observable in APV experiments is given by the value of $\sin \theta_W$ that is measured at low energies. The shift in $\sin^2 \theta_W$ caused by the presence of a new vector boson that mixes with the Z boson is found to be [58]

$$\Delta \sin^2 \theta_W = -0.42\epsilon\delta \frac{m_Z}{m_{Z'}} \frac{m_{Z'}^2}{m_{Z'}^2 + Q^2}, \quad (3.77)$$

where Q is the energy at which $\sin \theta_W$ is measured and $\Delta \sin^2 \theta_W$ refers to the error on the measurement of $\sin^2 \theta_W$ as shown in Table 3.5. By plugging the experimental error bar as displayed in the third column of Table 3.5 into Eq. (3.77) one can derive upper limits on ϵ as a function of δ as shown in the fourth column of Table 3.5. The first two rows in Table 3.5 refer to past experiments, whereas the remaining rows represent projected experimental sensitivities.

Anyways, one can see that the Q_{weak} experiment is not expected to be as sensitive to the kinetic mixing as the first measurements, but both Moller and MESA experiments should be able to surpass previous experiments yielding tight bounds on the kinetic mixing [104, 105, 106].

3.2.6 Muon Anomalous Magnetic Moment

Any charged particle has a magnetic dipole moment ($\vec{\mu}$) defined as

$$\vec{\mu} = g \left(\frac{q}{2m} \right) \vec{s}, \quad (3.78)$$

where s is the spin of the particle, g is the gyromagnetic ratio, $q = \pm e$ is the electric charge of a given charged particle, and m its mass (see [107] for a recent and extensive review). Loop corrections induce deviations from the tree-level value $g = 2$, which are parametrized for the muon in terms of $a_\mu = (g_\mu - 2)/2$, referred to as the anomalous magnetic moment. An enormous effort has been dedicated to precisely determine the SM contribution to $g - 2$ [108, 109, 110]. Interestingly, the SM prediction does not agree with recent measurements leading to [111]

$$\Delta a_\mu = a_\mu^{\text{exp}} - a_\mu^{\text{SM}} = (287 \pm 80) \times 10^{-11}, \quad (3.79)$$

which implies a 3.6σ evidence for new physics. Therefore, it is definitely worthwhile to explore new physics models capable of giving rise to a positive contribution to $g - 2$. In the $U(1)_X$ models under investigation, a particle that fulfills this role is the massive Z' that yields [107, 112, 113]

$$\Delta a_\mu(f, Z') = \frac{1}{8\pi^2} \frac{m_\mu^2}{m_{Z'}^2} \int_0^1 dx \sum_f \frac{|g_v^{f\mu}|^2 F^+(x) + |g_a^{f\mu}|^2 F^-(x)}{(1-x)(1-\lambda^2 x) + \epsilon_f^2 \lambda^2 x}, \quad (3.80a)$$

with

$$F^\pm = 2x(1-x)(x-2 \pm 2\epsilon_f) + \lambda^2 x^2 (1 \mp \epsilon_f)^2 (1-x \pm \epsilon_f) \quad (3.80b)$$

and $\epsilon_f \equiv \frac{m_f}{m_\mu}$, $\lambda \equiv \frac{m_\mu}{m_{Z'}}$. Here f are charged leptons. Since we are not dealing with flavor changing interactions in this work, $\epsilon_f \equiv 1$ and $m_f = m_\mu$. Moreover, in the limit of a Z' much heavier than the muon, the contribution simplifies to

$$\Delta a_\mu(Z') \simeq \frac{1}{12\pi^2} \frac{m_\mu^2}{m_{Z'}^2} (g_v^2 - 5g_a^2), \quad (3.81)$$

where g_v and g_a are the vector and axial vector couplings of the Z' with the muon. Notice that only models where the vector coupling is more than five times larger than the axial vector couplings are capable of addressing the $g - 2$ anomaly in agreement with [114]. This condition is satisfied only in the $U(1)_D$ and $U(1)_F$ models.

That said, the region that explain the $g - 2$ anomaly is easily obtained through the equality

$$\frac{g_v^2}{(m_{Z'}[\text{GeV}])^2} \simeq 3.3 \times 10^{-5}. \quad (3.82)$$

For instance, in the $U(1)_D$ model $g_v = -1.75g_X$. Keeping $g_X = 1$, we need $m_{Z'} \sim 540$ GeV to accommodate the $g - 2$ anomaly, which is way beyond the region of interest in this work. Anyways, such heavy gauge bosons are subject to stringent limits from dimuon searches as shown in [115, 116, 117, 118, 119, 120, 121, 122, 123, 124], preventing such gauge bosons to be a solution to the $g - 2$ anomaly. However, if we set $g_X = 10^{-4}$, then $m_{Z'} \sim 54$ MeV is required, being potentially able to explain the $g - 2$ anomaly, as long as the kinetic and mass mixing parameters are kept sufficiently small. A more thorough discussion of the possibility of explaining $g - 2$ in each of these models will be made elsewhere. It is interesting to see though, that one might be able to cure 2HDM from flavor changing interactions, generate neutrino masses, while solving a relevant and long standing anomaly in particle physics.

3.2.7 Neutrino-Electron Scattering

Intensity frontier constitutes a promising endeavor in the quest for new physics, being able to explore models inaccessible at high-energy frontiers. One canonical example are the precise measurements on neutrino-electron scattering using different targets, as measured by several experiments such as TEXONO, GEMMA, BOREXINO, LSND and CHARM. Since neutrino interactions are purely leptonic, they are subject to small uncertainties. Moreover, interesting models such as the dark photon and light Z' models such as ours, predict different signals at these experiments. Therefore, the use of neutrino-electron

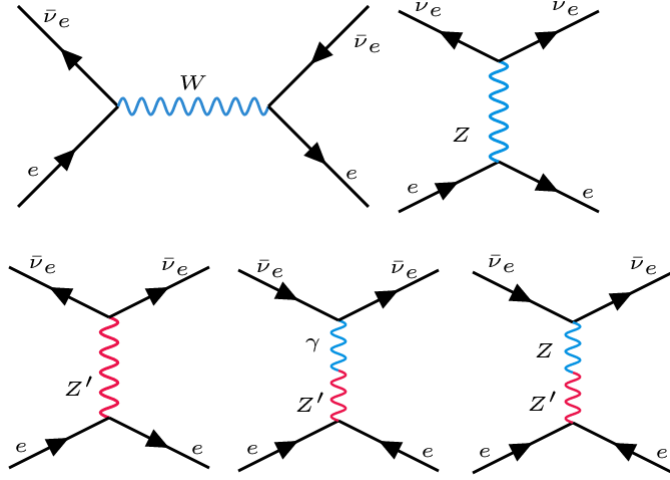


Figure 3.8: Feynman diagrams relevant for neutrino-electron scattering.

scattering to explore hints of new physics is both theoretically and experimentally well motivated.

That said, several works have been done to place limits on new physics models based on neutrino-electron scattering data [125, 126, 127, 128, 129, 130]. Here we will briefly review the concept behind these and derive constraints on the gauge couplings as a function of the Z' mass.

The physics behind these constraints lies on the computation of the neutrino-electron scattering due to new physics. In Fig. 3.8 we exhibit the SM diagram alongside the new physics ones. Following Ref. [131] the new physics neutrino-electron scattering cross section can be parametrized in terms of the $B - L$ model which is found to be [128]

$$\frac{d\sigma}{dE_R} = \frac{g_{B-L}^4 m_e}{4\pi E_\nu^2 (m_{Z'}^2 + 2m_e E_R)^2} (2E_\nu^2 + E_R^2 - eE_R E_\nu - m_e E_R) \quad (3.83)$$

where E_R is the electron recoil energy, E_ν is the energy of the incoming neutrino, m_e is the electron mass.

The idea is to compute the expected neutrino-scattering rate from new physics, $(dR/dE_R)_{NP}$, which is related to the neutrino-electron scattering through

$$\left(\frac{dR}{dE_R} \right)_{NP} = t \rho_e \int_{E_\nu^{min}}^{\infty} \frac{d\Phi}{dE_\nu} \frac{d\sigma}{dE_R} dE_\nu, \quad (3.84)$$

where Φ is the neutrino flux, t is period of mock data taking, and ρ_e is electron number density per kg of the target mass. Once that has been computed, one compares it with the measured rate and finds 90% level limits applying a χ^2 statistics as follows:

$$\chi^2 = \sum_{i=1} \frac{(R_{\text{exp } i} - (R_{\text{SM } i} + R_{\text{NP}}))^2}{\sigma_i} \quad (3.85)$$

Experiment	Type of neutrino	$\langle E_\nu \rangle$	T
TEXONO-NPCGe [132]	$\bar{\nu}_e$	1–2 MeV	0.35–12 keV
TEXONO-HPGe [133, 134]	$\bar{\nu}_e$	1–2 MeV	12–60 keV
TEXONO-CsI(Tl) [135]	$\bar{\nu}_e$	1–2 MeV	3–8 MeV
LSND [136]	ν_e	36 MeV	18–50 MeV
BOREXINO [137]	ν_e	862 keV	270–665 keV
GEMMA [138]	$\bar{\nu}_e$	1–2 MeV	3–25 keV
CHARM II [139]	ν_μ	23.7 GeV	3–24 GeV
CHARM II [139]	$\bar{\nu}_\mu$	19.1 GeV	3–24 GeV

Table 3.6: Summary of experiments that constrained $\nu - e$ scattering.

where R_{exp} , R_{SM} are the measured and SM predicted rates respectively, and σ_i is the statistical error on the measurement of R_{exp} . The index i runs through energy bins. Using data from several experiments subject to different energy threshold and type of incoming neutrino flavor as summarized in Table 3.2.7, constraints on the new physics have been placed [131]. The limits were interpreted in terms of the $B - L$ model, as shown in Fig. 3.9. These bounds are the most restrictive for $m_{Z'} \sim 100 \text{ MeV} - 1 \text{ GeV}$, as exhibited in Fig. 3.10 where all relevant constraints are put together. See [2] for a recent review on neutrino-electron scattering experiments.

One needs to apply these constraints to the $U(1)_X$ models under study with care. Obviously, for the $B - L$ model in Table 2, the limits in Fig. 3.10 are directly applicable. For the remaining $U(1)_X$ models, one can estimate the limits through rescaling. Since the kinetic and mass-mixing are constrained to be small, the leading diagram is the t -channel Z' exchange in Fig. 3.8. Therefore, the scattering cross section scales with $g_{Z' - \nu - \nu}^2 g_{Z' - e - e}^2$, where $g_{Z' - \nu - \nu}$, $g_{Z' - e - e}$ are the Z' vectorial couplings with the neutrinos and electrons respectively. These are easily obtained knowing that the vector coupling with a given fermion field is $g_{fv} = g_X/2(Q_{fL} + Q_{fR})$, where Q_{fL} and Q_{fR} are the charges of the left-handed and right-handed field components under $U(1)_X$ as displayed in Table 3.1. In summary, there is a plot similar to Fig. 3.9 for each $U(1)_X$ model in this work. Clearly this exercise is outside the scope of this work. Anyways, it is clear that neutrino-electron scattering provides a competitive probe for new physics and is relevant for the $U(1)_X$ models under study. These bounds can be circumvented by tuning the kinetic mixing to

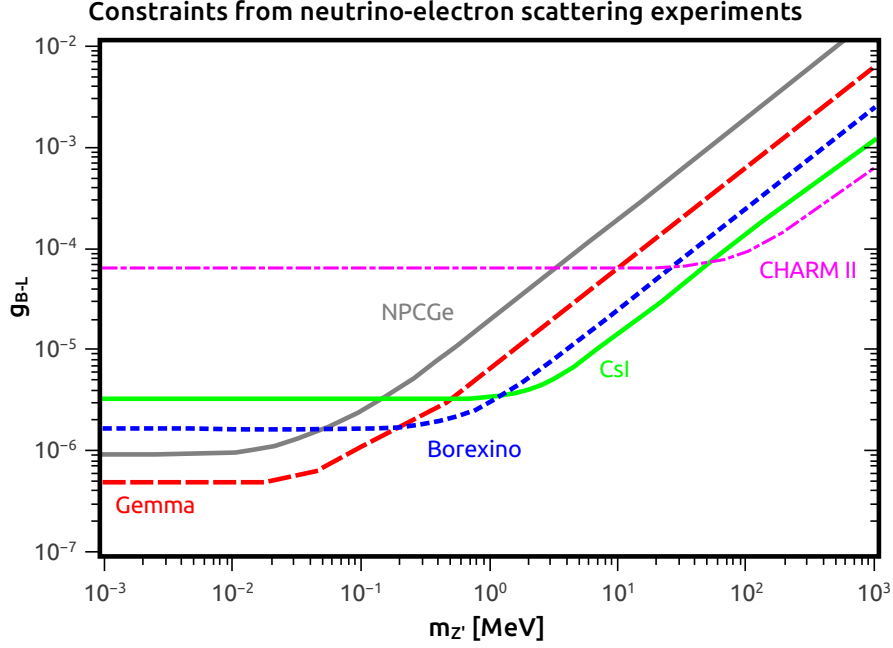


Figure 3.9: Constraints on the $B - L$ model based on measurements of neutrino-electron scattering.

sufficiently small values, similarly to the dark photon model.

3.2.8 Low Energy Accelerators

Low energy accelerators are capable of probing new physics models out of reach of high-energy colliders. Models with light mediators, such as the dark photon model are considered a benchmark [140, 141]. The sensitivity of low energy accelerators is driven by high-intensity beams and/or high precision detectors. Such accelerators are usually divided into two classes: (i) collider; (ii) fixed-target experiments. In the former, high-intensity beams of e^+e^- are capable of directly producing on-shell light mediators, whereas in the latter, light particles are produced as result of a decay chain created after the beam hits the target. In either case, the low-energy accelerators are excellent laboratories to spot new physics effects. In Fig. 3.11 we present a summary of current constraints on the dark photon model, with the dark photon, A' , decaying into charged leptons. With care, the limits exhibited in Fig. 3.11 can be applicable to the $U(1)_X$ under investigation. For instance, the BaBar experiment searched for the $e^+e^- \rightarrow \gamma A'$, with A' decaying into l^+l^- . The interaction of the dark photon with charged leptons reads $\epsilon \bar{l} \gamma_\mu l A'^\mu$. Having in mind that the two important quantities are the production cross section and the branching ratio into electrons, one can recast the BaBar upper limits on the dark photon kinetic mixing

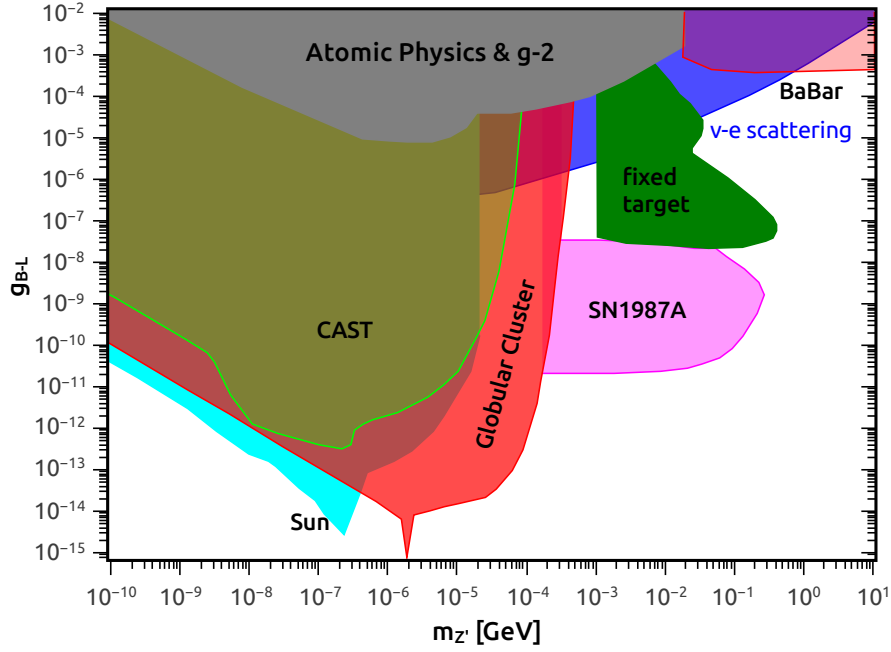


Figure 3.10: Summary of constraints from neutrino-electron scattering on $U(1)_X$ models with very light Z' gauge bosons. These constraints have been interpreted from dark photon searches.

(ϵ_{DP}) to other $U(1)_X$ models as follows

$$\epsilon_{\text{DP}}^2 \rightarrow (g_v^l)^2 BR(Z' \rightarrow l^+ l^-), \quad (3.86)$$

where $g_v^l = g_X/2(Q_L^l + Q_R^l)$ is the Z' vectorial coupling to charged leptons. Here Q_L^l and Q_R^l are the left-handed and right-handed charged lepton charges under $U(1)_X$.

In all $U(1)_X$ models that accommodate neutrino masses and are free from flavor changing interactions the Z' boson features a vectorial coupling with electrons. Since the SM fermions are charged under $U(1)_X$, in addition to the kinetic mixing term, a vectorial interaction proportional to g_X also arises. Therefore, Eq. (3.86) is valid when the term proportional to g_X is dominant, otherwise, the bounds in Fig. 3.11 are directly applicable. Hence, one can use Eq. (3.86) to obtain limits for each $U(1)_X$ model. A similar reasoning can be applied to other collider experiments.

As for fixed target experiments such as NA48/2, the rescaling is restricted to the branching ratio into charged leptons. Sometimes these experiments include both e^+e^- and $\mu^+\mu^-$ decay modes in the analysis, while other times they consider only one of those. Our goal here is not to describe each one of these searches individually but rather present to the reader the existence of limits on the kinetic-mixing stemming from low energy accelerators. The precise bound on ϵ for each $U(1)_X$ model is not relevant for us, since

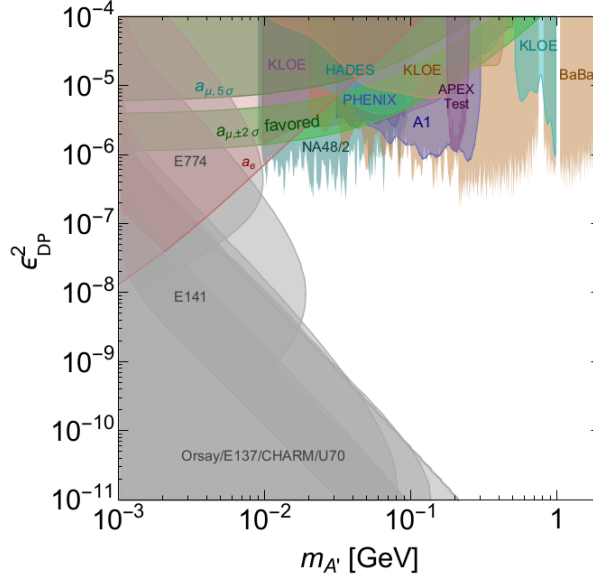


Figure 3.11: Summary of bounds from low energy accelerators constraints on the dark photon model [2]. After proper rescaling these constraints are also applicable to the $U(1)_X$ models in this work. In particular, the BaBar limits can be recast using the relation $\epsilon_{DP}^2 \rightarrow (g_v^l)^2 BR(Z' \rightarrow l^+ l^-)$. See text for details.

they can all be evaded by simply tuning down the free kinetic mixing parameter.

Furthermore, it is worth pointing out that there is also a similar plot considering only invisible decays of the dark photon. However, as far as the $U(1)_X$ models go, the only possible invisible decay modes are the active neutrinos and right-handed neutrinos. Except in the case of the $U(1)_{B-L}$ model, this branching ratio is expected to be small, substantially weakening the limits on ϵ . Thus the searches for visible decays are more constraining.

In summary, low energy accelerators yield very strong limits on the kinetic mixing parameter of the $U(1)_X$ models.

3.3 Discussion

We have discussed a variety of limits on the parameters δ and the kinetic mixing ϵ . They are model dependent. The bounds on δ were derived under the assumption that the fermions were uncharged under $U(1)_X$, where only the mass-mixing would dictate the Z' interactions with fermions. However, due to the presence of new interactions between the SM fermions and the Z' gauge boson these limits might be subject to changes by a factor of few depending on the value of g_X and fermion charges under $U(1)_X$. As for the limits

on the kinetic mixing, they were obtained assuming that the kinetic mixing alone dictates the observables since they were originally meant for the dark photon model. Since both δ and ϵ , in principle, are arbitrarily small, the constraints presented in this work might be circumvented. A more detailed analysis incorporating precise bounds on the $U(1)_X$ models is left for the future.

In summary, in this Chapter we presented new 2HDM gauge models capable of accommodating neutrino masses through type I seesaw and freeing the 2HDM from flavor changing interactions, as well as estimated what kind of phenomenology these models can generate. In the next Chapter we will see that the implementation of the type II seesaw mechanism is also possible in this framework and discuss its phenomenology.

Chapter 4

Neutrino Masses in a Two Higgs Doublet Model with a $U(1)$ Gauge Symmetry

In the Chapter 3 we have discussed how the FCNI problem in the 2HDM can be elegantly addressed by means of an Abelian gauge symmetry. In this 2HDM- $U(1)$ framework, we showed how neutrino masses could be generated via type-I seesaw mechanism. The requirement is the introduction of right-handed neutrinos and also a scalar singlet, in order to generate a neutrino Majorana mass term. A natural question that rises is then: is there a way to explain neutrino masses without adding right-handed neutrinos within the 2HDM- $U(1)$ framework?

Motivated by this question, in this Chapter we describe how one could accomplish that. We will study a new model, within the scope of 2HDM with $U(1)_X$ symmetry, in which neutrino masses are generated via type II seesaw mechanism which requires the introduction of a scalar triplet. As we will see, the anomaly cancellation in this case impose rather restrictive conditions on the possible models, and also, as there is not a scalar singlet, the Z' gauge boson is necessarily light.

4.1 Type II seesaw in the 2HDM- $U(1)$

A popular mechanism to explain the active neutrino masses without the presence of right-handed neutrinos is the so called type II seesaw mechanism [53, 56, 55, 142, 54]. In

the following, we will describe how it can be implemented in the 2HDM- $U(1)$ framework. First, recall from the Chapter 3 that the anomaly cancellation procedure for the type I 2HDM in the general case in which right-handed neutrinos are included, leads to the following charge relations,

$$\begin{aligned} q = \frac{1}{2}(u + d) \quad , \quad l = -\frac{3}{2}(u + d) \quad , \quad e = -(2u + d) \quad , \quad n = -(u + 2d), \\ Q_{X_1} = \frac{1}{2}(5u + 7d) \quad , \quad Q_{X_2} = \frac{1}{2}(u - d) \quad , \quad q_X = 2u + 4d, \end{aligned} \quad (4.1)$$

where u and d are the $U(1)_X$ charges of the up and down quarks respectively, q (l) the charge of the quark (lepton) doublet, e (n) the charge of the right-handed charged leptons (neutrinos), and lastly Q_{X_i} (q_X) the $U(1)_X$ charge of the scalar doublet (singlet). One of the anomaly cancellation conditions is $n = -(u + 2d)$, which comes from the $U(1)^3$ anomaly as shown in the Appendix A.1. Therefore, as we are interested in a case where there are no right-handed neutrinos, we must set $u = -2d$ to be free from gauge anomalies. Compared to the type I seesaw scenario, instead of having two independent charges (u and d), we now have only one, say d . That implies into,

$$\begin{aligned} q = -\frac{d}{2} \quad , \quad l = \frac{3d}{2} \quad , \quad e = 3d, \\ u = -2d \quad , \quad Q_{X_2} = -\frac{3d}{2}. \end{aligned} \quad (4.2)$$

The charge of the first doublet is free, as long as $Q_{X_1} \neq Q_{X_2}$, in order to recover the Yukawa Lagrangian (2.33) of the type I 2HDM, and keep the model free from FCNI. As shown in the Table 4.1, there is essentially only two different possibilities. One where the SM fermions are neutral and the other where they are charged under $U(1)_X$. If a particular nonzero value is chosen for d , any other multiple of this value would produce a physically equivalent model, because a change in d can be balanced by a rescaling on the gauge coupling constant g_X , so that the $U(1)_X$ interaction remains the same. In particular, taking $d = -2/3$ we notice that the charges of the SM fermions under $U(1)_X$ are similar to the SM weak hypercharge. In this way, it is clear that a type II seesaw realization in the 2HDM- $U(1)$ gives rise either to a fermiophobic or a sequential Z' boson.

The implementation of type II seesaw mechanism requires an $SU(2)_L$ scalar triplet $\Delta \sim (1, 3, 2, q_{X_t})$, where the quantum numbers refers to the transformation properties under the symmetry group $SU(3)_c \times SU(2)_L \times U(1)_Y \times U(1)_X$. The field Δ can be

Charges in Type II seesaw 2HDMs free from FCNI

Fields	u_R	d_R	Q_L	L_L	e_R	Δ	Φ_2	Φ_1
Charges	$-2d$	d	$-d/2$	$3d/2$	$3d$	$-3d$	$-3d/2$	$\neq Q_{X_2}$
$U(1)_N$	0	0	0	0	0	0	0	$\neq Q_{X_2}$
$U(1)_{Y'}$	4/3	-2/3	1/3	-1	-2	2	1	$\neq Q_{X_2}$

Table 4.1: The table shows anomaly free Type I 2HDM where neutrino masses are generated via a type II seesaw mechanism. The first row shows the generic charges as functions of the d_R quark charge, d . Two particular cases are shown for $d = 0$ and $d = -2/3$, which correspond to sequential Z' and dark photon models, respectively. Notice that to prevent FCNI the scalar doublets have different charges under the $U(1)_X$ gauge symmetry.

parameterized as,

$$\Delta = \begin{pmatrix} \Delta^+/\sqrt{2} & \Delta^{++} \\ \Delta^0 & -\Delta^+/\sqrt{2} \end{pmatrix}, \quad (4.3)$$

with,

$$\Delta^0 = \frac{\rho_t + v_t + i\eta_t}{\sqrt{2}}. \quad (4.4)$$

The $SU(2)_L$ symmetry allows the introduction of an interaction between Δ and the leptons via,

$$-\mathcal{L}_{Y_t} = y_L \bar{L}_L^c i\sigma^2 \Delta L_L + h.c. \quad (4.5)$$

which requires Δ to have hypercharge $Y_t = 2$ and lepton number $L_t = 2$, automatically forbidding interactions to quarks. The inclusion of Eq. (4.5) implies,

$$2l + q_{X_t} = 0, \quad (4.6)$$

and using eq. (4.2) we get,

$$q_{X_t} = -3d, \quad (4.7)$$

explaining the Δ charge shown in Table 4.1.

Since Δ carries lepton number, when the neutral scalar Δ^0 develops a VEV, v_t , lepton number is violated, and from eq. (4.5) we can easily see that it generates a Majorana mass term for the neutrinos with,

$$m_\nu = \sqrt{2}y_L v_t. \quad (4.8)$$

Thus, v_t has to be very small in order to accommodate neutrino masses in the sub-eV range. In the next section we study the mass spectrum of the model.

4.1.1 Mass Spectrum - Scalars

Our goal in this section is to study the spontaneous symmetry breaking pattern to find the physical scalars, gauge bosons, and neutrino masses. The SM charged lepton masses are the same as in the SM. That said, we begin our reasoning with the scalar sector.

The scalar sector is described by the Lagrangian,

$$\mathcal{L}_{\text{scalar}} = (D_\mu \Phi_i)^\dagger (D^\mu \Phi_i) + \text{Tr}[(D_\mu \Delta)^\dagger (D^\mu \Delta)] - V(\Phi_1, \Phi_2, \Delta), \quad (4.9)$$

where the covariant derivatives of the scalar doublets and the triplet read,

$$D_\mu \Phi_i = \partial_\mu \Phi_i + ig\tau^a W_\mu^a + ig' \frac{Y}{2} \hat{B}_\mu \Phi_i + ig_X \frac{Q_{X_i}}{2} \hat{X}_\mu \Phi_i, \quad (4.10)$$

$$D_\mu \Delta = \partial_\mu \Delta + ig[\tau^a W_\mu^a, \Delta] + ig' \frac{Y_t}{2} \hat{B}_\mu \Delta + ig_X \frac{q_{X_t}}{2} \hat{X}_\mu \Delta, \quad (4.11)$$

where τ^a are the generators of the $SU(2)_L$ group. The scalar potential in eq. (4.9), invariant under all gauge symmetries is given by

$$\begin{aligned} V(\Phi_1, \Phi_2, \Delta) = & m_1^2 \Phi_1^\dagger \Phi_1 + m_2^2 \Phi_2^\dagger \Phi_2 + m_\Delta^2 \text{Tr}(\Delta^\dagger \Delta) + \lambda_1 (\Phi_1^\dagger \Phi_1)^2 + \lambda_2 (\Phi_2^\dagger \Phi_2)^2 \\ & + \lambda_3 (\Phi_1^\dagger \Phi_1)(\Phi_2^\dagger \Phi_2) + \lambda_4 (\Phi_1^\dagger \Phi_2)(\Phi_2^\dagger \Phi_1) + \lambda_{t1} (\Phi_1^\dagger \Phi_1) \text{Tr}(\Delta^\dagger \Delta) \\ & + \lambda_{t2} (\Phi_2^\dagger \Phi_2) \text{Tr}(\Delta^\dagger \Delta) + \lambda_{tt1} \Phi_1^\dagger \Delta \Delta^\dagger \Phi_1 + \lambda_{tt2} \Phi_2^\dagger \Delta \Delta^\dagger \Phi_2 \\ & + \lambda_t [\text{Tr}(\Delta^\dagger \Delta)]^2 + \lambda_{tt} \text{Tr}(\Delta^\dagger \Delta)^2 + \mu_{t2} (\Phi_2^T i\sigma^2 \Delta^\dagger \Phi_2 + h.c.). \end{aligned} \quad (4.12)$$

Observe in the potential above that the terms $\Phi_1^T i\sigma^2 \Delta^\dagger \Phi_2$ and $\Phi_1^T i\sigma^2 \Delta^\dagger \Phi_1$ are forbidden by the $U(1)_X$ symmetry, as we require $Q_{X1} \neq Q_{X2}$. There is only one non-hermitian term $\Phi_2^T i\sigma^2 \Delta^\dagger \Phi_2$, which violates (explicitly) lepton number in two units. Such lepton number violation is a common feature in seesaw type II models. It is important to note that neutrino masses are generated when Δ^0 develops a vacuum expectation value as shown in eq.(4.8) and that would be related to lepton number violation since the scalar triplet carries lepton number. However, notice that the non-hermitian term in eq.(4.12) already explicitly violates lepton number, thus lepton number had been violated even before Δ^0 develops a non-trivial vacuum expectation value. We checked that without this non-hermitian term in the scalar potential the pseudoscalar from the scalar triplet field would remain massless, i.e. a majoron field [143].

Anyway, substituting the VEVs,

$$\langle \phi_i^0 \rangle = \frac{v_i}{\sqrt{2}}, \quad \langle \Delta^0 \rangle = \frac{v_t}{\sqrt{2}}, \quad (4.13)$$

in order to break spontaneously the gauge symmetries, we have the following constraint equations for a minimal point of the potential,

$$m_1^2 + \frac{1}{2} [2\lambda_1 v_1^2 + (\lambda_3 + \lambda_4)v_2^2 + (\lambda_{t1} + \lambda_{tt1})v_t^2] = 0, \quad (4.14)$$

$$m_2^2 + \frac{1}{2} [(\lambda_3 + \lambda_4)v_1^2 + 2\lambda_2 v_2^2 + (\lambda_{t2} + \lambda_{tt2})v_t^2 - 2\sqrt{2}\mu_{t2}v_t] = 0, \quad (4.15)$$

$$\frac{v_t}{2} [2m_t^2 + (\lambda_{t1} + \lambda_{tt1})v_1^2 + (\lambda_{t2} + \lambda_{tt2})v_2^2 + 2(\lambda_t + \lambda_{tt})v_t^2] - \frac{\mu_{t2}v_2^2}{\sqrt{2}} = 0. \quad (4.16)$$

In the SM, the symmetry is spontaneously broken when the m^2 term is negative. In the case of a type II seesaw, the mass terms m_1^2 , m_2^2 and m_t^2 in the scalar potential do not have to be all negative to break the symmetry (see, e. g., Ref. [144] for a detailed discussion about the type II seesaw vacuum). In fact, we will see later on that the mass term of the scalar triplet should be positive in order to generate a pseudoscalar with positive mass.

Assuming that $2m_t^2$ is the dominant term between the brackets in the constraint equation (4.16), we have a seesaw relation,

$$v_t \simeq \frac{\mu_{t2}v_2^2}{\sqrt{2}m_t^2}, \quad (4.17)$$

which leads to a naturally dwindled v_t for $|m_t^2| \gg |\mu_{t2}v_2|$. In this way, a small v_t can be understood as a simple consequence of having the coefficient of the bilinear term in Δ to be comparatively large with respect to the other energy scales of the scalar potential. Note that from eq. (4.17) we conclude that m_t^2 and μ_{t2} should have the same sign.

In the scalar sector, Φ_i and Δ render the existence of seven physical fields: 3 CP-even scalars, h , H and H_t ; one CP-odd, A ; two singly charged H^+ , H_t^+ and one doubly charged H^{++} . The other scalar degrees of freedom are absorbed as longitudinal components by the gauge bosons, W^\pm , Z and Z' , making them massive.

In the basis (ρ_1, ρ_2, ρ_t) the neutral scalars mix according to the following mass matrix,

$$M_{\text{CPeven}}^2 = \begin{pmatrix} 2\lambda_1 v_1^2 & (\lambda_3 + \lambda_4)v_1 v_2 & (\lambda_{t1} + \lambda_{tt1})v_1 v_t \\ (\lambda_3 + \lambda_4)v_1 v_2 & 2\lambda_2 v_2^2 & (\lambda_{t2} + \lambda_{tt2})v_2 v_t - \sqrt{2}\mu_{t2}v_2 \\ (\lambda_{t1} + \lambda_{tt1})v_1 v_t & (\lambda_{t2} + \lambda_{tt2})v_2 v_t - \sqrt{2}\mu_{t2}v_2 & 2(\lambda_t + \lambda_{tt})v_t^2 + \frac{\mu_{t2}v_2^2}{\sqrt{2}v_t} \end{pmatrix}. \quad (4.18)$$

From the diagonalization procedure of this mass matrix we will get three physical scalars, h , H and H_t . We can parametrize this diagonalization in terms of three mixing angles α ,

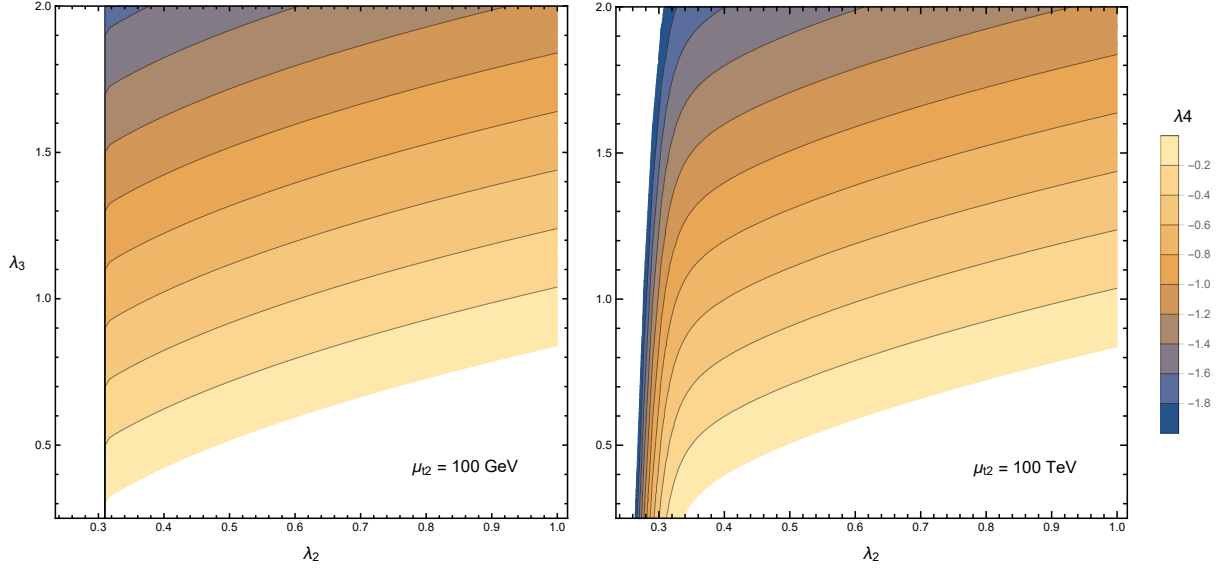


Figure 4.1: Region of parameter space that leads to a 125 GeV SM-like Higgs boson for $v_2 = 200$ GeV, $v_t = 1$ MeV and $\lambda_1 = 0.6$. In the left panel $\mu_{t2} = 100$ GeV and in the right panel, $\mu_{t2} = 100$ TeV.

α_1 and α_2 ,

$$\begin{pmatrix} h \\ H \\ H_t \end{pmatrix} = \begin{pmatrix} c_\alpha & s_\alpha & 0 \\ -s_\alpha & c_\alpha & 0 \\ 0 & 0 & 1 \end{pmatrix} \begin{pmatrix} c_{\alpha_1} & 0 & s_{\alpha_1} \\ 0 & 1 & 0 \\ -s_{\alpha_1} & 0 & c_{\alpha_1} \end{pmatrix} \begin{pmatrix} 1 & 0 & 0 \\ 0 & c_{\alpha_2} & s_{\alpha_2} \\ 0 & -s_{\alpha_2} & c_{\alpha_2} \end{pmatrix} \begin{pmatrix} \rho_1 \\ \rho_2 \\ \rho_t \end{pmatrix}, \quad (4.19)$$

where $s_{\alpha, \alpha_1, \alpha_2}$ and $c_{\alpha, \alpha_1, \alpha_2}$ are sine and cosine functions. We choose h to denote the 125 GeV SM-like Higgs found in the LHC. The angles are determined by the parameters of the potential and the scalar VEVs. Fully analytic expressions for the masses and eigenvectors are complicated but we can obtain approximate results. As shown in the Appendix B, in the limit $v_t \ll v_i$, the masses of the CP-even scalars are approximately,

$$m_h^2 = \lambda_1 v_1^2 + \lambda_2 v_2^2 - \sqrt{(\lambda_1 v_1^2 - \lambda_2 v_2^2)^2 + (\lambda_3 + \lambda_4)^2 v_1^2 v_2^2} - 2\sqrt{2} \sin^2 \alpha \mu_{t2} v_t \quad (4.20)$$

$$m_H^2 = \lambda_1 v_1^2 + \lambda_2 v_2^2 + \sqrt{(\lambda_1 v_1^2 - \lambda_2 v_2^2)^2 + (\lambda_3 + \lambda_4)^2 v_1^2 v_2^2} - 2\sqrt{2} \cos^2 \alpha \mu_{t2} v_t \quad (4.21)$$

$$m_{H_t}^2 = \frac{\mu_{t2} v_2^2}{\sqrt{2} v_t}. \quad (4.22)$$

The limit $v_t \ll v_i$, that will be assumed throughout this Chapter, yields a Higgs boson, h , with the correct mass is shown in Fig. 4.1. It is straightforward to see that we can easily find a Higgs with the correct mass for couplings of order one and μ_{t2} either at the weak or multi-TeV scale.

As for the pseudoscalars, in the basis (η_1, η_2, η_t) the mass matrix is given by,

$$M_{\text{CPodd}}^2 = \sqrt{2}\mu_{t2} \begin{pmatrix} 0 & 0 & 0 \\ 0 & 2v_t & -v_2 \\ 0 & -v_2 & \frac{v_2^2}{2v_t} \end{pmatrix}. \quad (4.23)$$

Note that η_1 is decoupled and massless. Thus it can be immediately recognized as a Goldstone boson, G_1 . After the diagonalization procedure we found another Goldstone boson, G_2 . These two massless pseudoscalars represent the degrees of freedom needed to generate the Z and Z' masses. In the diagonalization procedure we find the rotation matrix,

$$\begin{pmatrix} G_1 \\ G_2 \\ A \end{pmatrix} = \begin{pmatrix} 1 & 0 & 0 \\ 0 & c_{\beta'} & s_{\beta'} \\ 0 & -s_{\beta'} & c_{\beta'} \end{pmatrix} \begin{pmatrix} \eta_1 \\ \eta_2 \\ \eta_t \end{pmatrix}, \quad (4.24)$$

where,

$$\tan \beta' = \frac{2v_t}{v_2}, \quad (4.25)$$

which gives rise to two massless fields as aforementioned and a massive pseudoscalar, A , with mass,

$$m_A^2 = \frac{\mu_{t2}(v_2^2 + 4v_t^2)}{\sqrt{2}v_t}. \quad (4.26)$$

Observe that v_t and μ_{t2} must have the same sign in order to have $m_A^2 > 0$. We had concluded previously from Eq.(4.17) that μ_{t2} and m_t^2 should have the same sign to keep v_t positive definite, thus from Eq.(4.26) μ_{t2} must be positive to generate a positive squared mass for the pseudoscalar A . Hence, both μ_{t2} and m_t^2 are strictly positive.

It is important to stress that even with the introduction of a new gauge symmetry, the pseudoscalar A , which is a common figure in 2HDM, remains in the spectrum. Under the assumption that v_t is smaller than μ_{t2} the pseudoscalar can have a mass sufficiently large to evade existing bounds, as we shall discuss further.

The charged scalars mass matrix in the basis $(\phi_1^+, \phi_2^+, \Delta^+)$ is,

$$M_{\text{Charged}}^2 = \frac{1}{2} \begin{pmatrix} -\lambda_4 v_2^2 - \lambda_{t1} v_t^2 & \lambda_4 v_1 v_2 & \lambda_{t1} v_1 v_t / \sqrt{2} \\ \lambda_4 v_1 v_2 & -\lambda_4 v_1^2 - \lambda_{t2} v_t^2 + 2\sqrt{2}\mu_{t2} v_t & \frac{1}{2}(\sqrt{2}\lambda_{t2} v_t - 4\mu_{t2})v_2 \\ v_1 v_t \lambda_{t1} / \sqrt{2} & \frac{1}{2}(\sqrt{2}\lambda_{t2} v_t - 4\mu_{t2})v_2 & \frac{\sqrt{2}\mu_{t2} v_2^2}{v_t} - \frac{1}{2}(\lambda_{t1} v_1^2 + \lambda_{t2} v_2^2) \end{pmatrix}. \quad (4.27)$$

The physical fields are given by performing the following rotation,

$$\begin{pmatrix} G^+ \\ H^+ \\ H_t^+ \end{pmatrix} = \begin{pmatrix} c_\beta & s_\beta & 0 \\ -s_\beta & c_\beta & 0 \\ 0 & 0 & 1 \end{pmatrix} \begin{pmatrix} c_{\beta_1} & 0 & s_{\beta_1} \\ 0 & 1 & 0 \\ -s_{\beta_1} & 0 & c_{\beta_1} \end{pmatrix} \begin{pmatrix} 1 & 0 & 0 \\ 0 & c_{\beta_2} & s_{\beta_2} \\ 0 & -s_{\beta_2} & c_{\beta_2} \end{pmatrix} \begin{pmatrix} \phi_1^+ \\ \phi_2^+ \\ \Delta^+ \end{pmatrix}. \quad (4.28)$$

The Goldstone boson G^+ is absorbed by W^+ , and the physical states H^+ and H_t^+ have masses,

$$m_{H^+}^2 = \frac{1}{8}(A - \sqrt{A^2 - B}), \quad (4.29)$$

$$m_{H_t^+}^2 = \frac{1}{8}(A + \sqrt{A^2 - B}), \quad (4.30)$$

where,

$$A = -2\lambda_4 (v_1^2 + v_2^2) - \lambda_{tt1} (v_1^2 + 2v_t^2) - \lambda_{tt2} (v_2^2 + 2v_t^2) + 2\sqrt{2}\frac{\mu_{t2}}{v_t} (v_2^2 + 2v_t^2),$$

$$B = 8(v_1^2 + v_2^2 + 2v_t^2) \left[\lambda_4 (\lambda_{tt1}v_1^2 + \lambda_{tt2}v_2^2) + \lambda_{tt1}\lambda_{tt2}v_t^2 - 2\sqrt{2}\frac{\mu_{t2}}{v_t} (\lambda_4v_2^2 + \lambda_{tt1}v_t^2) \right].$$

The doubly charged scalar Δ^{++} does not mix any other field. This mass eigenstate, which we will denote henceforth by H^{++} , has a mass given by,

$$m_{H^{\pm\pm}}^2 = \frac{\mu_{t2}v_2^2}{\sqrt{2}v_t} - \frac{1}{2}(\lambda_{tt1}v_1^2 + \lambda_{tt2}v_2^2 + 2\lambda_{tt}v_t^2). \quad (4.31)$$

In summary, the scalar mass spectrum is largely controlled by the relative sizes of v_t , μ_{t2} and v_i . As v_i is fixed to be ~ 100 GeV and, as we will see later on, v_t is constrained to be $\lesssim O(1)$ GeV, we will always take $v_t \ll v_i$. In this limit, the masses of h , H and H^+ are rather insensitive to v_t and μ_{t2} , while the masses of H_t , A , H_t^+ and H^{++} strongly depend on them. As μ_{t2} , in principle, remains as a free parameter, we can distinguish three different regimes according to its size:

- $\mu_{t2} \sim v_t \ll v_i$: In this case, μ_{t2} has little influence on the masses of h and H . H remains always heavier than h , with a mass around the 100 – 300 GeV range, for λ 's of order ~ 1 . The masses of H_t , A , H_t^+ and H^{++} are controlled by the ratio μ_{t2}/v_t , with H_t and A nearly mass degenerate. In particular, for $\mu_{t2} = v_t$, the masses are around 200 GeV. Such low masses can be dangerous in light of existing bounds [145, 146, 147, 148, 149, 150, 151, 152, 153].
- $\mu_{t2} \sim v_i$: In this scenario the spectrum is shifted up and the scalar masses can be significantly larger than 100 GeV. A , H_t , H_t^+ and H^{++} are mass degenerate and

may reach masses in the TeV domain. For example, taking $\mu_{t2} = v_2 = 100$ GeV and $v_t = 100$ MeV, we obtain $m_h = 125$ GeV, $m_H = 404$ GeV, $m_{H^+} = 507$ GeV, $m_{H_t} \simeq m_A \simeq m_{H_t^+} \simeq m_{H^{++}} \simeq 2.65$ TeV. We have adopted $\lambda_1 = 1.6$, $\lambda_2 = 0.9$, $\lambda_3 = 7.7$, $\lambda_4 = -8.5$, $\lambda_{ti} = \lambda_{tti} = 0.5$.

- $\mu_{t2} \gg v_i$: This case can be recognized as the canonical type II seesaw scenario, in which m_t and μ_{t2} come from new physics at very high energy scale, like Grand Unification scale. In this case, only h , H and H^+ remain in the weak scale, while H_t , A , H_t^+ and H^{++} decouple and are still degenerate, getting very high masses of order $\sim v\sqrt{\mu_{t2}/v_t}$.

As stressed above, the masses of H_t , A , H_t^+ and H^{++} are always close to each other because they follow $m_{H_i}^2 = m_t^2 + O(v, v_t)$, with $m_t^2 \simeq \mu_{t2}v_2^2/\sqrt{2}v_t$. Thus, for small v_t , the m_t^2 term is the dominant one, so that the masses are all approximately given by $m_{H_i}^2 \simeq m_t^2$. The mass splittings are controlled by the scalar VEVs. At leading order,

$$\begin{aligned} m_{H_t}^2 - m_A^2 &\simeq O(v_t^2), \\ m_A^2 - m_{H_t^+}^2 &\simeq m_{H_t^+}^2 - m_{H^{++}}^2 \simeq \frac{1}{4}(\lambda_{tt1}v_1^2 + \lambda_{tt2}v_2^2). \end{aligned} \quad (4.32)$$

These mass splittings are noticeable only when the masses are small, i.e., for small μ_{t2} . For $\mu_{t2} \gtrsim v_i$, they are basically mass degenerate.

As aforementioned, the masses of h , H and H^+ are less sensitive to v_t and μ_{t2} , and depend mostly on the VEVs v_i and the λ_i 's. Therefore, they naturally lie at the weak scale. As for H^+ , we find $m_{H^+}^2 \simeq -\frac{1}{2}\lambda_4 v^2$ (see eq. (B.36) in the Appendix B), which requires λ_4 to be negative. If we took $|\lambda_4| > 1$, we would have charged scalar masses above 500 GeV, which can easily evade existing limits [154, 155, 156, 157, 158, 159, 160, 161]. In order to have scalar masses above 500 GeV we need couplings larger than the unit. This is typically true in seesaw type II models.

Returning to the mass expressions of the CP-even scalars, Eqs. (4.20) and (4.21), we see that if there were just the two scalar doublets, the neutral scalar masses would be given by these expressions with v_t, μ_{t2} set to zero. However, the scalar triplet generate negative correction terms proportional to $\mu_{t2}v_t$, so that these scalars become lighter than they would be if there was not the triplet. However, as shown in Figure 4.1, the parameter space allows to fit a mass $m_h = 125$ GeV for the Higgs boson h . Furthermore, the Eqs. (4.20) and (4.21) imply an upper bound in the combination $\mu_{t2}v_t$: a large value of μ_{t2}

must be balanced by a small value of v_t in order to avoid negative squared masses for h and H . Looking at these equations, we conclude that in order to preserve the masses positive, v_t must satisfy,

$$v_t \lesssim \frac{(\lambda v)^2}{\mu_{t2}}, \quad (4.33)$$

where we assume $\lambda v \sim 100$ GeV. For instance, $\mu_{t2} \sim 10^{14}$ GeV implies $v_t \lesssim 10^{-1}$ eV. Thus, one may naturally generate small v_t taking μ_{t2} at a Grand Unification scale [162]. Notice that Eq. (4.33) is another kind of seesaw relation between v_t and μ_{t2} valid in the limit $v_t \ll \mu_{t2}$, which is independent of the relation in Eq. (4.17).

Now that we have finished with the scalar sector, we will derive the masses of the gauge bosons.

4.1.2 Mass Spectrum - Gauge Bosons

The Lagrangian for the kinetic terms of the gauge fields associated to the hypercharge $U(1)_Y$ and the $U(1)_X$ symmetry is given by,

$$\mathcal{L}_{\text{gauge}} = -\frac{1}{4}\hat{B}_{\mu\nu}\hat{B}^{\mu\nu} + \frac{\epsilon}{2\cos\theta_W}\hat{X}_{\mu\nu}\hat{B}^{\mu\nu} - \frac{1}{4}\hat{X}_{\mu\nu}\hat{X}^{\mu\nu}, \quad (4.34)$$

where ϵ is the kinetic mixing parameter.

Similarly to what was done in the Chapter 3, a canonical gauge kinetic Lagrangian is obtained through a $GL(2, R)$ transformation on the fields \hat{B}_μ and \hat{X}_μ ,

$$\begin{aligned} \hat{X}_\mu &\simeq X_\mu \\ \hat{B}_\mu &\simeq B_\mu + \frac{\epsilon}{\cos\theta_W}X_\mu, \end{aligned} \quad (4.35)$$

so that the covariant derivatives (4.10) and (4.11) become,

$$D_\mu\Phi_i = \partial_\mu\Phi_i + ig\tau^a W_\mu^a + ig'\frac{Y}{2}B_\mu\Phi_i + \frac{i}{2}G_{X_i}X_\mu\Phi_i, \quad (4.36)$$

$$D_\mu\Delta = \partial_\mu\Delta + ig[T^a W_\mu^a, \Delta] + ig'\frac{Y_t}{2}B_\mu\Delta + \frac{i}{2}G_{X_t}X_\mu\Delta, \quad (4.37)$$

where $G_{X_i} = g'\frac{\epsilon Y_i}{\cos\theta_W} + g_X Q_{X_i}$ and $G_{X_t} = g'\frac{\epsilon Y_t}{\cos\theta_W} + g_X q_{X_t}$.

After spontaneous symmetry breaking and performing the electroweak rotation,

$$\begin{aligned} B_\mu &= \cos\theta_W A_\mu - \sin\theta_W Z_\mu^0, \\ W_\mu^3 &= \sin\theta_W A_\mu + \cos\theta_W Z_\mu^0, \end{aligned}$$

the spectrum of vector bosons turns out to be comprised of: the charged W_μ^\pm ; the photon, A_μ ; two neutral states, Z_μ^0 and X_μ , mixing to each other. They have the following mass Lagrangian

$$\mathcal{L}_{\text{mass}} = m_W^2 W_\mu^- W^{+\mu} + \frac{1}{2} m_{Z^0 X}^2 Z_\mu^0 Z^{0\mu} - m_{Z^0 X}^2 Z_\mu^0 X^\mu + \frac{1}{2} m_X^2 X_\mu X^\mu, \quad (4.38)$$

where,

$$m_W^2 = \frac{1}{4} g^2 (v^2 + 2v_t^2), \quad (4.39)$$

$$m_{Z^0}^2 = \frac{1}{4} g_Z^2 (v^2 + 4v_t^2), \quad (4.40)$$

$$m_{Z^0 X}^2 = \frac{1}{4} g_Z (G_{X1} v_1^2 + G_{X2} v_2^2 + 2G_{Xt} v_t^2), \quad (4.41)$$

$$m_X^2 = \frac{1}{4} (v_1^2 G_{X1}^2 + v_2^2 G_{X2}^2 + G_{Xt}^2 v_t^2), \quad (4.42)$$

with $g_Z^2 = g^2 + g'^2 = g^2 / \cos^2 \theta_W$, $v^2 = v_1^2 + v_2^2$ and $v^2 + 2v_t^2 = (246 \text{ GeV})^2$.

We see that the W_μ^\pm bosons are already the mass-eigenstates with mass m_W . The Z and Z' gauge bosons on the other hand mix and lead to the following mass matrix,

$$M_{Z'Z}^2 = \begin{pmatrix} m_{Z^0}^2 & -m_{Z^0 X}^2 \\ -m_{Z^0 X}^2 & m_X^2 \end{pmatrix}. \quad (4.43)$$

The diagonalization leads to,

$$\begin{aligned} m_Z^2 &= \frac{1}{2} \left[m_{Z^0}^2 + m_X^2 + \sqrt{(m_{Z^0}^2 - m_X^2)^2 + 4(m_{Z^0 X}^2)^2} \right], \\ m_{Z'}^2 &= \frac{1}{2} \left[m_{Z^0}^2 + m_X^2 - \sqrt{(m_{Z^0}^2 - m_X^2)^2 + 4(m_{Z^0 X}^2)^2} \right]. \end{aligned} \quad (4.44)$$

where,

$$\begin{pmatrix} Z_\mu \\ Z'_\mu \end{pmatrix} = \begin{pmatrix} \cos \xi & -\sin \xi \\ \sin \xi & \cos \xi \end{pmatrix} \begin{pmatrix} Z_\mu^0 \\ X_\mu \end{pmatrix}, \quad (4.45)$$

with ξ given by,

$$\tan 2\xi = \frac{2m_{Z^0 X}^2}{m_{Z^0}^2 - m_X^2}. \quad (4.46)$$

This mixing angle is constrained to be very small by the LEP electroweak precision measurements on the Z boson pole [163]. Thus,

$$\xi \simeq \frac{m_{Z^0 X}^2}{m_{Z^0}^2 - m_X^2}. \quad (4.47)$$

Also, as we are interested in a light Z' , we will assume the limit $m_{Z^0}^2 \gg m_X^2$ (which implies $m_{Z^0}^2 \gg m_{Z^0 X}^2$ as well). In this limit,

$$\xi \simeq \frac{m_{Z^0 X}^2}{m_{Z^0}^2}, \quad (4.48)$$

and we can write approximate expressions for the masses of Z and Z' as

$$\begin{aligned} m_{Z,Z'}^2 &= \frac{1}{2} \left\{ m_{Z^0}^2 + m_X^2 \pm (m_{Z^0}^2 - m_X^2) \left[1 + \frac{4(m_{Z^0 X}^2)^2}{(m_{Z^0}^2 - m_X^2)^2} \right]^{\frac{1}{2}} \right\} \\ &\simeq \frac{1}{2} \left[m_{Z^0}^2 + m_X^2 \pm \left(m_{Z^0}^2 - m_X^2 + \frac{2(m_{Z^0 X}^2)^2}{m_{Z^0}^2} \right) \right]. \end{aligned}$$

For the Z , we have

$$m_Z^2 \simeq m_{Z^0}^2 + \frac{(m_{Z^0 X}^2)^2}{m_{Z^0}^2},$$

and, at leading order, $m_Z^2 \simeq m_{Z^0}^2$,

$$m_Z^2 \simeq \frac{1}{4} g_Z^2 (v^2 + 4v_t^2). \quad (4.49)$$

For Z' ,

$$\begin{aligned} m_{Z'}^2 &\simeq m_X^2 - \frac{(m_{Z^0 X}^2)^2}{m_{Z^0}^2} \\ &\simeq \frac{g_X^2}{4} (Q_{X_1} - Q_{X_2})^2 \frac{v_1^2 v_2^2}{v^2} \left(1 - \frac{4v_t^2}{v^2} \right). \end{aligned}$$

In terms of β , defined by $\tan \beta = v_2/v_1$ (see Appendix B),

$$m_{Z'}^2 \simeq \frac{g_X^2}{4} (Q_{X_1} - Q_{X_2})^2 v^2 \sin^2 \beta \cos^2 \beta \left(1 - \frac{4v_t^2}{v^2} \right). \quad (4.50)$$

Note that the presence of the triplet induces only a tiny correction proportional to $(v_t/v)^2$, so that the addition of a triplet scalar cannot generate a heavy Z' , as opposed to the singlet case [164]. Thus, the Z' mass lies below the electroweak scale, being controlled by the value of g_X . For instance, taking $\tan \beta = 10$ and $Q_{X_1} - Q_{X_2} = 1$, $m_{Z'}$ varies from 1 MeV – 1 GeV, for g_X in the range of $10^{-3} - 10^{-1}$, regardless of the value of v_t , as long as $v_t < 2$ GeV.

In summary, we have proposed a type II seesaw mechanism for neutrino masses within the scope of 2HDM which prevent FCNI via gauge symmetries. Having discussed the mass spectrum of the model, we now will pay attention to some phenomenological constraints.

4.2 Phenomenological constraints

4.2.1 Electroweak Precision

In our model, the ρ parameter (see Eq. (1.22)) places an upper bound on the VEV of the triplet scalar, because it contributes to the masses of Z and W^\pm bosons according to eqs. (4.39) and (4.49), which translates into,

$$\rho = \frac{v^2 + 2v_t^2}{v^2 + 4v_t^2}. \quad (4.51)$$

Hence at 3σ level, we obtain,

$$v_t \leq 2.3 \text{ GeV}, \quad (4.52)$$

where we used $v^2 + 2v_t^2 = 246^2 \text{ GeV}^2$. As we are interested in a small v_t for the generation of tiny neutrino masses, this constraint can be easily satisfied in our model. Notice that as v_t becomes very small the scalar masses increase as can be seen, for instance in eq.(4.26) and eq.(4.31).

4.2.2 Collider Bounds

LHC - Z'

The $U(1)_X$ symmetry is spontaneously broken by the VEV of the doublets and the triplet, which also contributed to the mass generation of the Z' vector boson. As v_t is small and v is at the electroweak scale, the Z' mass will be at the electroweak scale or below, depending on the value of g_X and the other parameter such as $\tan \beta$. Such a light Z' is subject to a variety of experimental constraints, of the same nature as those discussed in Chapter 3. Notice that we have two possible Z' models ($U(1)_N$ or $U(1)_{Y'}$), one which resembles the sequential Z' model, and other the dark photon model. Concerning the latter, LHC bounds are weakened because the $Z' - Z$ mixing is necessarily small, and that would suppress its production cross section at the LHC [165, 166, 167].

As for the $U(1)_{Y'}$ model, we do not have much freedom since the SM fermions are charged under $U(1)_{Y'}$ the production cross section is much larger. In this scenario the LHC bounds are rather restrictive. Assuming $g_X = 1$ the LHC severely rules Z' masses below 3 TeV [168]. In our model the Z' mass is set by g_X . In order to have Z' masses around 100 GeV, g_X should be around 0.1, which is not sufficiently small to evade LHC

limits [116]. If we adopt $g_X = 0.01$ we will get $m_{Z'} = 1$ GeV, and for such small coupling we can easily evade LHC limits [116]. We have used eq. (4.50) and assumed Q_{X1} of the same order of Q_{X2} to find the corresponding Z' mass. We point out that the kinetic mixing parameter ϵ while not relevant for the Z' mass it is important to determine the Z' interactions with SM fermions. The conclusions drawn above are valid for sufficiently small kinetic mixing.

LHC - Doubly Charged Scalar

Regarding the scalar spectrum of our model, the most relevant ones come from LHC searches for heavy Higgs and triplet scalars. The cleanest signature signal is the doubly charged Higgs. We have then implemented the model in Madgraph [169, 170] and followed the recipe described in [171]. Assuming no hierarchy in the Yukawa couplings the doubly charged scalar decays essentially, with equal branching ratios, into charged leptons. That said, we found the current LHC bound with $\mathcal{L} = 36fb^{-1}$ of integrated luminosity and performed future prospects for the High Luminosity and High Energy LHC setups as summarized in the Table 4.2.

LHC 13TeV - $\mathcal{L} = 12.9fb^{-1}$	$m_{H^{++}} > 760$ GeV
LHC 13TeV - $\mathcal{L} = 36fb^{-1}$	$m_{H^{++}} > 980$ GeV
High-Luminosity LHC - $\mathcal{L} = 1000fb^{-1}$	$m_{H^{++}} > 1.9$ TeV
High-Energy LHC 27TeV, $\mathcal{L} = 1000fb^{-1}$	$m_{H^{++}} > 3$ TeV,

Table 4.2: Summary of collider bounds on the doubly charged scalar in our model using current and planned configurations. We used 13TeV of center-of-mass energy for the LHC configurations, whereas 27TeV for the high-energy upgrade. We can see that LHC and its upgrade will be paramount to probe the model up to the TeV scale.

In the light of current bounds our model is in agreement with existing bounds if we take $\mu_{t2} \leq v_i$ which predicts masses at the TeV scale as discussed previously. We highlight that we need couplings larger than one to find charged scalar masses above the TeV scale. Therefore, LHC and its planned upgrade will be important because it will probe a large portion of the model. The presence of a doubly charged scalar is the key signature of the type II seesaw mechanism.

4.2.3 LHC- Higgs

Now the Higgs decays to SM fermions and gauge bosons have been constrained [172, 173, 174], one can use Higgs data to place important limits on the model. The couplings of the Higgs-like scalar h with the SM fermions and gauge bosons are given by,

$$\mathcal{C}_{h\bar{f}f} = \frac{(s_\alpha c_{\alpha_2} - c_\alpha s_{\alpha_1} s_{\alpha_2})}{s_\beta} \mathcal{C}_{h\bar{f}f}^{SM} \quad (4.53)$$

$$\mathcal{C}_{hWW} = (c_\alpha c_{\alpha_1} c_\beta + s_\alpha c_{\alpha_2} s_\beta - c_\alpha s_{\alpha_1} s_{\alpha_2} s_\beta) \mathcal{C}_{hWW}^{SM} \quad (4.54)$$

$$\mathcal{C}_{hZZ} = (c_\alpha c_{\alpha_1} c_\beta + s_\alpha c_{\alpha_2} s_\beta - c_\alpha s_{\alpha_1} s_{\alpha_2} s_\beta) \mathcal{C}_{hZZ}^{SM}, \quad (4.55)$$

where $\mathcal{C}_{h\bar{f}f}^{SM} = \frac{m_f}{v}$, $\mathcal{C}_{hWW}^{SM} = \frac{1}{2}g^2v$ and $\mathcal{C}_{hZZ}^{SM} = \frac{1}{2}\frac{g^2v}{\cos^2\theta_W}$. In the expressions for the gauge bosons we have neglected small terms proportional to ϵ and $\sin\xi$. As shown in the Appendix B, the angles α_1 and α_2 (and also β_1 and β_2) are suppressed by v_t/v_2 , so they can be neglected at leading order. Taking $\alpha_1, \alpha_2 \rightarrow 0$ in the above expressions, we get,

$$\mathcal{C}_{h\bar{f}f} = \frac{s_\alpha}{s_\beta} \mathcal{C}_{h\bar{f}f}^{SM} \quad (4.56)$$

$$\mathcal{C}_{hWW} = c_{\beta-\alpha} \mathcal{C}_{hWW}^{SM} \quad (4.57)$$

$$\mathcal{C}_{hZZ} = c_{\beta-\alpha} \mathcal{C}_{hZZ}^{SM}, \quad (4.58)$$

with $c_{\beta-\alpha} \equiv \cos(\beta - \alpha)$. Therefore, when $\alpha_1, \alpha_2 \rightarrow 0$ and $\alpha = \beta$, we recover the alignment limit, in which h couples to the SM particles identically to the SM Higgs. For $\cos(\beta - \alpha) \sim 1$, $\tan\beta$ can take on essentially any value, as long as the Higgs-like decays are concerned.

Conversely, in this limit the couplings of the heavier Higgses H and H_t vanish, since they are proportional to $s_{\beta-\alpha}$ and s_{α_i} , respectively. An interesting signature of our model is the decay of the heavy Higgs H into gauge bosons [175]. From the Eq. (3.48) in the Chapter 3¹,

$$\Gamma(H \rightarrow Z'Z') = \frac{g^2}{128\pi} \frac{m_H^3}{m_{Z'}^2} (\delta \tan\beta)^4 \left(\frac{\cos^3\beta \cos\alpha - \sin^3\beta \sin\alpha}{\cos\beta \sin\beta} \right)^2. \quad (4.59)$$

This decay is kinematically available because the Z' gauge boson is very light. Depending on the magnitude of g_X , Z' might decay inside the detector. Thus, the possible signature of

¹Notice that the expression (3.48) refers to h instead of H . However, comparing Eqs.(3.46) and (4.19), we see that the convention used to define the α angle changes in the two situations (notice that the position of h and H are interchanged in the two expressions). Therefore, the equations for the h scalar in Chapter 3 correspond to the scalar H in this Chapter, and vice-versa.

this heavy scalar is the four lepton channel [176, 177]. However, if this channel becomes relevant, one has to check whether the decay of the SM-like Higgs $h \rightarrow Z'Z'$ is also significant, and assess the constraints. This is a possibility that deserves further analysis. Finally, regarding the charged Higgs H^+ , its coupling to fermions is suppressed by a factor of $\tan \beta$. Therefore, large values of $\tan \beta$ weakens the LHC limits. In summary, our model can be made fully consistent with the current constraints in the alignment limit.

Belle-II and KLOE2

Belle and KLOE collaborations represent e^+e^- colliders searching for light gauge bosons with the $\epsilon/2F^{\mu\nu}F'_{\mu\nu}$. The two models proposed here feature a similar term. In the $U(1)_N$ model SM fermions are uncharged under $U(1)_N$, thus the Z' will couple to SM fermions only via its mixing with the Z boson generated by the presence of the kinetic mixing. In this case, our model would be a UV complete version of the simplified dark photon model [178, 179]. This scenario for heavy Z' masses was investigated in [180]. For the $U(1)_{Y'}$ model, where the SM fermions are charged under the gauge symmetry, if we take $g_X \ll 1$ and $g_X < \epsilon$, again the model falls back to the dark photon model because the Z' interactions to SM via the kinetic mixing would be more pronounced, the experimental limits on dark photon become applicable to our study.

In summary, the experimental limits derived for dark photon models apply here, except in the case where $g_X \gg \epsilon$ and $m_{Z'} \gg 1$ GeV. Experimental collaborations usually display their bounds in terms of ϵ^2 . In Figure 4.2 we display a summary of the existing (gray) and planned (color) constraints. For $m_{Z'} \sim 10 - 30$ MeV, current bound imposes $\epsilon < 10^{-4}$, limiting the region of parameter of our model. Anyhow, we emphasize that we can still obey such bounds by taking g_X and ϵ to be very small as it is usually assumed in dark photon models.

4.2.4 Accelerators

There are several accelerators using electron/positron or hadronic beams which search for bremsstrahlung of dark photons or its appearance in meson decays. These bounds are inside the gray region in Figure 4.2. It is important to point out the future sensitivity on the flavor violating decay $\mu \rightarrow 3e$ [181], in case of no signal, will give rise to the upper limit in cyan. Moreover, The Heavy Photon Search Experiment (HPS) which

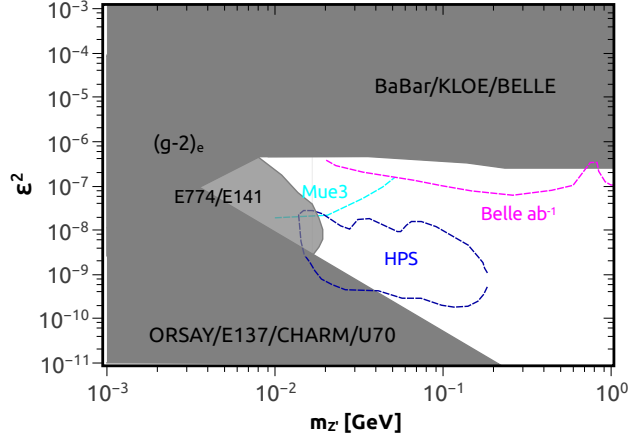


Figure 4.2: Summary of experimental limits applicable to the model $U(1)_N$ and to the model $U(1)_{Y'}$ assuming $g_X \ll \epsilon$. Current limits are in gray while projected ones in color.

was already installed at SLAC collides highly energetic electrons into a tungsten target, and in the process electrons may radiate dark photons. The experimental sensitivity of HPS is shown in blue.

4.2.5 Low Energy Probes

The muon anomalous magnetic moment $(g-2)$ [107], neutrino-electron scattering [182] and atomic parity violation [164] provide complementary but subdominant limits to our model. For instance, neutrino-electron scattering rules out $\epsilon > 10^{-5}$ [182]. One cannot accommodate $g-2$ with the $U(1)_{Y'}$ model because the electrons are charged under the gauge symmetry, and these couplings are subject to tight constraints [183, 184, 185]. In the $U(1)_N$ model, where our model resembles the dark photon one, the favored region to explain $g-2$ has already been excluded [107].

4.2.6 Dark Matter Possibility

In the two models described here, there are no dark matter candidates. One could simply add a vector-like fermion charged under the gauge symmetry while preserving the gauge anomaly cancellation. The dark matter relic abundance, direct detection and indirect detection signals would be governed by the kinetic mixing term and the g_X gauge coupling. For concreteness, if we take the $U(1)_N$ model, where SM fermions are not charged under the new gauge symmetry, the dark matter phenomenology would be similar to the dark photon portal investigated recently in the literature [186]. It has been shown

that in this setup if the dark matter mass is smaller than the Z' one, only s-channel processes would be relevant, and this case is nearly ruled out by current data for dark matter masses above 10 MeV. There is tiny region for $\epsilon \sim 10^{-5}$ and $m_{Z'} \sim 10$ MeV which obeys on existing limits and reproduce the correct relic density. If the dark matter particle is heavier than the Z' then the secluded dark matter setup arises [187], scenario which is much less restricted by data.

4.3 Discussion

There are important things to be stressed about the two models we proposed:

- The gauge symmetry imposed to distinguish Φ_1 from Φ_2 and then allow just one scalar doublet to couple to SM fermions gives rise to two very different type of models. In the $U(1)_N$ model, the SM fermions are uncharged under the gauge symmetry, and the corresponding massive Z' only couples to SM fermions via its mixing with the Z boson. In the $U(1)_{Y'}$ setup, the Z' gauge boson will have a neutral current with SM fermions determined by the $U(1)_{Y'}$ SM fermion charges, leading to a sequential Z' model [118].
- Since we have added a triplet scalar to explain neutrino masses via a type II seesaw mechanism, nothing prohibits one from considering off-diagonal Yukawa couplings, involving for instance the scalar triplet, to be non-vanishing. This will lead again to flavor changing interactions and give rise to $\mu \rightarrow e\gamma$, $\mu \rightarrow 3e$, $\mu - e$ conversion processes which are rather restricted by data. In particular, the product of the Yukawa terms are limited to be smaller than 10^{-7} [107]. Anyways, this feature is common in the models which extend the SM scalar sector and, thus, we can set to zero off-diagonal couplings involving the extra scalars without prejudice.
- The additional gauge symmetry allows us to easily introduce a dark matter candidate, a vector-like fermion, without spoiling the anomaly cancellation requirements. In summary, we argue that the addition of a gauge symmetry and a triplet scalar is well-motivated since it adds nice features to the original 2HDM proposal.
- The bounds discussed previously can be safely satisfied by taking g_X and ϵ to be sufficiently small, below 10^{-3} similarly to dark photon models.

In conclusion, in this Chapter we studied two models where neutrino masses are explained within the type II seesaw mechanism via the addition of a scalar triplet and a gauge symmetry that allows only one scalar doublet to couple to fermions. In this way we can simultaneously explain neutrino masses and avoid FCNI. We have investigated several constraints coming from low energy probes, electroweak precision and colliders. In particular, we derived collider bounds on the mass of the doubly charged scalar using current and planned LHC reach with high-luminosity and high-energy configurations. We discussed which regions of parameter space are consistent with current data to conclude that both models stand as viable alternatives to the original 2HDM proposal.

Chapter 5

Type I + II Seesaw in the Two Higgs Doublet Model

In the previous chapters we saw that the existence of right-handed neutrinos, scalar singlets or triplets allows different realizations of the seesaw mechanism. In view of the fact that there are several ways to accommodate neutrinos masses, in this Chapter we review these aspects in a general setting and show that one can combine the type I and type II seesaw, and assess under which conditions one seesaw dominates over the other. Several type I+II seesaw studies have been performed in the literature [188, 189, 190, 191, 192], but here we focus our discussion on the general realizations of type I, type II, and type I+II seesaw embedded in the well motivated 2HDM- $U(1)$ framework. We also highlight the general phenomenological features in each one of the scenarios.

5.1 Seesaw realizations in the 2HDM- $U(1)$

As discussed in Chapters 3 and 4, the charges of the fields under the $U(1)_X$ symmetry, which makes the 2HDM free from FCNI, are constrained by the Yukawa Lagrangian and by the anomaly cancellation. As we have seen, when there are right-handed neutrinos in the spectrum, the charges are given by,

$$\begin{aligned} q &= \frac{1}{2}(u + d) \quad , \quad l = -\frac{3}{2}(u + d) \quad , \quad Q_{X2} = \frac{1}{2}(u - d) \\ e &= -(2u + d) \quad , \quad n = -(u + 2d). \end{aligned} \tag{5.1}$$

For later convenience, we will refer to this as *charge assignment I* (see Table 5.1). However, it is also possible cancel the anomalies without extra fermions. In this case, in which the

BM	Fields	Charge Assignment	Yukawa Lagrangian	Seesaw Type	Neutrino Nature
1	N_R, Φ_s, Δ	I	$y^L \bar{L}_L^c i \sigma^2 \Delta L_L + y^D \bar{L}_L \tilde{\Phi}_2 N_R + y^R \bar{N}_R^c \Phi_s N_R$	Type I + II	Majorana
2	N_R, Φ_s	I	$y^D \bar{L}_L \tilde{\Phi}_2 N_R + y^R \bar{N}_R^c \Phi_s N_R$	Type I	Majorana
3	N_R, Δ	I	$y^L \bar{L}_L^c \Delta L_L + y^D \bar{L}_L \tilde{\Phi}_2 N_R$	Type II + Dirac	Majorana
4	N_R	I	$y^D \bar{L}_L \tilde{\Phi}_2 N_R$	Dirac	Dirac
5	Φ_s, Δ	II	$y^L \bar{L}_L^c \Delta L_L$	Type II	Majorana
6	Δ	II	$y^L \bar{L}_L^c \Delta L_L$	Type II	Majorana

Table 5.1: Summary of the six general benchmark cases in this work where we investigate neutrino mass generation with and without the presence of right-handed neutrinos, a scalar triplet, and scalar singlet. Each scenario yields different scalar potentials and neutrino masses. See text for details.

fermion content of the SM is maintained, the cancellation of the $[U(1)_X]^3$ anomaly forces the relation $u = -2d$, such that,

$$q = -\frac{d}{2} \quad , \quad l = \frac{3d}{2} \quad , \quad Q_{X_2} = -\frac{3d}{2}, \quad (5.2)$$

$$u = -2d \quad , \quad e = 3d,$$

We will refer to it as *charge assignment II*.

In this class of models, the implementation of the seesaw mechanism for the generation of neutrino masses calls for the presence of extra scalar fields. With right-handed neutrinos charged under $U(1)_X$, a bare Majorana mass term $M_R \bar{N}_R^c N_R$ is forbidden. Thus the type I seesaw mechanism cannot be realized. However, the inclusion of a scalar singlet Φ_s , allows for the coupling,

$$-\mathcal{L}_\nu = y^R \bar{N}_R^c \Phi_s N_R + h.c., \quad (5.3)$$

which, after spontaneous symmetry breaking of $U(1)_X$, generates a Majorana mass term. Note that Eq. (5.3) fixes the $U(1)_X$ charge of Φ_s as $q_{X_s} = 2u + 4d$.

If right-handed neutrinos are not included, neutrino masses can still be generated provided that we add to the model a scalar triplet, so that the Yukawa coupling,

$$-\mathcal{L}_\nu = y^L \bar{L}_L^c i \sigma^2 \Delta L_L + h.c., \quad (5.4)$$

generates a Majorana mass term for the neutrinos after Δ acquires a VEV. The term in Eq.(5.4) is only present if the $U(1)_X$ charge of Δ is $q_{X_t} = -3d$.

Notice that nothing forbids the possibility that these several fields may exist simultaneously, i. e., one can generate neutrino masses through type I and/or type II seesaw mechanisms in the 2HDM- $U(1)_X$ framework. Given the several ways to accommodate neutrino masses, we will divide them into six benchmark scenarios, as follows:

- **BM 1:** Is the scenario where right-handed neutrinos, a scalar triplet and a scalar singlet are added to the 2HDM, inducing a type I +II seesaw mechanism;
- **BM 2:** Concerns the setup where the 2HDM is augmented with only right-handed neutrinos and a scalar singlet, which leads to type I seesaw;
- **BM 3:** In this case, in addition to three right-handed neutrinos a scalar triplet is invoked, yielding a type II seesaw;
- **BM 4:** In this case only right-handed neutrinos are added to the 2HDM;
- **BM 5:** Refers to the case where there are no right-handed neutrinos but singlet and triplet scalar fields are invoked;
- **BM 6:** Is the setup where we simply add one scalar triplet.

We summarize these setups in Table 5.1 and will describe each one in more detail below.

5.1.1 Type I + II seesaw mechanism (BM 1)

It is possible to merge the Type I and Type II seesaw mechanisms by including both the scalar singlet and triplet. As right-handed neutrinos are also included, the charges follow the charge assignment I, under which the charge of the triplet is $q_{Xt} = 3(u + d)$. In this general case, the Yukawa Lagrangian relevant for neutrino masses is given by,

$$- \mathcal{L}_\nu = y^L \overline{L}_L^c i \sigma^2 \Delta L_L + y^D \bar{L}_L \tilde{\Phi}_2 N_R + y^R \overline{N}_R^c \Phi_s N_R + h.c. \quad (5.5)$$

As the scalars develop their respective VEVs, the neutrinos acquire masses according to

$$- \mathcal{L}_\nu = \frac{1}{2} \overline{\nu}_L^c M_L \nu_L + \bar{\nu}_L M_D N_R + \frac{1}{2} \overline{N}_R^c M_R N_R + h.c., \quad (5.6)$$

with,

$$\frac{1}{2} M_L = \frac{y^L v_t}{\sqrt{2}} \quad , \quad M_D = \frac{y^D v_2}{\sqrt{2}} \quad , \quad \frac{1}{2} M_R = \frac{y^R v_s}{\sqrt{2}}, \quad (5.7)$$

where v_t , v_2 and v_s are respectively the VEVs of Δ , Φ_2 and Φ_s . Although we have suppressed the flavor indices, it is to be understood that M_L , M_R , M_D and the corresponding Yukawa couplings are 3×3 matrices in flavor space.

We can arrange the left-handed active neutrinos and right-handed ones in a left-handed neutrino field as,

$$N_L = \begin{pmatrix} \nu_L \\ N_R^c \end{pmatrix}, \quad (5.8)$$

and rewrite Eq.(5.6) in a matrix form,

$$-\mathcal{L}_\nu = \frac{1}{2} \overline{N_L^c} M_\nu N_L + h.c., \quad (5.9)$$

with the mass matrix

$$M_\nu = \begin{pmatrix} M_L & M_D^T \\ M_D & M_R \end{pmatrix}, \quad (5.10)$$

whose eigenvalues give the physical neutrino masses.

As we are interested in estimating the order of magnitude of the physical neutrino masses, we will use the simplifying assumption that the matrices M_L , M_R and M_D are diagonal, i.e., $M_L = \text{diag}(m_L, m_L, m_L)$, $M_R = \text{diag}(m_R, m_R, m_R)$ and $M_D = \text{diag}(m_D, m_D, m_D)$, where these masses are real and positive. Consequently, M_ν reads,

$$M_\nu = \begin{pmatrix} m_L & 0 & 0 & m_D & 0 & 0 \\ 0 & m_L & 0 & 0 & m_D & 0 \\ 0 & 0 & m_L & 0 & 0 & m_D \\ m_D & 0 & 0 & m_R & 0 & 0 \\ 0 & m_D & 0 & 0 & m_R & 0 \\ 0 & 0 & m_D & 0 & 0 & m_R \end{pmatrix}, \quad (5.11)$$

and its eigenvalues are degenerate and given by,

$$m, M = \frac{1}{2} \left[m_L + m_R \mp \sqrt{4m_D^2 + (m_L - m_R)^2} \right], \quad (5.12)$$

where the minus (plus) sign corresponds to neutrino masses m (M). It should be clear that there are six eigenvalues actually, three of them equal to m and the others equal to M . This degeneracy is a result of our simplifying assumption on M_ν . Obviously, this scenario of mass degenerate neutrinos does not reproduce the neutrino oscillation data, but that can be easily achieved by letting M_L and M_D not be diagonal as shown in [193].

Depending on the relative sizes of m_D , m_R and m_L , there are several distinct scenarios for the neutrino masses. In the Table 5.2 approximate expressions for them are summarized, and the explicit derivation is shown in the Appendix C. We see that the

first four cases in Table 5.2 commonly feature $m_R \gg m_D$, i.e. the neutrino masses are essentially given by $m = m_L$ ($M = m_R$), so that to obtain active neutrino masses of order ~ 0.1 eV, m_L is forced to be very small, $m_L \lesssim 0.1$ eV.

In the next two rows which assume $m_D \gg m_R$, all the neutrinos are practically mass degenerate, with masses set by m_D , and are known as pseudo-Dirac neutrinos [194, 195, 196]. This scenario however is not realistic because, on one hand, CMB data constrains the sum of active neutrino masses [57],

$$\sum_i m_i \lesssim 0.1 \text{ eV}, \quad (5.13)$$

and on the other hand, stable right-neutrinos behave like dark matter, and successful structure formation impose, [197, 198, 199, 200, 201],

$$M \gtrsim 1 \text{ keV}, \quad (5.14)$$

ruling out this kind of pseudo-Dirac neutrinos. Nevertheless, if the right-handed neutrinos are unstable particles, then the bounds can be avoided and, in principle, would be possible to have M as low as 0.1 eV. Specifically in our model, this possibility could only be realized through the decay channel enabled by the Yukawa interaction,

$$-\mathcal{L}_\nu \supset y^D \bar{L}_L \tilde{\Phi}_2 N_R = \frac{y^D v_2}{\sqrt{2}} \bar{\nu}_L N_R + \frac{y^D}{\sqrt{2}} \bar{\nu}_L \rho_2 N_R,$$

where ρ_2 is the CP-even scalar of the Φ_2 doublet. However, with such a small mass of N_R this decay becomes kinematically forbidden, what makes right-handed neutrinos stable in our model, conclusively excluding this scenario.

In the last row, m_D and m_R being of the same order of magnitude imply that m and M are also of the same order or magnitude, but with m being slightly smaller than M , unless m_D and m_R are finely tuned. Therefore, this scenario is similar to the previous pseudo-Dirac case, in other words, ruled out.

Each one of the cases discussed previously will lead to a different scalar potential that we describe further. We remind the reader that we are focused on the 2HDM- $U(1)_X$ models where the doublet Φ_1 does not couple to the SM fermions. Therefore, there is freedom to choose different $U(1)_X$ charges, consequently leading to various scalar potentials. In general, the scalar potential can be written as,

$$V(\Phi_1, \Phi_2, \Phi_s, \Delta) = V_H + V_{NH}, \quad (5.15)$$

Limit	m	M	Neutrino Nature
$m_R \gg m_D \gg m_L$	$m_L - \frac{m_D^2}{2m_R}$	$m_R + \frac{m_D^2}{2m_R}$	Majorana
$m_R \gg m_L \gg m_D$	$m_L - \frac{m_L^2}{4m_R}$	$m_R + \frac{m_L^2}{4m_R}$	Majorana
$m_R \gg m_D, m_L$ and $m_D \sim m_L$	$m_L - \frac{m_D^2}{2m_R} - \frac{m_L^2}{4m_R}$	$m_R + \frac{m_D^2}{2m_R} + \frac{m_L^2}{4m_R}$	Majorana
$m_D \ll m_R, m_L$ and $m_R \sim m_L$	$m_L - \frac{m_D^2}{(m_R - m_L)}$	$m_R + \frac{m_D^2}{(m_R - m_L)}$	Majorana
$m_D \gg m_R \gg m_L$	$-m_D + \frac{1}{2}m_R - \frac{m_R^2}{8m_D}$	$m_D + \frac{1}{2}m_R + \frac{m_R^2}{8m_D}$	Pseudo-Dirac
$m_D \gg m_R, m_L$ and $m_R \sim m_L$	$-m_D + \frac{m_L + m_R}{2} - \frac{(m_L - m_R)^2}{8m_D}$	$m_D + \frac{m_L + m_R}{2} + \frac{(m_L - m_R)^2}{8m_D}$	Pseudo-Dirac
$m_L \ll m_R, m_D$ and $m_R \sim m_D$	$\frac{1}{2} \left[m_R - \sqrt{4m_D^2 + m_R^2} \right]$	$\frac{1}{2} \left[m_R + \sqrt{4m_D^2 + m_R^2} \right]$	Pseudo-Dirac

Table 5.2: Physical neutrino masses in different limits of the type I + II seesaw mechanism in 2HDM (benchmark scenario **BM 1**).

where V_H stands for the part of the potential that contains Hermitian terms,

$$\begin{aligned}
V_H = & m_1^2 \Phi_1^\dagger \Phi_1 + m_2^2 \Phi_2^\dagger \Phi_2 + m_s^2 \Phi_s^\dagger \Phi_s + m_t^2 \text{Tr}(\Delta^\dagger \Delta) + \lambda_1 (\Phi_1^\dagger \Phi_1)^2 + \lambda_2 (\Phi_2^\dagger \Phi_2)^2 \\
& + \lambda_s (\Phi_s^\dagger \Phi_s)^2 + \lambda_t [\text{Tr}(\Delta^\dagger \Delta)]^2 + \lambda_{tt} \text{Tr}(\Delta^\dagger \Delta)^2 + \lambda_3 (\Phi_1^\dagger \Phi_1) (\Phi_2^\dagger \Phi_2) + \lambda_4 (\Phi_1^\dagger \Phi_2) (\Phi_2^\dagger \Phi_1) \\
& + \lambda_{s1} (\Phi_1^\dagger \Phi_1) (\Phi_s^\dagger \Phi_s) + \lambda_{s2} (\Phi_2^\dagger \Phi_2) (\Phi_s^\dagger \Phi_s) + \lambda_{t1} (\Phi_1^\dagger \Phi_1) \text{Tr}(\Delta^\dagger \Delta) + \lambda_{t2} (\Phi_2^\dagger \Phi_2) \text{Tr}(\Delta^\dagger \Delta) \\
& + \lambda_{tt1} \Phi_1^\dagger \Delta \Delta^\dagger \Phi_1 + \lambda_{tt2} \Phi_2^\dagger \Delta \Delta^\dagger \Phi_2 + \lambda_{st} (\Phi_s^\dagger \Phi_s) \text{Tr}(\Delta^\dagger \Delta)
\end{aligned} \tag{5.16}$$

and V_{NH} corresponds to the remaining non-Hermitian ones.

There are three possibilities, depending on the charge of Φ_1 , Q_{X1} . These three possibilities rise after considering the Yukawa lagrangians which should remain intact. They read,

(i) for $Q_{X1} = \frac{1}{2}(5u + 7d)$ we get,

$$\begin{aligned}
V_{NH} = & \mu_s (\Phi_1^\dagger \Phi_2 \Phi_s + h.c.) + \mu_t (\Phi_1^T i \sigma^2 \Delta^\dagger \Phi_2 + h.c.) \\
& + \kappa'_1 (\Phi_1^T i \sigma^2 \Delta^\dagger \Phi_1 \Phi_s^\dagger + h.c.) \\
& + \kappa_2 (\Phi_2^T i \sigma^2 \Delta^\dagger \Phi_2 \Phi_s + h.c.);
\end{aligned} \tag{5.17}$$

(ii) for $Q_{X1} = \frac{3}{2}(u + d)$ we find,

$$V_{NH} = \mu_{t1} (\Phi_1^T i \sigma^2 \Delta^\dagger \Phi_1 + h.c.) + \kappa_2 (\Phi_2^T i \sigma^2 \Delta^\dagger \Phi_2 \Phi_s + h.c.); \tag{5.18}$$

(iii) and for $Q_{X1} = \frac{3}{2}(3u + 5d)$:

$$V_{NH} = \kappa' (\Phi_1^T i \sigma^2 \Delta^\dagger \Phi_2 \Phi_s^\dagger + h.c.) + \kappa_2 (\Phi_2^T i \sigma^2 \Delta^\dagger \Phi_2 \Phi_s + h.c.). \tag{5.19}$$

Notice that indeed there are three different distinct non-Hermitian scalar potentials which can be further modified depending on the presence or not of the scalar triplet and singlet field. We will consider these cases below.

5.1.2 Scalar singlet absent (BM 3)

In this section we shall consider the case in which the scalar sector is composed only by the doublets Φ_i and the triplet Δ . Without the scalar singlet Φ_s , the last term in equation (5.6) is absent, which amounts to a vanishing M_R , so that,

$$M_\nu = \begin{pmatrix} M_L & M_D^T \\ M_D & 0 \end{pmatrix}. \quad (5.20)$$

The eigenvalues of this matrix are,

$$m = \frac{1}{2} \left[\sqrt{4m_D^2 + m_L^2} - m_L \right], \quad (5.21)$$

and,

$$M = \frac{1}{2} \left[m_L + \sqrt{4m_D^2 + m_L^2} \right]. \quad (5.22)$$

In this setup there are *three* variants, summarized in Table 5.3. The first possibility is $m_D \gg m_L$. In this limit we get,

$$m, M \simeq m_D \mp \frac{1}{2}m_L + \frac{m_L^2}{8m_D},$$

which approximately means that,

$$m, M \simeq m_D. \quad (5.23)$$

Thus the neutrinos are pseudo-Dirac neutrinos, and as we discussed previously, this scenario is excluded.

The *second* possibility happens when $m_L \sim m_D$. If m_L and m_D are of the same order of magnitude the same happens for m and M , but with m being slightly smaller than M , unless again we invoke some fine tuning.

The *third* case occurs for $m_L \gg m_D$, which leads to,

$$m \simeq \frac{m_D^2}{m_L}, \quad (5.24)$$

and,

$$M \simeq m_L. \quad (5.25)$$

From eq.(5.24) we see that m can be very small for sufficiently large m_L . However, we must take into account the constraints coming from the ρ parameter, which preclude the VEV of the scalar triplet take on high values, thus limiting the maximum value of m_L . We

Limit	m	M	Neutrino Nature
$m_D \gg m_L$	m_D	m_D	pseudo-Dirac
$m_D \sim m_L$	$\frac{1}{2}[\sqrt{4m_D^2 + m_L^2} - m_L]$	$\frac{1}{2}[m_L + \sqrt{4m_D^2 + m_L^2}]$	Majorana
$m_D \ll m_L$	m_D^2/m_L	m_L	Majorana

Table 5.3: Physical neutrino masses in different limits of type II seesaw mechanism of benchmark scenario **BM 3** in 2HDM.

can expect $m_L \lesssim 1$ GeV as a reasonable upper limit. Therefore, the only way to achieve $m_L \gg m_D$ is to make the Yukawa couplings y^D very small. For example, assuming $v_2 \sim 100$ GeV and $m_L \sim 100$ MeV, we need $y^D \sim 10^{-8}$ to obtain $m \sim 0.1$ eV. Here, the right-handed neutrinos would have masses of $M \sim 100$ MeV. Right-handed neutrinos with masses around 100 MeV are fully consistent with structure formation bounds if they are potential dark matter candidates [202].

In this case, the Hermitian part of the potential is the same as the one in Eq. (5.16), omitting the terms which contain the singlet:

$$\begin{aligned}
V_H = & m_1^2 \Phi_1^\dagger \Phi_1 + m_2^2 \Phi_2^\dagger \Phi_2 + m_t^2 \text{Tr}(\Delta^\dagger \Delta) + \lambda_1 (\Phi_1^\dagger \Phi_1)^2 + \lambda_2 (\Phi_2^\dagger \Phi_2)^2 \\
& + \lambda_t [\text{Tr}(\Delta^\dagger \Delta)]^2 + \lambda_{tt} \text{Tr}(\Delta^\dagger \Delta)^2 + \lambda_3 (\Phi_1^\dagger \Phi_1) (\Phi_2^\dagger \Phi_2) + \lambda_4 (\Phi_1^\dagger \Phi_2) (\Phi_2^\dagger \Phi_1) \\
& + \lambda_{t1} (\Phi_1^\dagger \Phi_1) \text{Tr}(\Delta^\dagger \Delta) + \lambda_{t2} (\Phi_2^\dagger \Phi_2) \text{Tr}(\Delta^\dagger \Delta) + \lambda_{tt1} \Phi_1^\dagger \Delta \Delta^\dagger \Phi_1 + \lambda_{tt2} \Phi_2^\dagger \Delta \Delta^\dagger \Phi_2.
\end{aligned} \tag{5.26}$$

Regarding the non-Hermitian part of the potential there are some possibilities depending on the charge of Q_{X1} . Two straightforward possibilities are $Q_{X1} = \frac{1}{2}(5u + 7d)$ that yields,

$$V_{NH} = \mu_t (\Phi_1^T i \sigma^2 \Delta^\dagger \Phi_2 + h.c.), \tag{5.27}$$

and $Q_{X1} = \frac{3}{2}(u + d)$ which leads to,

$$V_{NH} = \mu_{t1} (\Phi_1^T i \sigma^2 \Delta^\dagger \Phi_1 + h.c.). \tag{5.28}$$

There is also a less obvious third option in which Q_{X1} remains free and u and d are not independent anymore, but satisfy $u = -2d$:

$$V_{NH} = \mu_{t2} (\Phi_2^T i \sigma^2 \Delta^\dagger \Phi_2 + h.c.). \tag{5.29}$$

The condition $u = -2d$ requires the scalar singlet to be neutral under the $U(1)_X$ symmetry, and thus it cannot break this symmetry spontaneously. However, as we are not including the singlet here, we do not have to worry about this. Note also that the condition

$u = -2d$ forces the right-handed neutrinos to have zero $U(1)_X$ charges. Consequently, the bare mass term $M_R \overline{N_R^c} N_R$ is now allowed going back to the case where a right-handed mass term is present. Albeit, the situation is fundamentally different because the entries of the matrix M_R are free parameters.

5.1.3 Scalar triplet absent - Type I seesaw (BM 2)

Without the presence of the scalar triplet, the first term in equation (5.5) is absent, so that,

$$-\mathcal{L}_{Y_{N_R}} = y_2^D \bar{L}_L \tilde{\Phi}_2 N_R + y^M \overline{N_R^c} \Phi_s N_R + h.c. \quad (5.30)$$

After spontaneous symmetry breaking, the Dirac and Majorana mass terms leads to the following mass matrix,

$$M_\nu = \begin{pmatrix} 0 & M_D^T \\ M_D & M_R \end{pmatrix} \quad (5.31)$$

The physical neutrino masses are,

$$m, M = \frac{1}{2} \left[m_R \pm \sqrt{4m_D^2 + m_R^2} \right]. \quad (5.32)$$

In the limit $m_R \gg m_D$, the type I seesaw mechanism is realized, so that,

$$m \simeq \frac{m_D^2}{m_R}, \quad (5.33)$$

$$M \simeq m_R. \quad (5.34)$$

In this scenario the scalar potential is uniquely defined with,

$$\begin{aligned} V = & m_1^2 \Phi_1^\dagger \Phi_1 + m_2^2 \Phi_2^\dagger \Phi_2 + m_s^2 \Phi_s^\dagger \Phi_s + \lambda_1 (\Phi_1^\dagger \Phi_1)^2 + \lambda_2 (\Phi_2^\dagger \Phi_2)^2 \\ & + \lambda_s (\Phi_s^\dagger \Phi_s)^2 + \lambda_3 (\Phi_1^\dagger \Phi_1) (\Phi_2^\dagger \Phi_2) + \lambda_4 (\Phi_1^\dagger \Phi_2) (\Phi_2^\dagger \Phi_1) \\ & + \lambda_{s1} (\Phi_s^\dagger \Phi_s) (\Phi_1^\dagger \Phi_1) + \lambda_{s2} (\Phi_s^\dagger \Phi_s) (\Phi_2^\dagger \Phi_2) + \mu_s (\Phi_1^\dagger \Phi_2 \Phi_s + h.c.), \end{aligned} \quad (5.35)$$

where $Q_{X1} = \frac{1}{2}(5u + 7d)$.

5.1.4 Scalar singlet and triplet absent - Dirac neutrinos (BM 4)

In the 2HDM without extra scalars, the Yukawa Lagrangian reduces to,

$$-\mathcal{L}_{Y_{N_R}} = y_2^D \bar{L}_L \tilde{\Phi}_2 N_R + h.c.. \quad (5.36)$$

In this case, the neutrinos are Dirac particles and acquire mass similarly to the other SM fermions,

$$m = \frac{y_2^D v_2}{\sqrt{2}}. \quad (5.37)$$

In this case, the smallness of neutrino masses requires small Yukawa couplings, as it happens when the SM is simply augmented by right-handed neutrinos. The scalar potential is given by,

$$\begin{aligned} V(\Phi_1, \Phi_2) = & m_1^2 \Phi_1^\dagger \Phi_1 + m_2^2 \Phi_2^\dagger \Phi_2 + \lambda_1 (\Phi_1^\dagger \Phi_1)^2 + \lambda_2 (\Phi_2^\dagger \Phi_2)^2 \\ & + \lambda_3 (\Phi_1^\dagger \Phi_1)(\Phi_2^\dagger \Phi_2) + \lambda_4 (\Phi_1^\dagger \Phi_2)(\Phi_2^\dagger \Phi_1), \end{aligned} \quad (5.38)$$

with the Φ_1 charge freely defined.

Since the scalar Φ_1 plays no role, in some models such scalar is assumed not to develop a vacuum expectation value as happens in the so-called scotogenic model [203, 204, 205]. It is nice to see that generally considering 2HDM- $U(1)_X$ models, one can find situations where such models mimic other well-known models in the literature. The key difference between them would be the presence of a Z' .

5.1.5 Right-handed neutrinos and scalar singlet absent - type II seesaw (BM 6)

In this setup only the first term in equation (5.5) is present, so that the matrix M_ν degenerates to a 3×3 matrix, $M_\nu = M_L$. The neutrino masses are given simply by,

$$m = \sqrt{2} y^L v_t. \quad (5.39)$$

In this case the potential is uniquely determined with,

$$\begin{aligned} V_H = & m_1^2 \Phi_1^\dagger \Phi_1 + m_2^2 \Phi_2^\dagger \Phi_2 + m_t^2 \text{Tr}(\Delta^\dagger \Delta) + \lambda_1 (\Phi_1^\dagger \Phi_1)^2 + \lambda_2 (\Phi_2^\dagger \Phi_2)^2 + \lambda_t [\text{Tr}(\Delta^\dagger \Delta)]^2 \\ & + \lambda_{tt} \text{Tr}(\Delta^\dagger \Delta)^2 + \lambda_3 (\Phi_1^\dagger \Phi_1)(\Phi_2^\dagger \Phi_2) + \lambda_4 (\Phi_1^\dagger \Phi_2)(\Phi_2^\dagger \Phi_1) + \lambda_{t1} (\Phi_1^\dagger \Phi_1) \text{Tr}(\Delta^\dagger \Delta) \\ & + \lambda_{t2} (\Phi_2^\dagger \Phi_2) \text{Tr}(\Delta^\dagger \Delta) + \lambda_{tt1} \Phi_1^\dagger \Delta \Delta^\dagger \Phi_1 + \lambda_{tt2} \Phi_2^\dagger \Delta \Delta^\dagger \Phi_2 + \mu_{t2} (\Phi_2^T i \sigma^2 \Delta^\dagger \Phi_2 + h.c.). \end{aligned} \quad (5.40)$$

where the Φ_1 charge is free. This is of course, the model studied in detail in Chapter 4.

5.1.6 Right-handed neutrinos absent - Type II seesaw + singlet (BM 5)

Similarly to the type II case, the neutrino masses are generated only by the scalar triplet. Therefore the expression for the neutrinos masses is the same as in Eq.(5.39). Concerning the scalars, the charge of Φ_1 and Φ_s are not fixed by Yukawa Lagrangian anymore, because right-handed neutrinos are absent. Fixing the value of q_{Xs} and keeping Q_{X1} free, we have the Hermitian part of the potential V_H identical to the one in the Eq. (5.40), and three possibilities for V_{NH} .

(i) For $q_{Xs} = Q_{X1} - Q_{X2}$ we find,

$$V_{NH} = \mu_s(\Phi_1^\dagger \Phi_2 \Phi_s + h.c.) + \mu_{t2}(\Phi_2^T i\sigma^2 \Delta^\dagger \Phi_2 + h.c.) + \kappa'(\Phi_1^T i\sigma^2 \Delta^\dagger \Phi_2 \Phi_s^\dagger + h.c.); \quad (5.41)$$

(ii) For $q_{Xs} = 2(Q_{X2} - Q_{X1})$ we obtain,

$$V_{NH} = \mu_{t2}(\Phi_2^T i\sigma^2 \Delta^\dagger \Phi_2 + h.c.) + \kappa_1(\Phi_1^T i\sigma^2 \Delta^\dagger \Phi_1 \Phi_s + h.c.); \quad (5.42)$$

(iii) For $q_{Xs} = 0$ we find,

$$V_{NH} = \mu_{t2}(\Phi_2^T i\sigma^2 \Delta^\dagger \Phi_2 \Phi_s^\dagger + h.c.) + \kappa_2(\Phi_2^T i\sigma^2 \Delta^\dagger \Phi_2 \Phi_s + h.c.). \quad (5.43)$$

In this last case, notice that the role of Φ_s is reduced because it contributes neither to neutrino masses (as there are no right-handed neutrinos) nor to Z' one, because it is uncharged under $U(1)_X$ (see next section). Nevertheless, it does not mean that Φ_s is totally irrelevant, as it mixes with the other scalars and induces effects on the Higgs properties.

5.2 Discussion

One of the nice features of the 2HDM- $U(1)_X$ is the presence of a new gauge boson, a Z' , which can be heavy or light and have different properties. These features are determined mostly by the charge assignments of the particles under $U(1)_X$ and by the scalar content of the model. For models that follow the charge assignment II (see Table 5.1), there are only two nontrivial particular charge assignments: one in which $d = 0$ in Eq.(5.2), i.e. where all fermions are neutral under $U(1)_X$; and another where $d = -2/3$

that leads to fermions with $U(1)_X$ charges identical to the SM hypercharge. Different values for d are in fact not distinct from the case $d = -2/3$, because it represents simply a rescaling on the $U(1)_X$ gauge coupling, g_X . Therefore, charge assignment II gives rise either to a fermiophobic or a sequential Z' [206]. We emphasize that collider bounds on such sequential Z' bound are rather stringent, excluding Z' masses below ~ 5 TeV [207], and future projection for the LHC upgrade expects to rule masses up to 10 TeV [208].

For the models that follow charge assignment I, the freedom in u and d charges in Eq. (5.1) yields more possibilities, including the fermiophobic and sequential Z' of the previous case, but also, a multitude of other cases, like fermiophilic Z' , $X = B - L$, etc [164].

It is important to highlight that when there are scalar doublets, like in the model of section 5.1.4 (**BM 4**), the Z' mass tends to be of the same order of the Z mass or smaller, given that the VEV of the doublets cannot be arbitrarily large, since $v_1^2 + v_2^2 = (246 \text{ GeV})^2$. In order to evade the collider bounds g_X must be very small because for a sufficiently light Z' boson, LHC loses sensitivity.

In the case of sections 5.1.2 and 5.1.5 (**BM 3** and **BM 6**) in which the triplet is included besides the doublets, the condition from the W boson mass reads $v^2 + 4v_t^2 = (246 \text{ GeV})^2$. However, the contribution of v_t to the Z' mass is rather restricted because of the bound from the ρ parameter, $v_t < 2 \text{ GeV}$. Therefore, in all the cases in which there are only doublets and the triplet, the Z' is necessarily light. In particular, for a Z' lighter than Z , we can generally write,

$$m_{Z'}^2 = \frac{g_X^2}{4v^2} [(Q_{X1} - Q_{X2})^2 v_1 v_2 + q_{Xs}^2 v_s^2] (v^2 - 4v_t^2). \quad (5.44)$$

Notice that, even with the presence of the scalar singlet, Z' can be light as long as v_s is not so large and g_X is very small. We stress that this expression for a light Z' can be applied to the several specific cases treated above by setting to zero the VEV of the corresponding scalar that is absent. For sufficiently low mass, Z' can behave like a dark photon when g_X is small and the Z' interactions with fermions is dominated by the kinetic mixing term $\epsilon/2 F^{\mu\nu} F'_{\mu\nu}$, as discussed in the previous chapters. For g_X not so small, the Z' is allowed to have more general interactions with fermions.

As the VEV of the singlet is unconstrained from above, this means that Z' can be made very heavy and easily evade LHC bounds that lie at the TeV scale. In this case,

the contribution of v_s dominates and we can approximate,

$$m_{Z'} = \frac{1}{2}g_X q_{Xs} v_s. \quad (5.45)$$

Hence, as long as v_s is sufficiently large, we can easily accommodate a heavy Z' , so that the models we discussed can be made consistent with existing bounds, while featuring a light or heavy Z' . Although we have not mentioned the bounds on the scalar fields masses, they can be circumvented by considering v_t sufficiently small and v_s sufficiently large.

In summary, in the 2HDM- $U(1)$ framework, the $U(1)$ gauge symmetry suffices to explain the absence of FCNI, the presence of massive active neutrinos and dark matter. As far as neutrino masses are concerned, we proposed models that can successfully realize combinations of the type I and/or type II seesaw. We have shown that some possibilities are already excluded by data, while others remain viable, containing either relatively light or very heavy right-handed neutrinos. Such models stand as plausible alternatives to the 2HDM, because they are theoretically compelling, and also experimentally attractive for being subject to searches for right-handed neutrinos, dark matter, doubly charged scalars, dark photon or Z' fields.

Chapter 6

Conclusions and Perspectives

In this document, we have reviewed some key aspects of the Standard Model and neutrino masses. Later on, we have addressed the problem of neutrino masses in a well motivated Standard Model extension, Two Higgs Doublet Model, encompassing several implementations of the seesaw mechanism. We have shown that such Two Higgs Doublet Model is plagued with flavor changing neutral interactions, which are subject to stringent flavor bounds. We have proposed a solution to this flavor problem by implementing a new Abelian gauge symmetry that discriminates the two Higgs doublets present in our study. This discrimination is exactly what we need to solve the flavor problem. Nevertheless, this new gauge symmetry is anomalous and requires the existence of new chiral fermions. We have shown that the addition of three right-handed neutrinos suffices to keep the model anomaly free. These right-handed neutrinos are the key players of the so-called type I seesaw mechanism. There are other ways to cancel such gauge anomaly as we explored in this work and they lead to different and interesting phenomenological signatures and allow us to accommodate a type II seesaw. Moreover, a vector gauge boson arises as a result of this symmetry. This vector boson has been searched for at several low and high energy experiment and result of these searches have been explored in this document. Therefore, we discussed models that are capable of solving an important problem in the canonical Two Higgs Doublet Model, and in addition offer viable mechanism to generate neutrino masses. We highlight that these models free Two Higgs Doublet Models from flavor changing interactions and generate neutrino masses while being consistent with current data. Our findings were published in journals with high scientific impact as listed in the beginning of the document.

In the near future we plan to connect neutrino physics and dark matter to explore signatures at neutrino detectors, and tease out the correlation between neutrino mass ordering and lepton flavor violation.

Appendix A

Appendix A

A.1 Conditions for Anomaly Freedom

Generically we will call the $U(1)_X$ charges Y' , where $Y' = l, q, e, u, d$. The anomaly free conditions can be read as:

$[SU(3)_c]^2 U(1)_X$:

$$\begin{aligned}\mathcal{A} &= \text{Tr} \left[\left\{ \frac{\lambda^a}{2}, \frac{\lambda^b}{2} \right\} Y'_R \right] - \text{Tr} \left[\left\{ \frac{\lambda^a}{2}, \frac{\lambda^b}{2} \right\} Y'_L \right] \\ \mathcal{A} &\propto \sum_{\text{quarks}} Y'_R - \sum_{\text{quarks}} Y'_L = [3u + 3d] - [3 \cdot 2q] = 0.\end{aligned}$$

Therefore,

$$u + d - 2q = 0. \quad (\text{A.1})$$

$[SU(2)_L]^2 U(1)_X$:

$$\mathcal{A} = -\text{Tr} \left[\left\{ \frac{\sigma^a}{2}, \frac{\sigma^b}{2} \right\} Y'_L \right] \propto -\sum Y_L = -[2l + 3 \cdot 2q] = 0.$$

Therefore,

$$l = -3q. \quad (\text{A.2})$$

$[U(1)_Y]^2 U(1)_X$:

$$\begin{aligned}\mathcal{A} &= \text{Tr} [\{Y_R, Y_R\} Y'_R] - \text{Tr} [\{Y_L, Y_L\} Y'_L] \propto \sum Y_R^2 Y'_R - \sum Y_L^2 Y'_L \\ \mathcal{A} &\propto \left[(-2)^2 e + 3 \left(\frac{4}{3} \right)^2 u + 3 \left(-\frac{2}{3} \right)^2 d \right] - \left[2(-1)^2 l + 3 \cdot 2 \left(\frac{1}{3} \right)^2 q \right] = 0.\end{aligned}$$

Therefore,

$$6e + 8u + 2d - 3l - q = 0. \quad (\text{A.3})$$

$U(1)_Y [U(1)_X]^2$:

$$\begin{aligned}\mathcal{A} &= \text{Tr} [\{Y'_R, Y'_R\} Y_R] - \text{Tr} [\{Y'_L, Y'_L\} Y_L] \propto \sum Y_R Y_R'^2 - \sum Y_L Y_L'^2 \\ \mathcal{A} &\propto \left[(-2) e^2 + 3 \left(\frac{4}{3} \right) u^2 + 3 \left(-\frac{2}{3} \right) d^2 \right] - \left[2(-1) l^2 + 3 \cdot 2 \left(\frac{1}{3} \right) q^2 \right] = 0.\end{aligned}$$

Therefore,

$$-e^2 + 2u^2 - d^2 + l^2 - q^2 = 0. \quad (\text{A.4})$$

$[U(1)_X]^3$:

$$\begin{aligned}\mathcal{A} &= \text{Tr} [\{Y'_R, Y'_R\} Y'_R] - \text{Tr} [\{Y'_L, Y'_L\} Y'_L] \propto \sum Y_R'^3 - \sum Y_L'^3 \\ \mathcal{A} &\propto [e^3 + 3u^3 + 3d^3] - [2l^3 + 3 \cdot 2q^3] = 0.\end{aligned}$$

Therefore,

$$e^3 + 3u^3 + 3d^3 - 2l^3 - 6q^3 = 0. \quad (\text{A.5})$$

A.2 Gauge bosons

We will now derive the physical gauge boson spectrum, first of all let us write the covariant derivative Eq. (3.24) in terms of ϵ as

$$D_\mu = \partial_\mu + igT^a W_\mu^a + ig' \frac{Q_Y}{2} B_\mu + \frac{i}{2} \left(g' \frac{\epsilon Q_Y}{\cos \theta_W} + g_X Q_X \right) X_\mu, \quad (\text{A.6})$$

or explicitly,

$$D_\mu = \partial_\mu + \frac{i}{2} \begin{pmatrix} gW_\mu^3 + g'Q_Y B_\mu + G_X X_\mu & g\sqrt{2}W_\mu^+ \\ g\sqrt{2}W_\mu^- & -gW_\mu^3 + g'Q_Y B_\mu + G_X X_\mu \end{pmatrix}, \quad (\text{A.7})$$

where we defined for simplicity

$$G_{X_i} = \frac{g' \epsilon Q_{Y_i}}{\cos \theta_W} + g_X Q_{X_i} \quad (\text{A.8})$$

with Q_{Y_i} being the hypercharge of the scalar doublet under $SU(2)_L$, which in the 2HDM is taken to equal to +1 for both scalar doublets; Q_{X_i} is charge of the scalar doublet i under $U(1)_X$.

We will use $D_\mu \Phi_i$ to refer to the action of the covariant derivative on the i scalar doublet of $Y = 1$ ($i = 1, 2$). Disregarding the term ∂_μ we have

$$D_\mu \Phi_i = \frac{i}{2\sqrt{2}} \begin{pmatrix} gW_\mu^3 + g'B_\mu + G_{X_i} X_\mu & g\sqrt{2}W_\mu^+ \\ g\sqrt{2}W_\mu^- & -gW_\mu^3 + g'B_\mu + G_{X_i} X_\mu \end{pmatrix} \begin{pmatrix} 0 \\ v_i \end{pmatrix}, \quad (\text{A.9})$$

$$D_\mu \Phi_i = \frac{i}{2\sqrt{2}} v_i \begin{pmatrix} \sqrt{2} g W_\mu^+ \\ -g W_\mu^3 + g' B_\mu + G_{Xi} X_\mu \end{pmatrix}. \quad (\text{A.10})$$

Consequently,

$$\begin{aligned} (D_\mu \Phi_i)^\dagger (D^\mu \Phi_i) &= \frac{1}{4} v_i^2 g^2 W_\mu^- W^{+\mu} + \frac{1}{8} v_i^2 [g^2 W_\mu^3 W^{3\mu} + g'^2 B_\mu B^\mu + G_{Xi}^2 X_\mu X^\mu] \\ &\quad + \frac{1}{8} v_i^2 [-2gg' W_\mu^3 B^\mu - 2gG_{Xi} W_\mu^3 X^\mu + 2g'G_{Xi} B_\mu X^\mu]. \end{aligned} \quad (\text{A.11})$$

Carrying out the electroweak rotation as usual,

$$\begin{aligned} B_\mu &= \cos \theta_W A_\mu - \sin \theta_W Z_\mu^0 \\ W_\mu^3 &= \sin \theta_W A_\mu + \cos \theta_W Z_\mu^0, \end{aligned} \quad (\text{A.12})$$

we obtain

$$(D_\mu \Phi_i)^\dagger (D^\mu \Phi_i) = \frac{1}{4} v_i^2 g^2 W_\mu^- W^{+\mu} + \frac{1}{8} v_i^2 [g_Z^2 Z_\mu^0 Z^{0\mu} + G_{Xi}^2 X_\mu X^\mu - 2g_Z G_{Xi} Z_\mu^0 X^\mu], \quad (\text{A.13})$$

where $g_Z^2 = g^2 + g'^2 = g^2 / \cos^2 \theta_W$. As we can see, after the rotation Eq. (A.12) the field A_μ identified as the photon is massless, as it must be.

For the singlet Φ_S (with $Q_Y = 0$ and $T^a = 0$ and disregarding the ∂_μ term) we obtain

$$D_\mu \Phi_S = \frac{i}{2\sqrt{2}} v_s g_X q_X X_\mu, \quad (\text{A.14})$$

so that

$$(D_\mu \Phi_S)^\dagger (D^\mu \Phi_S) = \frac{1}{8} v_s^2 g_X^2 q_X^2 X_\mu X^\mu. \quad (\text{A.15})$$

Notice from Eq. (A.15) that the singlet only contributes to the $U(1)_X$ gauge boson mass. Then:

$$\begin{aligned} \mathcal{L}_{\text{mass}} &= (D_\mu \Phi_1)^\dagger (D^\mu \Phi_1) + (D_\mu \Phi_2)^\dagger (D^\mu \Phi_2) + (D_\mu \Phi_S)^\dagger (D^\mu \Phi_S) \\ &= \frac{1}{4} g^2 v^2 W_\mu^- W^{+\mu} + \frac{1}{8} g_Z^2 v^2 Z_\mu^0 Z^{0\mu} - \frac{1}{4} g_Z (G_{X1} v_1^2 + G_{X2} v_2^2) Z_\mu^0 X^\mu \\ &\quad + \frac{1}{8} (v_1^2 G_{X1}^2 + v_2^2 G_{X2}^2 + v_s^2 g_X^2 q_X^2) X_\mu X^\mu, \end{aligned} \quad (\text{A.16})$$

where $v^2 = v_1^2 + v_2^2$. Finally Eq. (A.16) can be written as

$$\mathcal{L}_{\text{mass}} = m_W^2 W_\mu^- W^{+\mu} + \frac{1}{2} m_{Z^0}^2 Z_\mu^0 Z^{0\mu} - \Delta^2 Z_\mu^0 X^\mu + \frac{1}{2} m_X^2 X_\mu X^\mu, \quad (\text{A.17})$$

where

$$m_W^2 = \frac{1}{4}g^2v^2, \quad (\text{A.18})$$

$$m_{Z^0}^2 = \frac{1}{4}g_Z^2v^2, \quad (\text{A.19})$$

$$\Delta^2 = \frac{1}{4}g_Z (G_{X1}v_1^2 + G_{X2}v_2^2), \quad (\text{A.20})$$

$$m_X^2 = \frac{1}{4}(v_1^2G_{X1}^2 + v_2^2G_{X2}^2 + v_s^2g_X^2q_X^2). \quad (\text{A.21})$$

Summarizing, after the symmetry breaking pattern of this model we realize that there is a remaining mixing between Z_μ^0 and X_μ , that may expressed through the matrix

$$m_{Z^0X}^2 = \frac{1}{2} \begin{pmatrix} m_{Z^0}^2 & -\Delta^2 \\ -\Delta^2 & m_X^2 \end{pmatrix}, \quad (\text{A.22})$$

or explicitly

$$m_{Z^0X}^2 = \frac{1}{8} \begin{pmatrix} g_Z^2v^2 & -g_Z (G_{X1}v_1^2 + G_{X2}v_2^2) \\ -g_Z (G_{X1}v_1^2 + G_{X2}v_2^2) & v_1^2G_{X1}^2 + v_2^2G_{X2}^2 + v_s^2g_X^2q_X^2 \end{pmatrix} \quad (\text{A.23})$$

The above expression Eq. (A.23) for the mixing between the Z_μ^0 and X_μ bosons is given as function of arbitrary $U(1)_X$ charges of doublets/singlet scalars. It is important to note that when $Q_{X1} = Q_{X2}$, and there is not singlet contribution, the determinant of the matrix Eq.(A.23) is zero.

Eq. (A.23) is diagonalized through a rotation $O(\xi)$

$$\begin{pmatrix} Z_\mu \\ Z'_\mu \end{pmatrix} = \begin{pmatrix} \cos \xi & -\sin \xi \\ \sin \xi & \cos \xi \end{pmatrix} \begin{pmatrix} Z_\mu^0 \\ X_\mu \end{pmatrix}, \quad (\text{A.24})$$

and its eigenvalues are:

$$\begin{aligned} m_Z^2 &= \frac{1}{2} \left[m_{Z^0}^2 + m_X^2 + \sqrt{(m_{Z^0}^2 - m_X^2)^2 + 4(\Delta^2)^2} \right] \\ m_{Z'}^2 &= \frac{1}{2} \left[m_{Z^0}^2 + m_X^2 - \sqrt{(m_{Z^0}^2 - m_X^2)^2 + 4(\Delta^2)^2} \right]. \end{aligned} \quad (\text{A.25})$$

The ξ angle is given by

$$\tan 2\xi = \frac{2\Delta^2}{m_{Z^0}^2 - m_X^2}. \quad (\text{A.26})$$

The expressions for the gauge boson masses above are general but not very intuitive. We will simplify these equations by working in the limit in which the mass mixing is small

and the Z' is much lighter than the Z boson. That said, we can find a reduced formula for the masses as follows

$$m_Z^2 \simeq \frac{1}{2} \left[m_{Z^0}^2 + \sqrt{m_{Z^0}^4 + 4(\Delta^2)^2} \right] \simeq \frac{1}{2} [m_{Z^0}^2 + m_{Z^0}^2].$$

In this case:

$$m_Z^2 \simeq m_{Z^0}^2 = \frac{1}{4} g_Z^2 v^2, \quad (\text{A.27})$$

being $g_Z = \frac{g}{\cos \theta_W}$. Similarly for the Z' one finds

$$\begin{aligned} m_{Z'}^2 &= \frac{1}{2} \left[m_{Z^0}^2 + m_X^2 - \sqrt{(m_{Z^0}^2 - m_X^2)^2 + 4(\Delta^2)^2} \right] \\ &= \frac{1}{2} \left\{ m_{Z^0}^2 + m_X^2 - (m_{Z^0}^2 - m_X^2) \left[1 + \frac{4(\Delta^2)^2}{(m_{Z^0}^2 - m_X^2)^2} \right]^{\frac{1}{2}} \right\} \\ &\simeq \frac{1}{2} \left\{ m_{Z^0}^2 + m_X^2 - (m_{Z^0}^2 - m_X^2) \left[1 + \frac{2(\Delta^2)^2}{(m_{Z^0}^2 - m_X^2)^2} \right] \right\} \\ &\simeq \frac{1}{2} \left[m_{Z^0}^2 + m_X^2 - m_{Z^0}^2 + m_X^2 - \frac{2(\Delta^2)^2}{m_{Z^0}^2} \right] \\ &\simeq m_X^2 - \frac{(\Delta^2)^2}{m_{Z^0}^2}, \end{aligned} \quad (\text{A.28})$$

We may also further simplify Eq. (A.28) by working out explicitly Δ in the small-mixing regime of interest. The mixing angle must satisfy $\xi \ll 1$ by the measurements of LEP experiment, i.e.

$$\tan 2\xi \simeq \sin 2\xi \simeq 2\xi \quad (\text{A.29})$$

with which one gets

$$\xi \simeq \frac{\Delta^2}{m_{Z^0}^2 - m_X^2}. \quad (\text{A.30})$$

For the case $m_{Z^0}^2 \gg m_X^2$ we find

$$\xi \simeq \frac{\Delta^2}{m_{Z^0}^2} = \frac{1}{g_Z} (G_{X1} \cos^2 \beta + G_{X2} \sin^2 \beta). \quad (\text{A.31})$$

Substituting the Eq. (A.8) into Eq. (A.31) we obtain

$$\xi \simeq \frac{1}{g_Z} \left[\left(\frac{g' \epsilon Q_{Y1}}{\cos \theta_W} + g_X Q_{X1} \right) \cos^2 \beta + \left(\frac{g' \epsilon Q_{Y2}}{\cos \theta_W} + g_X Q_{X2} \right) \sin^2 \beta \right]. \quad (\text{A.32})$$

which simplifies to

$$\xi \simeq \frac{1}{g_Z} \left[(g_X Q_{X1} \cos^2 \beta + g_X Q_{X2} \sin^2 \beta) + \left(\frac{g' \epsilon Q_{Y1}}{\cos \theta_W} \cos^2 \beta + \frac{g' \epsilon Q_{Y2}}{\cos \theta_W} \sin^2 \beta \right) \right]. \quad (\text{A.33})$$

Since both Higgs doublets have the same hypercharge equal to $+1$, $g' = e/\sin\theta_W$ and $g = e/\cos\theta_W$, we further reduce Eq. (A.33) to

$$\xi \simeq \frac{\Delta^2}{m_{Z^0}^2} = \frac{g_X}{g_Z}(Q_{X1}\cos^2\beta + Q_{X2}\sin^2\beta) + \epsilon\tan\theta_W, \quad (\text{A.34})$$

which can also be written as

$$\xi = \epsilon_Z + \epsilon\tan\theta_W \quad (\text{A.35})$$

where

$$\epsilon_Z \equiv \frac{g_X}{g_Z}(Q_{X1}\cos^2\beta + Q_{X2}\sin^2\beta). \quad (\text{A.36})$$

Eq. (A.34) is the general expression for the mass-mixing between the Z boson and the Z' stemming from an arbitrary $U(1)_X$ symmetry in the limit $m_{Z'} \ll m_Z$.

In particular, for the $B-L$ case it is straightforward to prove that Eq. (A.34) becomes

$$\xi \simeq \frac{\Delta^2}{m_{Z^0}^2} \simeq 2\frac{g_X}{g_Z}\cos^2\beta + \epsilon\tan\theta_W = \epsilon_Z + \epsilon\tan\theta_W, \quad (\text{A.37})$$

where

$$\epsilon_Z = 2\frac{g_X}{g_Z}\cos^2\beta, \quad (\text{A.38})$$

in agreement with [62]. The parameter ϵ_Z appears often throughout the manuscript via its connection to the ξ in Eq. (A.34).

Anyways, with Eq. (A.34) we can obtain the general expression for the Z' mass. To do so, we need a few ingredients. Firstly, notice that

$$\begin{aligned} \frac{\Delta^4}{m_Z^2} = & \frac{g_X^2 v^2}{4} Q_{X1} \cos^2\beta (1 - \sin^2\beta) + \frac{g_X^2 v^2}{2} Q_{X1} Q_{X2} \cos^2\beta \sin^2\beta \\ & + \frac{g_X^2 v^2}{4} Q_{X2}^2 \sin^2\beta (1 - \cos^2\beta) + \frac{g_Z^2 v^2 \epsilon^2}{4} \tan^2\theta_W \\ & + \frac{g_X g_Z v^2}{2} (Q_{X1} \cos^2\beta + Q_{X2} \sin^2\beta) \epsilon \tan\theta_W, \end{aligned} \quad (\text{A.39})$$

with m_Z^2 defined in Eq. (A.19). Secondly, expanding Eq. (A.21) we get

$$m_X^2 = \frac{1}{4} [v_1^2 (g_X Q_{X1} + g_Z \epsilon \tan\theta_W Q_{Y1})^2 + v_2^2 (g_X Q_{X2} + g_Z \epsilon \tan\theta_W Q_{Y2})^2 + v_s^2 g_X^2 q_X^2] \quad (\text{A.40})$$

which simplifies to

$$\begin{aligned} m_X^2 = & \frac{g_Z^2 \epsilon^2 \tan^2\theta_W v^2}{4} + \frac{g_X^2}{4} (Q_{X1}^2 v_1^2 + Q_{X2}^2 v_2^2) \\ & + \frac{g_X g_Z \epsilon \tan\theta_W}{2} (Q_{X1} v_1^2 + Q_{X2} v_2^2) + \frac{v_s^2 g_X^2 q_X^2}{4}. \end{aligned} \quad (\text{A.41})$$

Now substituting Eq. (A.39) and Eq. (A.41) into Eq. (A.28) we find

$$m_{Z'}^2 = \frac{v_s^2}{4} g_X^2 q_X^2 + \frac{g_X^2 v^2}{4} Q_{X1}^2 \sin^2 \beta \cos^2 \beta + \frac{g_X^2 v^2}{4} Q_{X2}^2 \cos^2 \beta \sin^2 \beta - \frac{g_X^2 v^2}{2} Q_{X1} Q_{X2} \cos^2 \beta \sin^2 \beta \quad (\text{A.42})$$

which reduces to

$$m_{Z'}^2 = \frac{v_s^2}{4} g_X^2 q_X^2 + \frac{g_X^2 v^2 \cos^2 \beta \sin^2 \beta}{4} (Q_{X1} - Q_{X2})^2. \quad (\text{A.43})$$

We emphasize that q_X , Q_{X1} , Q_{X2} are the charges under $U(1)_X$ of the singlet scalar, Higgs doublets Φ_1 and Φ_2 respectively, $\tan \beta = v_2/v_1$, $v = 246$ GeV, v_s sets the $U(1)_X$ scale of spontaneous symmetry breaking, and g_X is the coupling constant of the $U(1)_X$ symmetry. Eq. (A.43) accounts for the Z' mass for every single $U(1)_X$ models studied in this work.

A few remarks are in order:

- (i) The Z' mass is controlled by g_X . Thus in order to achieve $m_{Z'} \ll m_Z$ one needs to sufficiently suppress this coupling.
- (ii) The Z' mass is generated via spontaneous symmetry breaking and for this reason it depends on the v_s which sets the $U(1)_X$ breaking and v due to the $Z - Z'$ mass mixing.
- (iii) The Z' mass as expected depends on the $U(1)_X$ charges of the scalar doublets and the singlet scalar since they all enter into the covariant derivative of the respective scalar field from which the Z and Z' are obtained.
- (iv) If $(Q_{X1} - Q_{X2})^2$ is not much larger than four as occurs for many $U(1)_X$ models in Table 4.1, then $m_{Z'}$ is approximately

$$m_{Z'}^2 = \frac{v_s^2}{4} g_X^2 q_X^2. \quad (\text{A.44})$$

For instance, in the $B - L$ model, $Q_{X1} = 2$, $q_X = 2$, $Q_{X2} = 0$, implying that

$$B - L : m_{Z'}^2 = v_s^2 g_X^2 + g_X^2 v^2 \cos^2 \beta \sin^2 \beta. \quad (\text{A.45})$$

Setting $v_s = 1$ TeV, we need $g_X = 10^{-3} - 10^{-6}$ to achieve $m_{Z'} = 1$ MeV – 1 GeV. Notice that this small coupling constant is a feature common to all dark photon-like models such as ours.

A.3 δ Parameter

Defining $\tan \beta_d = \frac{v_s}{v_1}$, we can write $m_{Z'}$ from (A.43) as:

$$\begin{aligned} m_{Z'}^2 &= \frac{g_X^2 v^2 \cos^2 \beta [\sin^2 \beta (Q_{X1} - Q_{X2})^2 + \tan^2 \beta_d q_X^2]}{4}, \\ &= \frac{g_X^2 v^2 \cos^2 \beta [q_X^2 + \cos^2 \beta_d (\sin^2 \beta (Q_{X1} - Q_{X2})^2 - q_X^2)]}{4 \cos^2 \beta_d}, \end{aligned} \quad (\text{A.46})$$

$$\begin{aligned} \Rightarrow m_{Z'} &= g_X v \cos^2 \beta \frac{\sqrt{[q_X^2 + \cos^2 \beta_d (\sin^2 \beta (Q_{X1} - Q_{X2})^2 - q_X^2)]}}{2 \cos \beta \cos \beta_d}, \\ &= \frac{g_X v \cos^2 \beta}{\delta}, \end{aligned} \quad (\text{A.47})$$

with

$$\delta = \frac{2 \cos \beta \cos \beta_d}{\sqrt{[q_X^2 + \cos^2 \beta_d (\sin^2 \beta (Q_{X1} - Q_{X2})^2 - q_X^2)]}}. \quad (\text{A.48})$$

Even in this general scenario we realize that there is a relation among the masses of the neutral gauge bosons and ϵ_Z from Eq. (A.36):

$$\delta = \frac{m_Z}{m_{Z'}} \epsilon_Z. \quad (\text{A.49})$$

In the $B - L$ model where $Q_{X1} = 2, q_X = 2, Q_{X2} = 0$, δ from Eq. (A.48) is reduced to

$$\delta = \frac{\cos \beta \cos \beta_d}{\sqrt{1 - \cos^2 \beta \cos^2 \beta_d}}, \quad (\text{A.50})$$

and Eq. (A.49) is reproduced for the $m_{Z'}$ and δ values given in equations Eq. (A.45) and Eq. (A.50), respectively. In the doublets only case, $v_s = 0$, $\cos \beta_d = 1$ and consequently (A.50) becomes

$$\delta \tan \beta = 1. \quad (\text{A.51})$$

On the other hand, in the limit $v_2 \gg v_1$ and $v_s \gg v_1$:

$$\delta \simeq \cos \beta \cos \beta_d \simeq \frac{1}{\tan \beta \tan \beta_d}. \quad (\text{A.52})$$

A.4 Currents for Z and Z'

In this section we will derive the generalized interactions among fermions and gauge bosons from the following Lagrangian:

$$\mathcal{L}_{\text{fermion}} = \sum_{\text{fermions}} \bar{\Psi}^L i \gamma^\mu D_\mu \Psi^L + \bar{\Psi}^R i \gamma^\mu D_\mu \Psi^R. \quad (\text{A.53})$$

After the electroweak rotation (A.12) the covariant derivative Eq. (3.24) for neutral gauge bosons becomes (the charged interactions are the same as those of the SM):

$$D_\mu^L = igT^3 (\sin \theta_W A_\mu + \cos \theta_W Z_\mu^0) + ig' \frac{Q_Y}{2} (\cos \theta_W A_\mu - \sin \theta_W Z_\mu^0) + \frac{i}{2} \left(g' Q_Y \frac{\epsilon}{\cos \theta_W} + g_X Q_X \right) X_\mu. \quad (\text{A.54})$$

In Appendix A.2 we have demonstrated that after the final SSB process a mixing between Z_μ^0 and X_μ remains, and this is the origin of δ . Replacing Z_μ^0 and X_μ as function of the physical bosons Z_μ and Z'_μ , Eq. (A.24), we obtain

$$\begin{aligned} \bar{\Psi}^L i \gamma^\mu D_\mu^L \Psi^L = & -e Q_f \bar{\psi}_f^L \gamma^\mu \psi_f^L A_\mu \\ & - \left[g_Z (T_{3f}^L - Q_f \sin^2 \theta_W) \cos \xi - \frac{1}{2} (\epsilon g_Z Q_{Yf}^L \tan \theta_W + g_X Q_{Xf}^L) \sin \xi \right] \bar{\psi}_f^L \gamma^\mu \psi_f^L Z_\mu \\ & - \left[g_Z (T_{3f}^L - Q_f \sin^2 \theta_W) \sin \xi + \frac{1}{2} (\epsilon g_Z Q_{Yf}^L \tan \theta_W + g_X Q_{Xf}^L) \cos \xi \right] \bar{\psi}_f^L \gamma^\mu \psi_f^L Z'_\mu, \end{aligned} \quad (\text{A.55})$$

where the relations $g \sin \theta_W = g' \cos \theta_W = e$, $g_Z = g / \cos \theta_W$, $g' = g_Z \sin \theta_W$ and $T^3 + Q_Y/2 = Q_f$ have been used. For the right-handed fields it suffices to replace T_{3f}^L for $T_{3f}^R = 0$, in which case:

$$\begin{aligned} \bar{\Psi}^R i \gamma^\mu D_\mu^R \Psi^R = & -e Q_f \bar{\psi}_f^R \gamma^\mu \psi_f^R A_\mu \\ & - \left[-g_Z Q_f \sin^2 \theta_W \cos \xi - \frac{1}{2} (\epsilon g_Z Q_{Yf}^R \tan \theta_W + g_X Q_{Xf}^R) \sin \xi \right] \bar{\psi}_f^R \gamma^\mu \psi_f^R Z_\mu \\ & - \left[-g_Z Q_f \sin^2 \theta_W \sin \xi + \frac{1}{2} (\epsilon g_Z Q_{Yf}^R \tan \theta_W + g_X Q_{Xf}^R) \cos \xi \right] \bar{\psi}_f^R \gamma^\mu \psi_f^R Z'_\mu. \end{aligned} \quad (\text{A.56})$$

The generalized interactions among fermions and gauge bosons, Eq. (A.53), is the sum of the contributions (A.55) and (A.56), and can be written as follows:

$$\begin{aligned}
\mathcal{L}_{\text{fermion}} = & -eQ_f \bar{\psi}_f \gamma^\mu \psi_f A_\mu \\
& - \left[g_Z (T_{3f} - Q_f \sin^2 \theta_W) \cos \xi - \frac{1}{2} \epsilon g_Z Q_{Yf}^L \tan \theta_W \sin \xi \right] \bar{\psi}_f^L \gamma^\mu \psi_f^L Z_\mu \\
& - \left[-g_Z Q_f \sin^2 \theta_W \cos \xi - \frac{1}{2} \epsilon g_Z Q_{Yf}^R \tan \theta_W \sin \xi \right] \bar{\psi}_f^R \gamma^\mu \psi_f^R Z_\mu \\
& - \left[g_Z (T_{3f} - Q_f \sin^2 \theta_W) \sin \xi + \frac{1}{2} \epsilon g_Z Q_{Yf}^L \tan \theta_W \cos \xi \right] \bar{\psi}_f^L \gamma^\mu \psi_f^L Z'_\mu \\
& - \left[-g_Z Q_f \sin^2 \theta_W \sin \xi + \frac{1}{2} \epsilon g_Z Q_{Yf}^R \tan \theta_W \cos \xi \right] \bar{\psi}_f^R \gamma^\mu \psi_f^R Z'_\mu \\
& + \frac{1}{2} g_X Q_{Xf}^L \sin \xi \bar{\psi}_f^L \gamma^\mu \psi_f^L Z_\mu + \frac{1}{2} g_X Q_{Xf}^R \sin \xi \bar{\psi}_f^R \gamma^\mu \psi_f^R Z_\mu - \frac{1}{2} g_X Q_{Xf}^L \cos \xi \bar{\psi}_f^L \gamma^\mu \psi_f^L Z'_\mu \\
& - \frac{1}{2} g_X Q_{Xf}^R \cos \xi \bar{\psi}_f^R \gamma^\mu \psi_f^R Z'_\mu.
\end{aligned} \tag{A.57}$$

The last two lines of (A.57) are the contributions introduced when the charges of the fermions under $U(1)_X$ are non-zero. In Appendix A.5 we derive explicitly the neutral currents of both Z and Dark Z bosons of reference [62] ($Q_X^{L,R} = 0$ case). After that Eq. (A.57) can be written as

$$\begin{aligned}
\mathcal{L} = & -eJ_{em}^\mu A_\mu - \frac{g_Z}{2} J_{NC}^\mu Z_\mu - \left(\epsilon e J_{em}^\mu + \frac{\epsilon_Z g_Z}{2} J_{NC}^\mu \right) Z'_\mu \\
& + \frac{1}{4} g_X \sin \xi \left[(Q_{Xf}^R + Q_{Xf}^L) \bar{\psi}_f \gamma^\mu \psi_f + (Q_{Xf}^R - Q_{Xf}^L) \bar{\psi}_f \gamma^\mu \gamma_5 \psi_f \right] Z_\mu \\
& - \frac{1}{4} g_X \cos \xi \left[(Q_{Xf}^R + Q_{Xf}^L) \bar{\psi}_f \gamma^\mu \psi_f - (Q_{Xf}^R - Q_{Xf}^L) \bar{\psi}_f \gamma^\mu \gamma_5 \psi_f \right] Z'_\mu.
\end{aligned} \tag{A.58}$$

Eq. (A.58) is the general neutral current for all $U(1)_X$ models studied in this work. Since we are interested in the regime in which the mixing angle is much smaller than one, $\xi \ll 1$, and $g_X \ll 1$, then Z properties will be kept unmodified.

For concreteness, we shall obtain again the neutral current for a well-known model, such as the $U(1)_{B-L}$ model. In this case, we find

$$\begin{aligned}
\mathcal{L} = & -eJ_{em}^\mu A_\mu - \frac{g_Z}{2} J_{NC}^\mu Z_\mu - \left(\epsilon e J_{em}^\mu + \frac{\epsilon_Z g_Z}{2} J_{NC}^\mu \right) Z'_\mu \\
& - \frac{\epsilon_Z g_Z}{2} \left[\frac{a}{4 \cos^2 \beta} \bar{\psi}_f \gamma^\mu \psi_f \right] Z'_\mu,
\end{aligned} \tag{A.59}$$

Here $a = -2$ for charged leptons and $a = 2/3$ for quarks. Notice that in our case we have a new vector coupling for Z' when compared to the Z' of the Dark 2HDM [62].

A.5 Comparison with the 2HDM with Gauged $U(1)_N$

It is important to cross-check our findings with the existing literature. In [62] a 2HDM similar to the $U(1)_N$ model in Table 4.1 was studied. Therefore, in this setup all fermions are uncharged under the $U(1)_X$ symmetry, i.e. $Q_X^{L,R} = 0$. Using Eq. (A.57) the neutral current involving the Z boson reads

$$\mathcal{L}_Z = -\frac{g_Z}{2} \cos \xi J_{NC}^\mu Z_\mu - \epsilon g_Z \tan \theta_W \sin \xi \left[\left(\frac{T_{3f}}{2} - Q_f \right) \bar{\psi}_f \gamma^\mu \psi_f - \frac{T_{3f}}{2} \bar{\psi}_f \gamma^\mu \gamma_5 \psi_f \right] Z_\mu. \quad (\text{A.60})$$

Since the mixing angle (ξ) and the kinetic mixing (ϵ) are much smaller than one, only the SM neutral current, the first term of Eq. (A.60) is left. In other words, the Z properties are kept identical to the SM.

As for the neutral current of the Z' boson, we get from Eq. (A.57) that

$$\begin{aligned} \mathcal{L}_{Z'} = & -g_Z \sin \xi \left[\left(\frac{T_{3f}}{2} - Q_f \sin^2 \theta_W \right) \bar{\psi}_f \gamma^\mu \psi_f - \frac{T_{3f}}{2} \bar{\psi}_f \gamma^\mu \gamma_5 \psi_f \right] Z'_\mu \\ & + \epsilon g_Z \tan \theta_W \cos \xi \left[\left(\frac{T_{3f}}{2} - Q_f \right) \bar{\psi}_f \gamma^\mu \psi_f - \frac{1}{2} T_{3f} \bar{\psi}_f \gamma^\mu \gamma_5 \psi_f \right] Z'_\mu. \end{aligned} \quad (\text{A.61})$$

Using Eq. (A.37) and taking $\xi \ll 1$, we find

$$\mathcal{L}_{Z'} = -\epsilon e Q_f \bar{\psi}_f \gamma^\mu \psi_f Z'_\mu - \frac{\epsilon_Z g_Z}{2} [(T_{3f} - 2Q_f \sin^2 \theta_W) \bar{\psi}_f \gamma^\mu \psi_f - T_{3f} \bar{\psi}_f \gamma^\mu \gamma_5 \psi_f] Z'_\mu \quad (\text{A.62})$$

which simplifies to

$$\mathcal{L}_{Z'} = -\left(\epsilon e J_{em}^\mu + \frac{\epsilon_Z g_Z}{2} J_{NC}^\mu \right) Z'_\mu. \quad (\text{A.63})$$

Our limiting case of the $U(1)_N$ model matches the result of [62], once again validating our findings.

A.6 Higgs Interactions to Vector Bosons

In this section we summarize the Higgs-gauge boson vertices under the assumption that the mixing between the Higgs doublets and the singlet scalar is suppressed. We find that

$$\mathcal{C}_{H-Z-Z} = \frac{g_Z^2 v}{2} \cos(\beta - \alpha), \quad (\text{A.64})$$

$$\mathcal{C}_{H-Z-Z'} = -g_Z g_X v \cos \beta \sin \beta \sin(\beta - \alpha), \quad (\text{A.65})$$

$$\mathcal{C}_{H-Z'-Z'} = 2g_X^2 v \cos \beta \sin \beta (\cos^3 \beta \sin \alpha + \sin^3 \beta \cos \alpha), \quad (\text{A.66})$$

$$\mathcal{C}_{h-Z-Z} = \frac{g_Z^2 v}{2} \sin(\beta - \alpha), \quad (\text{A.67})$$

$$\mathcal{C}_{h-Z-Z'} = -g_Z g_X v \cos \beta \sin \beta \cos(\beta - \alpha), \quad (\text{A.68})$$

$$\mathcal{C}_{h-Z'-Z'} = 2g_X^2 v \cos \beta \sin \beta (\cos^3 \beta \sin \alpha - \sin^3 \beta \cos \alpha). \quad (\text{A.69})$$

Appendix B

Appendix B

In this Appendix we show in details how to obtain approximate expressions for the masses and mixing angles for the physical scalars in the relevant regime adopted in the Chapter 3, $v_i \sim 100$ GeV, $v_t \ll v_i$. In the first section we treat the CP-even scalars, and in the next we treat the charged scalars.

CP-even scalars

In general, it is not possible to obtain analytic expressions for the diagonalization of the mass matrix M_{CPeven}^2 , given in eq. (4.18). The masses of the neutral scalars (eigenvalues of that matrix) are given implicitly as the solutions of the polynomial equation,

$$ax^3 + bx^2 + cx + d = 0, \quad (\text{B.1})$$

with a , b , c and d given by,

$$a = 8v_1v_2v_t, \quad (\text{B.2})$$

$$b = -16v_1v_2v_t[\lambda_1v_1^2 + \lambda_2v_2^2 + v_t^2(\lambda_t + \lambda_{tt})] - 4\sqrt{2}\mu_{t2}(v_1^2v_2^2 + v_1^2v_t^2 + v_2^2v_t^2) \quad (\text{B.3})$$

$$\begin{aligned} c = & 8v_1v_2v_t[4\lambda_1\lambda_2v_1^2v_2^2 - (\lambda_3 + \lambda_4)^2v_1^2v_2^2 + (4\lambda_1\lambda_t - \lambda_{t1}^2)v_1^2v_t^2 + (4\lambda_2\lambda_t - \lambda_{t2}^2)v_2^2v_t^2 \\ & + 4\lambda_{tt}v_t^2(\lambda_1v_1^2 + \lambda_2v_2^2) - 2v_t^2(\lambda_{t1}\lambda_{tt1}v_1^2 + \lambda_{t2}\lambda_{tt2}v_2^2) - v_t^2(\lambda_{tt1}^2v_1^2 + \lambda_{tt2}^2v_2^2)] \\ & + 8\sqrt{2}\mu_{t2}[\lambda_1v_1^4(v_2^2 + v_t^2) + \lambda_2v_2^4(v_1^2 + v_t^2) + \lambda_tv_t^4(v_1^2 + v_2^2) + \lambda_{tt}v_t^4(v_1^2 + v_2^2) \\ & + (\lambda_3 + \lambda_4)v_1^2v_2^2v_t^2 + (\lambda_{t1} + \lambda_{t2})v_1^2v_2^2v_t^2 + (\lambda_{tt1} + \lambda_{tt2})v_1^2v_2^2v_t^2] \end{aligned} \quad (\text{B.4})$$

$$\begin{aligned}
d = & 16v_1^3v_2^3v_t^3\{\lambda_1(\lambda_{t2} + \lambda_{tt2})^2 + \lambda_2(\lambda_{t1} + \lambda_{tt1})^2 + (\lambda_t + \lambda_{tt})[(\lambda_3 + \lambda_4)^2 - 4\lambda_1\lambda_2] \\
& - (\lambda_3 + \lambda_4)(\lambda_{t1} + \lambda_{tt1})(\lambda_{t2} + \lambda_{tt2})\} - 4\sqrt{2}\mu_{t2}\{[4\lambda_1\lambda_2 - (\lambda_3 + \lambda_4)^2]v_1^4v_2^4 \\
& + [4\lambda_2(\lambda_t + \lambda_{tt}) - (\lambda_{t2} + \lambda_{tt2})^2]v_2^4v_t^4 + [4\lambda_1(\lambda_t + \lambda_{tt}) - (\lambda_{t1} + \lambda_{tt1})^2]v_1^4v_t^4\} \\
& + 8\sqrt{2}\mu_{t2}v_1^2v_2^2v_t^2\{[(\lambda_{t1} + \lambda_{tt1})(\lambda_{t2} + \lambda_{tt2}) - 2(\lambda_3 + \lambda_4)(\lambda_t + \lambda_{tt})]v_t^2 \\
& + [(\lambda_3 + \lambda_4)(\lambda_{t1} + \lambda_{tt1}) - 2\lambda_1(\lambda_{t2} + \lambda_{tt2})]v_1^2 + [(\lambda_3 + \lambda_4)(\lambda_{t2} + \lambda_{tt2}) - 2\lambda_2(\lambda_{t1} + \lambda_{tt1})]v_2^2\} \\
& - 16\mu_{t2}^2v_1v_2v_t[(\lambda_3 + \lambda_4)v_1^2v_2^2 + (\lambda_{t1} + \lambda_{tt1})v_1^2v_t^2 + (\lambda_{t2} + \lambda_{tt2})v_2^2v_t^2] + 8\sqrt{2}\mu_{t2}^3v_1^2v_2^2v_t^2,
\end{aligned} \tag{B.5}$$

This equation can be solved numerically once the set of parameters is fixed. For the mixing angles, it is very difficult even to furnish an equation that determine them in terms of the parameters of the potential, because of the difficulty in computing the eigenvectors of M_{CPeven}^2 .

There are some limits, however, in which these expressions are calculable. The idea is to take advantage of the different energy scales involved and decompose the original matrix into matrices whose entries belong to the same scale.

Let us decompose M_{CPeven}^2 ,

$$M_{\text{CPeven}}^2 = \begin{pmatrix} 2\lambda_1v_1^2 & (\lambda_3 + \lambda_4)v_1v_2 & (\lambda_{t1} + \lambda_{tt1})v_1v_t \\ (\lambda_3 + \lambda_4)v_1v_2 & 2\lambda_2v_2^2 & (\lambda_{t2} + \lambda_{tt2})v_2v_t - \sqrt{2}\mu_{t2}v_2 \\ (\lambda_{t1} + \lambda_{tt1})v_1v_t & (\lambda_{t2} + \lambda_{tt2})v_2v_t - \sqrt{2}\mu_{t2}v_2 & 2(\lambda_t + \lambda_{tt})v_t^2 + \frac{\mu_{t2}v_2^2}{\sqrt{2}v_t} \end{pmatrix},$$

in the following way,

$$\begin{aligned}
M_{\text{CPeven}}^2 &= M_1^2 + M_2^2 \\
&= v_1v_2 \begin{pmatrix} 2\lambda_1\frac{v_1}{v_2} & \lambda_3 + \lambda_4 & 0 \\ \lambda_3 + \lambda_4 & 2\lambda_2\frac{v_2}{v_1} & 0 \\ 0 & 0 & 0 \end{pmatrix} \\
&+ \sqrt{2}\mu_{t2}v_2 \begin{pmatrix} 0 & 0 & (\lambda_{t1} + \lambda_{tt1})\frac{v_1v_t}{\sqrt{2}\mu_{t2}v_2} \\ 0 & 0 & (\lambda_{t2} + \lambda_{tt2})\frac{v_t}{\sqrt{2}\mu_{t2}} - 1 \\ (\lambda_{t1} + \lambda_{tt1})\frac{v_1v_t}{\sqrt{2}\mu_{t2}v_2} & (\lambda_{t2} + \lambda_{tt2})\frac{v_t}{\sqrt{2}\mu_{t2}} - 1 & (\lambda_t + \lambda_{tt})\frac{2v_t^2}{\sqrt{2}\mu_{t2}v_2} + \frac{v_2}{2v_t} \end{pmatrix}.
\end{aligned} \tag{B.6}$$

The matrix M_1^2 would be the mixing matrix of the neutral scalars in case there were just the two doublets, while M_2^2 account for the effects of the presence of the triplet. Let us first consider the limit $v_t, \mu_{t2} \ll v_i$. In this case, the decomposition (B.6) makes it clear

that the triplet decouples from the doublets. The matrix M_1^2 remains the same and M_2^2 reduces to $M_2^2 = \text{diag}(0, 0, \mu_{t2}v_2^2/\sqrt{2}v_t)$, from which we obtain immediately the mass of H_t . To diagonalize M_1^2 we need only one mixing angle, so that we can make $\alpha_1, \alpha_2 \rightarrow 0$ in eq.(4.19), leading to the following physical fields,

$$\begin{pmatrix} h \\ H \\ H_t \end{pmatrix} = \begin{pmatrix} c_\alpha & s_\alpha & 0 \\ -s_\alpha & c_\alpha & 0 \\ 0 & 0 & 1 \end{pmatrix} \begin{pmatrix} \rho_1 \\ \rho_2 \\ \rho_t \end{pmatrix}$$

with α given by,

$$\tan 2\alpha = \frac{(\lambda_3 + \lambda_4)v_1v_2}{\lambda_1v_1^2 - \lambda_2v_2^2}. \quad (\text{B.7})$$

From the eigenvalues of M_1^2 and M_2^2 , we have the masses,

$$m_{h,H}^{\prime 2} = \lambda_1v_1^2 + \lambda_2v_2^2 \pm \sqrt{(\lambda_1v_1^2 - \lambda_2v_2^2)^2 + (\lambda_3 + \lambda_4)^2v_1^2v_2^2} \quad (\text{B.8})$$

$$m_{H_t}^2 = \frac{\mu_{t2}v_2^2}{\sqrt{2}v_t}, \quad (\text{B.9})$$

with $m'_h < m'_H$ ¹.

Now, relaxing the condition on μ_{t2} and allowing it to increase to the same order of v_i or higher, this comparatively large value of μ_{t2} produces a sizable perturbation on the spectrum obtained above, but as we will see, the mass expressions are somewhat similar to the ones obtained in eqs. (B.8) and (B.9). In this case, it is still possible to diagonalize the matrices M_1^2 and M_2^2 almost independently. First, as v_t is always taken to be small but now μ_{t2} can be large, M_2^2 can be approximated by,

$$M_2^2 = \sqrt{2}\mu_{t2}v_2 \begin{pmatrix} 0 & 0 & 0 \\ 0 & 0 & -1 \\ 0 & -1 & \frac{v_2}{2v_t} \end{pmatrix}. \quad (\text{B.10})$$

M_2^2 is diagonalized by moving to an intermediate basis (H_1, H_2, H_3) through a rotation R_{α_2} ,

$$\begin{pmatrix} H_1 \\ H_2 \\ H_3 \end{pmatrix} = \begin{pmatrix} 1 & 0 & 0 \\ 0 & c_{\alpha_2} & s_{\alpha_2} \\ 0 & -s_{\alpha_2} & c_{\alpha_2} \end{pmatrix} \begin{pmatrix} \rho_1 \\ \rho_2 \\ \rho_t \end{pmatrix}, \quad (\text{B.11})$$

¹The prime in $m_{h,H}^{\prime 2}$ was inserted here to differentiate these mass expressions from the masses $m_{h,H}^2$, given in eqs. (B.19) and (B.20), which are the masses of h and H calculated in another limit.

with,

$$\sin \alpha_2 = \frac{2v_t}{v_2} \quad , \quad \cos \alpha_2 \simeq 1, \quad (\text{B.12})$$

so that,

$$\begin{aligned} M_{2\text{diag}}^2 &= R_{\alpha_2} M_2^2 R_{\alpha_2}^T \\ &= \sqrt{2} \mu_{t2} v_2 \begin{pmatrix} 0 & 0 & 0 \\ 0 & -\frac{2v_t}{v_2} & O(\frac{v_t^2}{v_2^2}) \\ 0 & O(\frac{v_t^2}{v_2^2}) & \frac{v_2}{2v_t} \end{pmatrix}. \end{aligned} \quad (\text{B.13})$$

The effect of this rotation on M_1^2 is

$$R_{\alpha_2} M_1^2 R_{\alpha_2}^T = v_1 v_2 \begin{pmatrix} 2\lambda_1 \frac{v_1}{v_2} & (\lambda_3 + \lambda_4) c_{\alpha_2} & -(\lambda_3 + \lambda_4) s_{\alpha_2} \\ (\lambda_3 + \lambda_4) c_{\alpha_2} & 2\lambda_2 \frac{v_2}{v_1} c_{\alpha_2}^2 & -2\lambda_2 \frac{v_2}{v_1} s_{\alpha_2} c_{\alpha_2} \\ -(\lambda_3 + \lambda_4) s_{\alpha_2} & -2\lambda_2 \frac{v_2}{v_1} s_{\alpha_2} c_{\alpha_2} & 2\lambda_2 \frac{v_2}{v_1} s_{\alpha_2}^2 \end{pmatrix}. \quad (\text{B.14})$$

As $\sin \alpha_2 \ll 1$, at leading order we have $R_{\alpha_2} M_1^2 R_{\alpha_2}^T \simeq M_1^2$, and the rotation R_{α_2} does not change M_1^2 . Then, rotating M_1^2 by R_α , with α given in eq. (B.7), we move to the physical basis,

$$\begin{pmatrix} h \\ H \\ H_t \end{pmatrix} = \begin{pmatrix} c_\alpha & s_\alpha & 0 \\ -s_\alpha & c_\alpha & 0 \\ 0 & 0 & 1 \end{pmatrix} \begin{pmatrix} H_1 \\ H_2 \\ H_3 \end{pmatrix}, \quad (\text{B.15})$$

such that,

$$\begin{aligned} M_{1\text{diag}}^2 &= R_\alpha M_1^2 R_\alpha^T \\ &= \begin{pmatrix} m_h'^2 & 0 & 0 \\ 0 & m_H'^2 & 0 \\ 0 & 0 & 0 \end{pmatrix}, \end{aligned} \quad (\text{B.16})$$

where $m_h'^2$ and $m_H'^2$ are as given in eq. (B.8). This second rotation R_α , albeit diagonalize M_1^2 , tends to disturb the previous diagonalization of M_2^2 , by generating corrections to the diagonal elements and also off-diagonal elements in $M_{2\text{diag}}^2$,

$$M_{2\text{diag}}'^2 = R_\alpha M_{2\text{diag}}^2 R_\alpha^T = \sqrt{2} \mu_{t2} v_2 \begin{pmatrix} -2s_\alpha^2 \frac{v_t}{v_2} & O(\frac{v_t}{v_2}) & 0 \\ O(\frac{v_t}{v_2}) & -2c_\alpha^2 \frac{v_t}{v_2} & 0 \\ 0 & 0 & \frac{v_2}{2v_t} \end{pmatrix}. \quad (\text{B.17})$$

This matrix is diagonal up to $O(v_t/v_2)$ terms, which can be discarded for sufficiently small v_t . As we are interested in extracting the leading order correction to the masses of h and H , we shall keep the diagonal elements.

In summary what we have done is,

$$\begin{aligned}
\boldsymbol{\rho}^T M_{\text{CPeven}}^2 \boldsymbol{\rho} &= \boldsymbol{\rho}^T (M_1^2 + M_2^2) \boldsymbol{\rho} \\
&= \mathbf{H}_1^T (R_{\alpha_2} M_1^2 R_{\alpha_2}^T + R_{\alpha_2} M_2^2 R_{\alpha_2}^T) \mathbf{H}_1 \\
&\simeq \mathbf{H}_1^T (M_1^2 + M_{2\text{diag}}^2) \mathbf{H}_1 \\
&= \mathbf{H}^T (R_\alpha M_1^2 R_\alpha^T + R_\alpha M_{2\text{diag}}^2 R_\alpha^T) \mathbf{H} \\
\boldsymbol{\rho}^T M_{\text{CPeven}}^2 \boldsymbol{\rho} &\simeq \mathbf{H}^T (M_{1\text{diag}}^2 + M_{2\text{diag}}'^2) \mathbf{H}.
\end{aligned}$$

From,

$$M_{1\text{diag}}^2 + M_{2\text{diag}}'^2 = \begin{pmatrix} m_h'^2 - 2\sqrt{2}s_\alpha^2 \mu_{t2} v_t & 0 & 0 \\ 0 & m_H'^2 - 2\sqrt{2}c_\alpha^2 \mu_{t2} v_t & 0 \\ 0 & 0 & \frac{\mu_{t2} v_2^2}{\sqrt{2}v_t} \end{pmatrix}, \quad (\text{B.18})$$

we can read the scalar masses,

$$m_h^2 = \lambda_1 v_1^2 + \lambda_2 v_2^2 - \sqrt{(\lambda_1 v_1^2 - \lambda_2 v_2^2)^2 + (\lambda_3 + \lambda_4)^2 v_1^2 v_2^2} - 2\sqrt{2} \sin^2 \alpha \mu_{t2} v_t \quad (\text{B.19})$$

$$m_H^2 = \lambda_1 v_1^2 + \lambda_2 v_2^2 + \sqrt{(\lambda_1 v_1^2 - \lambda_2 v_2^2)^2 + (\lambda_3 + \lambda_4)^2 v_1^2 v_2^2} - 2\sqrt{2} \cos^2 \alpha \mu_{t2} v_t \quad (\text{B.20})$$

$$m_{H_t}^2 = \frac{\mu_{t2} v_2^2}{\sqrt{2}v_t}. \quad (\text{B.21})$$

Note that the expressions obtained agree with those given in eq. (B.8)-(B.9) if we take $\mu_{t2} \ll v_i$, as expected. The main difference in the expressions in these two limits is the presence of the correction terms $-2\sqrt{2} \sin^2 \alpha \mu_{t2} v_t$ and $-2\sqrt{2} \cos^2 \alpha \mu_{t2} v_t$ in m_h^2 and m_H^2 , respectively, which pushes down their values, making h and H lighter than it would be in the absence of the triplet. Notice also that in this approximation, we managed to perform the diagonalization using only two mixing angles, α and α_2 , instead of the three angles needed in the general case.

Charged scalars

In this section we will apply to the charged scalars mass matrix the same method used in the previous section for the neutral scalars. First note that the matrix (4.27),

$$M_{\text{Charged}}^2 = \frac{1}{2} \begin{pmatrix} -\lambda_4 v_2^2 - \lambda_{tt1} v_t^2 & \lambda_4 v_1 v_2 & \lambda_{tt1} v_1 v_t / \sqrt{2} \\ \lambda_4 v_1 v_2 & -\lambda_4 v_1^2 - \lambda_{tt2} v_t^2 + 2\sqrt{2} \mu_{t2} v_t & \frac{1}{2} (\sqrt{2} \lambda_{tt2} v_t - 4\mu_{t2}) v_2 \\ v_1 v_t \lambda_{tt1} / \sqrt{2} & \frac{1}{2} (\sqrt{2} \lambda_{tt2} v_t - 4\mu_{t2}) v_2 & \frac{\sqrt{2} \mu_{t2} v_2^2}{v_t} - \frac{1}{2} (\lambda_{tt1} v_1^2 + \lambda_{tt2} v_2^2) \end{pmatrix},$$

can be decomposed as,

$$\begin{aligned}
M_{\text{Charged}}^2 &= M_{1+}^2 + M_{2+}^2 \\
&= \frac{1}{2} \begin{pmatrix} -\lambda_4 v_2^2 & \lambda_4 v_1 v_2 & 0 \\ \lambda_4 v_1 v_2 & -\lambda_4 v_1^2 & 0 \\ 0 & 0 & 0 \end{pmatrix} \\
&\quad + \frac{1}{2} \begin{pmatrix} -\lambda_{tt1} v_t^2 & 0 & \lambda_{tt1} v_1 v_t / \sqrt{2} \\ 0 & -\lambda_{tt2} v_t^2 + 2\sqrt{2} \mu_{t2} v_t & \frac{1}{2}(\sqrt{2} \lambda_{tt2} v_t - 4\mu_{t2}) v_2 \\ v_1 v_t \lambda_{tt1} / \sqrt{2} & \frac{1}{2}(\sqrt{2} \lambda_{tt2} v_t - 4\mu_{t2}) v_2 & \frac{\sqrt{2} \mu_{t2} v_2^2}{v_t} - \frac{1}{2}(\lambda_{tt1} v_1^2 + \lambda_{tt2} v_2^2) \end{pmatrix}.
\end{aligned} \tag{B.22}$$

In the matrix M_{2+}^2 are contained all the mixing effects among the doublets and the triplet. If M_{2+}^2 vanished, there would be mixing only between the two doublets, as described by M_{1+}^2 , leading to a charged Goldstone boson and a charged physical scalar, as in the usual 2HDM. Let's again consider the limit $v_t, \mu_{t2} \ll v_i$, in which M_{1+}^2 remains the same and M_{2+}^2 reduces to $M_{2+}^2 = \text{diag}(0, 0, \sqrt{2} \mu_{t2} v_2^2 / 2v_t - \lambda_{tt1} v_1^2 / 2 - \lambda_{tt2} v_2^2 / 2)$, so that the triplet completely decouples from the doublets, which still mix with themselves. In this case, it is necessary only one angle in the diagonalization and we can make $\beta_1, \beta_2 \rightarrow 0$ in eq.(4.28), leading to the following physical fields,

$$\begin{pmatrix} G^+ \\ H^+ \\ H_t^+ \end{pmatrix} = \begin{pmatrix} c_\beta & s_\beta & 0 \\ -s_\beta & c_\beta & 0 \\ 0 & 0 & 1 \end{pmatrix} \begin{pmatrix} \phi_1^+ \\ \phi_2^+ \\ \Delta^+ \end{pmatrix}$$

with,

$$\tan 2\beta = \frac{2v_1 v_2}{v_1^2 - v_2^2}, \tag{B.23}$$

which can be put in the form $\tan 2\beta = 2 \tan \beta / (1 - \tan^2 \beta)$ by dividing numerator and denominator by v_1^2 , so that

$$\tan \beta = \frac{v_2}{v_1}. \tag{B.24}$$

The masses of H^+ and H_t^+ in this approximation are,

$$m_{H^+}^2 = -\frac{1}{2} \lambda_4 v^2, \tag{B.25}$$

$$m_{H_t^+}^2 = \frac{\mu_{t2} v_2^2}{\sqrt{2} v_t} - \frac{1}{4} (\lambda_{tt1} v_1^2 + \lambda_{tt2} v_2^2). \tag{B.26}$$

As mentioned early, for $\mu_{t2} \simeq v_t$ the mass of H_t^+ is small and may be in tension with existing bounds, so that in this limit $\mu_{t2}/v_t > 1$ is favored.

Now, allowing μ_{t2} be large but keeping v_t small, M_{2+}^2 reduces to,

$$M_{2+}^2 = \mu_{t2} \begin{pmatrix} 0 & 0 & 0 \\ 0 & \sqrt{2}v_t & -v_2 \\ 0 & -v_2 & \frac{v_2^2}{\sqrt{2}v_t} \end{pmatrix}. \quad (\text{B.27})$$

M_{2+}^2 is diagonalized by moving to an intermediate basis (H_1^+, H_2^+, H_3^+) through a rotation R_{β_2} ,

$$\begin{pmatrix} H_1^+ \\ H_2^+ \\ H_3^+ \end{pmatrix} = \begin{pmatrix} 1 & 0 & 0 \\ 0 & c_{\beta_2} & s_{\beta_2} \\ 0 & -s_{\beta_2} & c_{\beta_2} \end{pmatrix} \begin{pmatrix} \phi_1^+ \\ \phi_2^+ \\ \Delta^+ \end{pmatrix}, \quad (\text{B.28})$$

so that,

$$R_{\beta_2} M_{2+}^2 R_{\beta_2}^T = M_{2+\text{diag}}^2, \quad (\text{B.29})$$

with,

$$\sin \beta_2 = \frac{\sqrt{2}v_t}{\sqrt{v_2^2 + 2v_t^2}} \simeq \frac{\sqrt{2}v_t}{v_2}, \quad (\text{B.30})$$

and,

$$\cos \beta_2 = \frac{v_2}{\sqrt{v_2^2 + 2v_t^2}} \simeq 1. \quad (\text{B.31})$$

The effect of this rotation on M_{1+}^2 is

$$R_{\beta_2} M_{1+}^2 R_{\beta_2}^T = \frac{1}{2} \begin{pmatrix} -\lambda_4 v_2^2 & \lambda_4 v_1 v_2 c_{\beta_2} & \lambda_4 v_1 v_2 s_{\beta_2} \\ \lambda_4 v_1 v_2 c_{\beta_2} & -\lambda_4 v_1^2 c_{\beta_2}^2 + \frac{\lambda_{tt1} v_1^2 + \lambda_{tt2} v_2^2}{2} s_{\beta_2}^2 & -(\lambda_4 v_1^2 + \frac{\lambda_{tt1} v_1^2 + \lambda_{tt2} v_2^2}{2}) s_{\beta_2} c_{\beta_2} \\ -\lambda_4 v_1 v_2 s_{\beta_2} & (\lambda_4 v_1^2 + \frac{\lambda_{tt1} v_1^2 + \lambda_{tt2} v_2^2}{2}) s_{\beta_2} c_{\beta_2} & -\frac{\lambda_{tt1} v_1^2 + \lambda_{tt2} v_2^2}{2} s_{\beta_2}^2 + \lambda_4 v_1^2 c_{\beta_2}^2 \end{pmatrix} \quad (\text{B.32})$$

As $\sin \beta_2 \ll 1$, at leading order we have $R_{\beta_2} M_{1+}^2 R_{\beta_2}^T \simeq M_{1+}^2$, and the rotation R_{β_2} does not change M_{1+}^2 , as we wanted. Then, rotating M_{1+}^2 by a matrix R_β , with β given by eq. (B.24), we move to the physical basis,

$$\begin{pmatrix} G_1^+ \\ H^+ \\ H_t^+ \end{pmatrix} = \begin{pmatrix} c_\beta & s_\beta & 0 \\ -s_\beta & c_\beta & 0 \\ 0 & 0 & 1 \end{pmatrix} \begin{pmatrix} H_1^+ \\ H_2^+ \\ H_3^+ \end{pmatrix}. \quad (\text{B.33})$$

Note that this second rotation R_β does not disturb the diagonalization of M_{2+}^2 ,

$$R_\beta M_{2+\text{diag}}^2 R_\beta^T = \begin{pmatrix} c_\beta & s_\beta & 0 \\ -s_\beta & c_\beta & 0 \\ 0 & 0 & 1 \end{pmatrix} \begin{pmatrix} 0 & 0 & 0 \\ 0 & 0 & 0 \\ 0 & 0 & \frac{\mu_{t2} v_2^2}{\sqrt{2} v_t} \end{pmatrix} \begin{pmatrix} c_\beta & -s_\beta & 0 \\ s_\beta & c_\beta & 0 \\ 0 & 0 & 1 \end{pmatrix} = \begin{pmatrix} 0 & 0 & 0 \\ 0 & 0 & 0 \\ 0 & 0 & \frac{\mu_{t2} v_2^2}{\sqrt{2} v_t} \end{pmatrix} = M_{2+\text{diag}}^2. \quad (\text{B.34})$$

Thus, the diagonalization of M_{1+}^2 and M_{2+}^2 leads to,

$$M_{1+\text{diag}}^2 + M_{2+\text{diag}}^2 = \begin{pmatrix} 0 & 0 & 0 \\ 0 & -\frac{1}{2} \lambda_4 v^2 & 0 \\ 0 & 0 & \frac{\mu_{t2} v_2^2}{\sqrt{2} v_t} \end{pmatrix}, \quad (\text{B.35})$$

from which we obtain the masses for H^+ and H_t^+ ,

$$m_{H^+}^2 = -\frac{1}{2} \lambda_4 v^2, \quad (\text{B.36})$$

$$m_{H_t^+}^2 = \frac{\mu_{t2} v_2^2}{\sqrt{2} v_t}. \quad (\text{B.37})$$

As a consistency check, notice that taking the limit $v_t \ll v_i$ directly in the eqs. (4.29) and (4.30), we obtain as result the eqs. (B.36) and (B.37). Finally, note that for the diagonalization in this limit we need to use only two mixing angles, β and β_2 , instead of the three angles needed in the general case.

Appendix C

Appendix C

In this appendix we will describe in more detail the limiting cases of type I and type II seesaw dominance considering different scales for the m_R , m_D and m_L masses. We will consider the case in which we have the complete scalar sector, with the two doublets Φ_i , the triplet Δ and the singlet Φ_s , so that it is necessary to analyze the full mass matrix Eq.(5.11). As we assume that the block matrix components of M_ν have equal diagonal elements, we obtain degenerate eigenvalues given by,

$$m = \frac{1}{2} \left[m_L + m_R - \sqrt{4m_D^2 + (m_L - m_R)^2} \right], \quad (\text{C.1})$$

and,

$$M = \frac{1}{2} \left[m_L + m_R + \sqrt{4m_D^2 + (m_L - m_R)^2} \right]. \quad (\text{C.2})$$

As there are different limits, we can classify them based on the relative size of m_L, m_R and m_D :

- (i) The three variables are of the same order of magnitude:

$$m_D \sim m_R \sim m_L.$$

(ii) The three variables are of different orders:

$$m_R \gg m_D \gg m_L,$$

$$m_R \gg m_L \gg m_D,$$

$$m_L \gg m_D \gg m_R,$$

$$m_L \gg m_R \gg m_D,$$

$$m_D \gg m_R \gg m_L,$$

$$m_D \gg m_L \gg m_R.$$

(iii) Two of them are of the same order and the third one is much larger than the others:

$$m_R \gg m_D, m_L \quad \text{and} \quad m_D \sim m_L,$$

$$m_L \gg m_D, m_R \quad \text{and} \quad m_D \sim m_R,$$

$$m_D \gg m_R, m_L \quad \text{and} \quad m_R \sim m_L.$$

(iv) Two of them are of the same order and the third one is much smaller than the others:

$$m_L \ll m_R, m_D \quad \text{and} \quad m_D \sim m_R,$$

$$m_R \ll m_L, m_D \quad \text{and} \quad m_D \sim m_L,$$

$$m_D \ll m_R, m_L \quad \text{and} \quad m_R \sim m_L.$$

Instead of considering all these possibilities, we can deal with a reduced number of them, by noting that the masses m and M are symmetrical under the exchange of m_R and m_L . So, we are left with:

(i) The three variables are of the same order of magnitude:

$$m_D \sim m_R \sim m_L.$$

(ii) The three variables are of different orders:

$$m_R \gg m_D \gg m_L,$$

$$m_R \gg m_L \gg m_D,$$

$$m_D \gg m_R \gg m_L.$$

(iii) Two of them are of the same order and the third one is much larger than the others:

$$\begin{aligned} m_R &\gg m_D, m_L \quad \text{and} \quad m_D \sim m_L, \\ m_D &\gg m_R, m_L \quad \text{and} \quad m_R \sim m_L. \end{aligned}$$

(iv) Two of them are of the same order and the third one is much smaller than the others:

$$\begin{aligned} m_R &\ll m_L, m_D \quad \text{and} \quad m_D \sim m_L, \\ m_D &\ll m_R, m_L \quad \text{and} \quad m_R \sim m_L. \end{aligned}$$

The remaining cases are obtained by swapping m_R and m_L in the corresponding expressions.

For the case $m_D \sim m_R \sim m_L$, the Eq. (C.1) and Eq.(C.2) should be used without modification, as they are not amenable to simplifications in this regime. Now, for $m_R \gg m_D, m_L$, we can use the approximation:

$$\begin{aligned} \sqrt{4m_D^2 + (m_L - m_R)^2} &\simeq m_R \left(1 + \frac{m_D^2}{m_R^2} + \frac{m_L^2}{2m_R^2} - \frac{m_L}{m_R} \right) \\ &= m_R - m_L + \frac{m_D^2}{m_R} + \frac{m_L^2}{2m_R}. \end{aligned}$$

Then, using Eq. (C.1) and Eq.(C.2), we get,

• If $m_D \sim m_L$, then,

$$m \simeq m_L - \frac{m_D^2}{2m_R} - \frac{m_L^2}{4m_R}, \quad (\text{C.3})$$

and,

$$M \simeq m_R + \frac{m_D^2}{2m_R} + \frac{m_L^2}{4m_R}. \quad (\text{C.4})$$

• If $m_D \gg m_L$, then,

$$m \simeq m_L - \frac{m_D^2}{2m_R}, \quad (\text{C.5})$$

and,

$$M \simeq m_R + \frac{m_D^2}{2m_R}. \quad (\text{C.6})$$

- If $m_L \gg m_D$, then,

$$m \simeq m_L - \frac{m_L^2}{4m_R}, \quad (\text{C.7})$$

and,

$$M \simeq m_R + \frac{m_L^2}{4m_R}. \quad (\text{C.8})$$

Now, for $m_D \gg m_R, m_L$ we use the approximation:

$$\begin{aligned} \sqrt{4m_D^2 + (m_L - m_R)^2} &\simeq 2m_D \left[1 + \frac{(m_L - m_R)^2}{8m_D^2} \right] \\ &= 2m_D + \frac{(m_L - m_R)^2}{4m_D}. \end{aligned}$$

Hence:

- If $m_R \sim m_L$, then,

$$m \simeq -m_D + \frac{m_L + m_R}{2} - \frac{(m_L - m_R)^2}{8m_D}, \quad (\text{C.9})$$

and,

$$M \simeq m_D + \frac{m_L + m_R}{2} + \frac{(m_L - m_R)^2}{8m_D}. \quad (\text{C.10})$$

- If $m_R \gg m_L$, then,

$$m \simeq -m_D + \frac{1}{2}m_R - \frac{m_R^2}{8m_D}, \quad (\text{C.11})$$

and,

$$M \simeq m_D + \frac{1}{2}m_R + \frac{m_R^2}{8m_D}. \quad (\text{C.12})$$

Now, if $m_R \ll m_L, m_D$ and $m_L \sim m_D$:

$$\sqrt{4m_D^2 + (m_L - m_R)^2} \simeq \sqrt{4m_D^2 + m_L^2}.$$

Hence,

$$m \simeq \frac{1}{2} \left[m_L - \sqrt{4m_D^2 + m_L^2} \right], \quad (\text{C.13})$$

and,

$$M \simeq \frac{1}{2} \left[m_L + \sqrt{4m_D^2 + m_L^2} \right], \quad (\text{C.14})$$

Finally, for $m_D \ll m_R, m_L$ and $m_R \sim m_L$:

$$\begin{aligned} \sqrt{4m_D^2 + (m_L - m_R)^2} &= -(m_L - m_R) \left(1 + \frac{2m_D^2}{(m_L - m_R)^2} \right) \\ &= m_R - m_L - \frac{2m_D^2}{(m_L - m_R)}. \end{aligned}$$

Hence,

$$m \simeq m_L - \frac{m_D^2}{(m_R - m_L)}, \quad (\text{C.15})$$

and,

$$M \simeq m_R + \frac{m_D^2}{(m_R - m_L)}. \quad (\text{C.16})$$

Bibliography

- [1] R. N. Cahn, D. A. Dwyer, S. J. Freedman, W. C. Haxton, R. W. Kadel, Yu. G. Kolomensky, K. B. Luk, P. McDonald, G. D. Orebi Gann, and A. W. P. Poon, *White Paper: Measuring the Neutrino Mass Hierarchy*, in *Proceedings, 2013 Community Summer Study on the Future of U.S. Particle Physics: Snowmass on the Mississippi (CSS2013): Minneapolis, MN, USA, July 29-August 6, 2013*, 2013.
- [2] J. Alexander *et. al.*, *Dark Sectors 2016 Workshop: Community Report*, 2016.
- [3] A. Alves, S. Profumo, and F. S. Queiroz, *The dark Z' portal: direct, indirect and collider searches*, *JHEP* **04** (2014) 063.
- [4] S. Weinberg, *A Model of Leptons*, *Phys. Rev. Lett.* **19** (1967) 1264–1266.
- [5] S. L. Glashow, *Partial Symmetries of Weak Interactions*, *Nucl. Phys.* **22** (1961) 579–588.
- [6] **ATLAS** Collaboration, G. Aad *et. al.*, *Observation of a new particle in the search for the Standard Model Higgs boson with the ATLAS detector at the LHC*, *Phys. Lett.* **B716** (2012) 1–29.
- [7] **CMS** Collaboration, S. Chatrchyan *et. al.*, *Observation of a new boson at a mass of 125 GeV with the CMS experiment at the LHC*, *Phys. Lett.* **B716** (2012) 30–61.
- [8] G. C. Branco, P. M. Ferreira, L. Lavoura, M. N. Rebelo, M. Sher, and J. P. Silva, *Theory and phenomenology of two-Higgs-doublet models*, *Phys. Rept.* **516** (2012) 1–102.
- [9] **LHC Dark Matter Working Group** Collaboration, T. Abe *et. al.*, *LHC Dark Matter Working Group: Next-generation spin-0 dark matter models*, *arXiv:1810.09420* (2018).

- [10] P. W. Higgs, *Broken symmetries, massless particles and gauge fields*, *Phys.Lett.* **12** (1964) 132–133.
- [11] F. Englert and R. Brout, *Broken Symmetry and the Mass of Gauge Vector Mesons*, *Phys.Rev.Lett.* **13** (1964) 321–323.
- [12] **ATLAS, CMS** Collaboration, G. Aad *et. al.*, *Combined Measurement of the Higgs Boson Mass in pp Collisions at $\sqrt{s} = 7$ and 8 TeV with the ATLAS and CMS Experiments*, *Phys. Rev. Lett.* **114** (2015) 191803.
- [13] **Particle Data Group** Collaboration, M. Tanabashi *et. al.*, *Review of Particle Physics*, *Phys. Rev.* **D98** (2018), no. 3 030001.
- [14] I. J. R. Aitchison, *Supersymmetry and the MSSM: An Elementary introduction*, .
- [15] L. Randall and R. Sundrum, *A Large mass hierarchy from a small extra dimension*, *Phys. Rev. Lett.* **83** (1999) 3370–3373.
- [16] N. Arkani-Hamed, A. G. Cohen, and H. Georgi, *Electroweak symmetry breaking from dimensional deconstruction*, *Phys. Lett.* **B513** (2001) 232–240.
- [17] P. W. Graham, D. E. Kaplan, and S. Rajendran, *Cosmological Relaxation of the Electroweak Scale*, *Phys. Rev. Lett.* **115** (2015), no. 22 221801.
- [18] J. E. Kim and G. Carosi, *Axions and the Strong CP Problem*, *Rev. Mod. Phys.* **82** (2010) 557–602. [erratum: *Rev. Mod. Phys.* 91,no.4,049902(2019)].
- [19] E. W. Kolb, A. D. Linde, and A. Riotto, *GUT baryogenesis after preheating*, *Phys. Rev. Lett.* **77** (1996) 4290–4293.
- [20] D. E. Morrissey and M. J. Ramsey-Musolf, *Electroweak baryogenesis*, *New J. Phys.* **14** (2012) 125003.
- [21] M. Fukugita and T. Yanagida, *Baryogenesis Without Grand Unification*, *Phys. Lett.* **B174** (1986) 45–47.
- [22] C. L. Cowan, F. Reines, F. B. Harrison, H. W. Kruse, and A. D. McGuire, *Detection of the free neutrino: A Confirmation*, *Science* **124** (1956) 103–104.

- [23] C. S. Wu, E. Ambler, R. W. Hayward, D. D. Hoppes, and R. P. Hudson, *Experimental Test of Parity Conservation in Beta Decay*, *Phys. Rev.* **105** (1957) 1413–1414.
- [24] M. Goldhaber, L. Grodzins, and A. W. Sunyar, *Helicity of Neutrinos*, *Phys. Rev.* **109** (1958) 1015–1017.
- [25] B. T. Cleveland, T. Daily, R. Davis, Jr., J. R. Distel, K. Lande, C. K. Lee, P. S. Wildenhain, and J. Ullman, *Measurement of the solar electron neutrino flux with the Homestake chlorine detector*, *Astrophys. J.* **496** (1998) 505–526.
- [26] **Super-Kamiokande** Collaboration, Y. Fukuda *et. al.*, *Evidence for oscillation of atmospheric neutrinos*, *Phys. Rev. Lett.* **81** (1998) 1562–1567.
- [27] **SNO** Collaboration, Q. R. Ahmad *et. al.*, *Measurement of the rate of $\nu_e + d \rightarrow p + p + e^-$ interactions produced by 8B solar neutrinos at the Sudbury Neutrino Observatory*, *Phys. Rev. Lett.* **87** (2001) 071301.
- [28] B. Pontecorvo, *Neutrino Experiments and the Problem of Conservation of Leptonic Charge*, *Sov. Phys. JETP* **26** (1968) 984–988. [*Zh. Eksp. Teor. Fiz.*53,1717(1967)].
- [29] Z. Maki, M. Nakagawa, and S. Sakata, *Remarks on the unified model of elementary particles*, *Prog. Theor. Phys.* **28** (1962) 870–880. [,34(1962)].
- [30] C. Giunti and C. W. Kim, *Fundamentals of Neutrino Physics and Astrophysics*. 2007.
- [31] S. M. Bilenky and C. Giunti, *Neutrinoless double-beta decay: A brief review*, *Mod. Phys. Lett.* **A27** (2012) 1230015.
- [32] **DUNE** Collaboration, R. Acciarri *et. al.*, *Long-Baseline Neutrino Facility (LBNF) and Deep Underground Neutrino Experiment (DUNE)*, .
- [33] **KATRIN** Collaboration, M. Aker *et. al.*, *An improved upper limit on the neutrino mass from a direct kinematic method by KATRIN*, *Phys. Rev. Lett.* **123** (2019), no. 22 221802.
- [34] **KATRIN** Collaboration, M. Aker *et. al.*, *First operation of the KATRIN experiment with tritium*, *arXiv:1909.06069* (2019).

- [35] I. Esteban, M. C. Gonzalez-Garcia, M. Maltoni, I. Martinez-Soler, and T. Schwetz, *Updated fit to three neutrino mixing: exploring the accelerator-reactor complementarity*, *JHEP* **01** (2017) 087.
- [36] P. Langacker, *Grand Unified Theories and Proton Decay*, *Phys. Rept.* **72** (1981) 185.
- [37] T. D. Lee, *A Theory of Spontaneous T Violation*, *Phys. Rev.* **D8** (1973) 1226–1239. [,516(1973)].
- [38] A. T. Davies, C. D. Froggatt, G. Jenkins, and R. G. Moorhouse, *Baryogenesis constraints on two Higgs doublet models*, *Phys. Lett.* **B336** (1994) 464–470.
- [39] J. M. Cline, K. Kainulainen, and M. Trott, *Electroweak Baryogenesis in Two Higgs Doublet Models and B meson anomalies*, *JHEP* **11** (2011) 089.
- [40] Z.-G. Mou, P. M. Saffin, and A. Tranberg, *Cold Baryogenesis from first principles in the Two-Higgs Doublet model with Fermions*, *JHEP* **06** (2015) 163.
- [41] A. Alves, D. A. Camargo, A. G. Dias, R. Longas, C. C. Nishi, and F. S. Queiroz, *Collider and Dark Matter Searches in the Inert Doublet Model from Peccei-Quinn Symmetry*, *JHEP* **10** (2016) 015.
- [42] A. Celis, J. Fuentes-Martín, and H. Serôdio, *Effective Aligned 2HDM with a DFSZ-like invisible axion*, *Phys. Lett.* **B737** (2014) 185–190.
- [43] N. G. Deshpande and E. Ma, *Pattern of Symmetry Breaking with Two Higgs Doublets*, *Phys. Rev.* **D18** (1978) 2574.
- [44] Q.-H. Cao, E. Ma, and G. Rajasekaran, *Observing the Dark Scalar Doublet and its Impact on the Standard-Model Higgs Boson at Colliders*, *Phys. Rev.* **D76** (2007) 095011.
- [45] Ya. B. Zeldovich, I. Yu. Kobzarev, and L. B. Okun, *Cosmological Consequences of the Spontaneous Breakdown of Discrete Symmetry*, *Zh. Eksp. Teor. Fiz.* **67** (1974) 3–11. [Sov. Phys. JETP40,1(1974)].
- [46] E. A. Paschos, *Diagonal Neutral Currents*, *Phys. Rev.* **D15** (1977) 1966.

- [47] S. L. Glashow and S. Weinberg, *Natural Conservation Laws for Neutral Currents*, *Phys. Rev.* **D15** (1977) 1958.
- [48] M. Aoki, S. Kanemura, K. Tsumura, and K. Yagyu, *Models of Yukawa interaction in the two Higgs doublet model, and their collider phenomenology*, *Phys. Rev.* **D80** (2009) 015017.
- [49] M. Carena, I. Low, N. R. Shah, and C. E. M. Wagner, *Impersonating the Standard Model Higgs Boson: Alignment without Decoupling*, *JHEP* **04** (2014) 015.
- [50] J. F. Gunion and H. E. Haber, *The CP conserving two Higgs doublet model: The Approach to the decoupling limit*, *Phys. Rev.* **D67** (2003) 075019.
- [51] P. Ko, Y. Omura, and C. Yu, *A Resolution of the Flavor Problem of Two Higgs Doublet Models with an Extra $U(1)_H$ Symmetry for Higgs Flavor*, *Phys. Lett.* **B717** (2012) 202–206.
- [52] P. Minkowski, *$\mu \rightarrow e\gamma$ at a Rate of One Out of 10^9 Muon Decays?*, *Phys. Lett.* **67B** (1977) 421–428.
- [53] R. N. Mohapatra and G. Senjanovic, *Neutrino Mass and Spontaneous Parity Nonconservation*, *Phys. Rev. Lett.* **44** (1980) 912. [,231(1979)].
- [54] G. Lazarides, Q. Shafi, and C. Wetterich, *Proton Lifetime and Fermion Masses in an $SO(10)$ Model*, *Nucl. Phys.* **B181** (1981) 287–300.
- [55] R. N. Mohapatra and G. Senjanovic, *Neutrino Masses and Mixings in Gauge Models with Spontaneous Parity Violation*, *Phys. Rev.* **D23** (1981) 165.
- [56] J. Schechter and J. W. F. Valle, *Neutrino Masses in $SU(2) \times U(1)$ Theories*, *Phys. Rev.* **D22** (1980) 2227.
- [57] **Planck** Collaboration, P. A. R. Ade *et. al.*, *Planck 2015 results. XIII. Cosmological parameters*, *Astron. Astrophys.* **594** (2016) A13.
- [58] H. Davoudiasl, H.-S. Lee, and W. J. Marciano, *Muon Anomaly and Dark Parity Violation*, *Phys. Rev. Lett.* **109** (2012) 031802.

- [59] H. Davoudiasl, H.-S. Lee, and W. J. Marciano, '*Dark*' *Z* implications for Parity Violation, Rare Meson Decays, and Higgs Physics, *Phys. Rev.* **D85** (2012) 115019.
- [60] H. Davoudiasl, H.-S. Lee, I. Lewis, and W. J. Marciano, *Higgs Decays as a Window into the Dark Sector*, *Phys. Rev.* **D88** (2013), no. 1 015022.
- [61] H.-S. Lee and E. Ma, *Gauged $B - x_i L$ origin of R Parity and its implications*, *Phys. Lett.* **B688** (2010) 319–322.
- [62] H.-S. Lee and M. Sher, *Dark Two Higgs Doublet Model*, *Phys. Rev.* **D87** (2013), no. 11 115009.
- [63] H.-S. Lee, *Muon $g-2$ anomaly and dark leptonic gauge boson*, *Phys. Rev.* **D90** (2014), no. 9 091702.
- [64] H. Davoudiasl, H.-S. Lee, and W. J. Marciano, *Muon $g - 2$, rare kaon decays, and parity violation from dark bosons*, *Phys. Rev.* **D89** (2014), no. 9 095006.
- [65] B. Batell, R. Essig, and Z. Surujon, *Strong Constraints on Sub-GeV Dark Sectors from SLAC Beam Dump E137*, *Phys. Rev. Lett.* **113** (2014), no. 17 171802.
- [66] W. Rodejohann and C. E. Yaguna, *Scalar dark matter in the $B\hat{a}^{\prime}L$ model*, *JCAP* **1512** (2015), no. 12 032.
- [67] K. Kaneta, Z. Kang, and H.-S. Lee, *Right-handed neutrino dark matter under the $B - L$ gauge interaction*, *JHEP* **02** (2017) 031.
- [68] B. Batell, M. Pospelov, and B. Shuve, *Shedding Light on Neutrino Masses with Dark Forces*, *JHEP* **08** (2016) 052.
- [69] A. Alves, G. Arcadi, Y. Mambrini, S. Profumo, and F. S. Queiroz, *Augury of darkness: the low-mass dark Z' portal*, *JHEP* **04** (2017) 164.
- [70] K. S. Babu, C. F. Kolda, and J. March-Russell, *Implications of generalized $Z - Z'$ -prime mixing*, *Phys. Rev.* **D57** (1998) 6788–6792.
- [71] P. Langacker, *The Physics of Heavy Z' Gauge Bosons*, *Rev. Mod. Phys.* **81** (2009) 1199–1228.

- [72] S. Gopalakrishna, S. Jung, and J. D. Wells, *Higgs boson decays to four fermions through an abelian hidden sector*, *Phys. Rev.* **D78** (2008) 055002.
- [73] M. Klasen, F. Lyonnet, and F. S. Queiroz, *NLO+NLL collider bounds, Dirac fermion and scalar dark matter in the B-L model*, *Eur. Phys. J.* **C77** (2017), no. 5 348.
- [74] **E865** Collaboration, R. Appel *et. al.*, *A New measurement of the properties of the rare decay $K^+ \rightarrow \pi^+ e^+ e^-$* , *Phys. Rev. Lett.* **83** (1999) 4482–4485.
- [75] **NA48/2** Collaboration, J. R. Batley *et. al.*, *Precise measurement of the $K^{+-} \rightarrow \pi^+ e^+ e^-$ decay*, *Phys. Lett.* **B677** (2009) 246–254.
- [76] **Particle Data Group** Collaboration, C. Patrignani *et. al.*, *Review of Particle Physics*, *Chin. Phys.* **C40** (2016), no. 10 100001.
- [77] L. J. Hall and M. B. Wise, *Flavor Changing Higgs - Boson Couplings*, *Nucl. Phys.* **B187** (1981) 397–408.
- [78] A. J. Buras, *New physics patterns in ε'/ε and ε_K with implications for rare kaon decays and ΔM_K* , *JHEP* **04** (2016) 071.
- [79] A. Crivellin, G. D’Ambrosio, M. Hoferichter, and L. C. Tunstall, *Violation of lepton flavor and lepton flavor universality in rare kaon decays*, *Phys. Rev.* **D93** (2016), no. 7 074038.
- [80] N. H. Christ, X. Feng, A. Juttner, A. Lawson, A. Portelli, and C. T. Sachrajda, *First exploratory calculation of the long-distance contributions to the rare kaon decays $K \rightarrow \pi \ell^+ \ell^-$* , *Phys. Rev.* **D94** (2016), no. 11 114516.
- [81] M. Ibe, W. Nakano, and M. Suzuki, *Constraints on $L_\mu - L_\tau$ gauge interactions from rare kaon decay*, *Phys. Rev.* **D95** (2017), no. 5 055022.
- [82] C.-W. Chiang and P.-Y. Tseng, *Probing a dark photon using rare leptonic kaon and pion decays*, *Phys. Lett.* **B767** (2017) 289–294.
- [83] B. Batell, M. Pospelov, and A. Ritz, *Multi-lepton Signatures of a Hidden Sector in Rare B Decays*, *Phys. Rev.* **D83** (2011) 054005.

- [84] M. Freytsis, Z. Ligeti, and J. Thaler, *Constraining the Axion Portal with $B \rightarrow K l^+ l^-$* , *Phys. Rev.* **D81** (2010) 034001.
- [85] **BaBar** Collaboration, G. Eigen, *Branching Fraction and CP Asymmetry Measurements in Inclusive $B \rightarrow X_s l^+ l^-$ and $B \rightarrow X_s \gamma$ Decays from BaBar*, *Nucl. Part. Phys. Proc.* **273-275** (2016) 1459–1464.
- [86] **BaBar** Collaboration, B. Aubert *et. al.*, *Direct CP, Lepton Flavor and Isospin Asymmetries in the Decays $B \rightarrow K^{(*)} l^+ l^-$* , *Phys. Rev. Lett.* **102** (2009) 091803.
- [87] **Belle** Collaboration, J. T. Wei *et. al.*, *Measurement of the Differential Branching Fraction and Forward-Backward Asymmetry for $B \rightarrow K^{(*)} l^+ l^-$* , *Phys. Rev. Lett.* **103** (2009) 171801.
- [88] **ALEPH** Collaboration, R. Barate *et. al.*, *Search for an invisibly decaying Higgs boson in $e^+ e^-$ collisions at 189-GeV*, *Phys. Lett.* **B466** (1999) 50–60.
- [89] **L3** Collaboration, P. Achard *et. al.*, *Search for an invisibly-decaying Higgs boson at LEP*, *Phys. Lett.* **B609** (2005) 35–48.
- [90] **OPAL** Collaboration, G. Abbiendi *et. al.*, *Search for invisibly decaying Higgs bosons in $e^+ e^- \rightarrow Z0 h0$ production at $s^{*(1/2)} = 183\text{-GeV} - 209\text{-GeV}$* , *Phys. Lett.* **B682** (2010) 381–390.
- [91] M. Carena, A. de Gouvea, A. Freitas, and M. Schmitt, *Invisible Z boson decays at $e^+ e^-$ colliders*, *Phys. Rev.* **D68** (2003) 113007.
- [92] P. M. Ferreira, R. Santos, M. Sher, and J. P. Silva, *Could the LHC two-photon signal correspond to the heavier scalar in two-Higgs-doublet models?*, *Phys. Rev.* **D85** (2012) 035020.
- [93] **OPAL, DELPHI, L3, ALEPH, LEP Higgs Working Group for Higgs boson searches** Collaboration, *Search for charged Higgs bosons: Preliminary combined results using LEP data collected at energies up to 209-GeV*, in *Lepton and photon interactions at high energies. Proceedings, 20th International Symposium, LP 2001, Rome, Italy, July 23-28, 2001*, 2001.

- [94] M. Jung, A. Pich, and P. Tuzon, *Charged-Higgs phenomenology in the Aligned two-Higgs-doublet model*, *JHEP* **11** (2010) 003.
- [95] M. Aoki, R. Guedes, S. Kanemura, S. Moretti, R. Santos, and K. Yagyu, *Light Charged Higgs bosons at the LHC in 2HDMs*, *Phys. Rev.* **D84** (2011) 055028.
- [96] **ATLAS Collaboration** Collaboration, G. Aad *et. al.*, *Search for charged Higgs bosons decaying via $H^+ \rightarrow \tau\nu$ in top quark pair events using pp collision data at $\sqrt{s} = 7$ TeV with the ATLAS detector*, *JHEP* **1206** (2012) 039.
- [97] A. Djouadi, J. Kalinowski, and P. M. Zerwas, *Two and three-body decay modes of SUSY Higgs particles*, *Z. Phys.* **C70** (1996) 435–448.
- [98] A. G. Akeroyd, *Three body decays of Higgs bosons at LEP-2 and application to a hidden fermiophobic Higgs*, *Nucl. Phys.* **B544** (1999) 557–575.
- [99] R. Ramos and M. Sher, *The Dark Z and Charged Higgs Decay*, *arXiv:1312.0013* (2013).
- [100] C. Bouchiat and P. Fayet, *Constraints on the parity-violating couplings of a new gauge boson*, *Phys. Lett.* **B608** (2005) 87–94.
- [101] W. J. Marciano and A. Sirlin, *Radiative Corrections To Atomic Parity Violation*, *Phys. Rev.* **D27** (1983) 552.
- [102] S. G. Porsev, K. Beloy, and A. Derevianko, *Precision determination of weak charge of ^{133}Cs from atomic parity violation*, *Phys. Rev.* **D82** (2010) 036008.
- [103] S. C. Bennett and C. E. Wieman, *Measurement of the $6S \rightarrow 7S$ transition polarizability in atomic cesium and an improved test of the Standard Model*, *Phys. Rev. Lett.* **82** (1999) 2484–2487. [Erratum: *Phys. Rev. Lett.* 83,889(1999)].
- [104] **MOLLER** Collaboration, J. Benesch *et. al.*, *The MOLLER Experiment: An Ultra-Precise Measurement of the Weak Mixing Angle Using Møller Scattering*, *arXiv:1411.4088* (2014).
- [105] N. Berger *et. al.*, *Measuring the weak mixing angle with the P2 experiment at MESA*, *J. Univ. Sci. Tech. China* **46** (2016), no. 6 481–487.

- [106] R. Bucoveanu, M. Gorchtein, and H. Spiesberger, *Precision Measurement of $\sin^2 \theta_w$ at MESA*, *PoS LL2016* (2016) 061.
- [107] M. Lindner, M. Platscher, and F. S. Queiroz, *A Call for New Physics : The Muon Anomalous Magnetic Moment and Lepton Flavor Violation*, *Phys. Rept.* **731** (2018) 1–82.
- [108] R. L. Garwin, D. P. Hutchinson, S. Penman, and G. Shapiro, *Accurate Determination of the μ^+ Magnetic Moment*, *Phys. Rev.* **118** (1960) 271–283.
- [109] T. Burnett and M. J. Levine, *Intermediate vector boson contribution to the muon’s anomalous magnetic moment*, *Phys. Lett.* **24B** (1967) 467–468.
- [110] T. Kinoshita and R. J. Oakes, *Hadronic contributions to the muon magnetic moment*, *Phys. Lett.* **25B** (1967) 143–145.
- [111] T. Blum, A. Denig, I. Logashenko, E. de Rafael, B. Lee Roberts, T. Teubner, and G. Venanzoni, *The Muon ($g-2$) Theory Value: Present and Future*, *arXiv:1311.2198* (2013).
- [112] J. P. Leveille, *The Second Order Weak Correction to ($G-2$) of the Muon in Arbitrary Gauge Models*, *Nucl. Phys.* **B137** (1978) 63–76.
- [113] F. Jegerlehner and A. Nyffeler, *The Muon $g-2$* , *Phys. Rept.* **477** (2009) 1–110.
- [114] F. S. Queiroz and W. Shepherd, *New Physics Contributions to the Muon Anomalous Magnetic Moment: A Numerical Code*, *Phys. Rev.* **D89** (2014), no. 9 095024.
- [115] S. Profumo and F. S. Queiroz, *Constraining the Z' mass in 331 models using direct dark matter detection*, *Eur. Phys. J.* **C74** (2014), no. 7 2960.
- [116] B. Allanach, F. S. Queiroz, A. Strumia, and S. Sun, *Z^2 models for the LHCb and $g - 2$ muon anomalies*, *Phys. Rev.* **D93** (2016), no. 5 055045. [Erratum: *Phys. Rev.* **D95**, no. 11, 119902 (2017)].
- [117] A. Alves, A. Berlin, S. Profumo, and F. S. Queiroz, *Dirac-fermionic dark matter in $U(1)_X$ models*, *JHEP* **10** (2015) 076.

- [118] A. Alves, A. Berlin, S. Profumo, and F. S. Queiroz, *Dark Matter Complementarity and the Z' Portal*, *Phys. Rev.* **D92** (2015), no. 8 083004.
- [119] S. Patra, F. S. Queiroz, and W. Rodejohann, *Stringent Dilepton Bounds on Left-Right Models using LHC data*, *Phys. Lett.* **B752** (2016) 186–190.
- [120] **CMS** Collaboration, V. Khachatryan *et. al.*, *Search for narrow resonances in dilepton mass spectra in proton-proton collisions at $\sqrt{s} = 13$ TeV and combination with 8 TeV data*, *Phys. Lett.* **B768** (2017) 57–80.
- [121] M. Lindner, F. S. Queiroz, and W. Rodejohann, *Dilepton bounds on left–right symmetry at the LHC run II and neutrinoless double beta decay*, *Phys. Lett.* **B762** (2016) 190–195.
- [122] W. Altmannshofer, S. Gori, S. Profumo, and F. S. Queiroz, *Explaining dark matter and B decay anomalies with an $L_\mu - L_\tau$ model*, *JHEP* **12** (2016) 106.
- [123] **ATLAS** Collaboration, T. A. collaboration, *Search for new high-mass phenomena in the dilepton final state using 36.1 fb^{-1} of proton-proton collision data at $\sqrt{s} = 13$ TeV with the ATLAS detector*, *CERN Document Server* (2017).
- [124] G. Arcadi, M. Dutra, P. Ghosh, M. Lindner, Y. Mambrini, M. Pierre, S. Profumo, and F. S. Queiroz, *The waning of the WIMP? A review of models, searches, and constraints*, *Eur. Phys. J.* **C78** (2018), no. 3 203.
- [125] O. G. Miranda, V. B. Semikoz, and J. W. F. Valle, *Neutrino electron scattering and electroweak gauge structure: Probing the masses of a new Z boson*, in *Lepton and baryon number violation in particle physics, astrophysics and cosmology. Proceedings, 1st International Symposium, Lepton-baryon’98, Trento, Italy, April 20-25, 1998*, pp. 683–690, 1998.
- [126] S. Ciechanowicz, W. Sobkow, and M. Misiaszek, *Scattering of neutrinos on a polarized electron target as a test for new physics beyond the standard model*, *Phys. Rev.* **D71** (2005) 093006.
- [127] J. Kopp, P. A. N. Machado, and S. J. Parke, *Interpretation of MINOS data in terms of non-standard neutrino interactions*, *Phys. Rev.* **D82** (2010) 113002.

- [128] R. Harnik, J. Kopp, and P. A. N. Machado, *Exploring ν Signals in Dark Matter Detectors*, *JCAP* **1207** (2012) 026.
- [129] W. Liao, X.-H. Wu, and H. Zhou, *Electron events from the scattering with solar neutrinos in the search of keV scale sterile neutrino dark matter*, *Phys. Rev.* **D89** (2014), no. 9 093017.
- [130] W. Rodejohann, X.-J. Xu, and C. E. Yaguna, *Distinguishing between Dirac and Majorana neutrinos in the presence of general interactions*, *JHEP* **05** (2017) 024.
- [131] S. Bilmis, I. Turan, T. M. Aliev, M. Deniz, L. Singh, and H. T. Wong, *Constraints on Dark Photon from Neutrino-Electron Scattering Experiments*, *Phys. Rev.* **D92** (2015), no. 3 033009.
- [132] J.-W. Chen, H.-C. Chi, H.-B. Li, C. P. Liu, L. Singh, H. T. Wong, C.-L. Wu, and C.-P. Wu, *Constraints on millicharged neutrinos via analysis of data from atomic ionizations with germanium detectors at sub-keV sensitivities*, *Phys. Rev.* **D90** (2014), no. 1 011301.
- [133] **TEXONO** Collaboration, H. B. Li *et. al.*, *Limit on the electron neutrino magnetic moment from the Kuo-Sheng reactor neutrino experiment*, *Phys. Rev. Lett.* **90** (2003) 131802.
- [134] **TEXONO** Collaboration, H. T. Wong *et. al.*, *A Search of Neutrino Magnetic Moments with a High-Purity Germanium Detector at the Kuo-Sheng Nuclear Power Station*, *Phys. Rev.* **D75** (2007) 012001.
- [135] **TEXONO collaboration** Collaboration, M. Deniz *et. al.*, *Measurement of Neutrino-Electron Scattering Cross-Section with a CsI(Tl) Scintillating Crystal Array at the Kuo-Sheng Nuclear Power Reactor*, *Phys. Rev.* **D81** (2010) 072001.
- [136] **LSND collaboration** Collaboration, L. B. Auerbach *et. al.*, *Measurement of electron-neutrino electron elastic scattering*, *Phys. Rev.* **D63** (2001) 112001.
- [137] G. Bellini, J. Benziger, D. Bick, S. Bonetti, G. Bonfini, *et. al.*, *Precision measurement of the ^7Be solar neutrino interaction rate in Borexino*, *Phys.Rev.Lett.* **107** (2011) 141302.

- [138] A. G. Beda, E. V. Demidova, A. S. Starostin, V. B. Brudanin, V. G. Egorov, D. V. Medvedev, M. V. Shirchenko, and T. Vylov, *GEMMA experiment: Three years of the search for the neutrino magnetic moment*, *Phys. Part. Nucl. Lett.* **7** (2010) 406–409.
- [139] **CHARM-II** Collaboration, P. Vilain *et. al.*, *Measurement of differential cross-sections for muon-neutrino electron scattering*, *Phys. Lett.* **B302** (1993) 351–355.
- [140] M. Pospelov, A. Ritz, and M. B. Voloshin, *Secluded WIMP Dark Matter*, *Phys. Lett.* **B662** (2008) 53–61.
- [141] M. Pospelov, *Secluded $U(1)$ below the weak scale*, *Phys. Rev.* **D80** (2009) 095002.
- [142] M. Magg and C. Wetterich, *Neutrino Mass Problem and Gauge Hierarchy*, *Phys. Lett.* **94B** (1980) 61–64.
- [143] F. S. Queiroz and K. Sinha, *The Poker Face of the Majoron Dark Matter Model: LUX to keV Line*, *Phys. Lett.* **B735** (2014) 69–74.
- [144] A. Arhrib, R. Benbrik, M. Chabab, G. Moultaka, M. C. Peyranere, L. Rahili, and J. Ramadan, *The Higgs Potential in the Type II Seesaw Model*, *Phys. Rev.* **D84** (2011) 095005.
- [145] L. Basso, A. Lipniacka, F. Mahmoudi, S. Moretti, P. Osland, G. M. Pruna, and M. Purmohammadi, *Probing the charged Higgs boson at the LHC in the CP-violating type-II 2HDM*, *JHEP* **11** (2012) 011.
- [146] H. S. Cheon and S. K. Kang, *Constraining parameter space in type-II two-Higgs doublet model in light of a 126 GeV Higgs boson*, *JHEP* **09** (2013) 085.
- [147] O. Eberhardt, U. Nierste, and M. Wiebusch, *Status of the two-Higgs-doublet model of type II*, *JHEP* **07** (2013) 118.
- [148] A. Broggio, E. J. Chun, M. Passera, K. M. Patel, and S. K. Vempati, *Limiting two-Higgs-doublet models*, *JHEP* **11** (2014) 058.
- [149] S. von Buddenbrock, N. Chakrabarty, A. S. Cornell, D. Kar, M. Kumar, T. Mandal, B. Mellado, B. Mukhopadhyaya, R. G. Reed, and X. Ruan,

- Phenomenological signatures of additional scalar bosons at the LHC*, *Eur. Phys. J.* **C76** (2016), no. 10 580.
- [150] A. Dery, C. Frugiuele, and Y. Nir, *Large Higgs-electron Yukawa coupling in 2HDM*, *JHEP* **04** (2018) 044.
- [151] P. Basler, P. M. Ferreira, M. Muhlleitner, and R. Santos, *High scale impact in alignment and decoupling in two-Higgs doublet models*, *Phys. Rev.* **D97** (2018), no. 9 095024.
- [152] R. Patrick, P. Sharma, and A. G. Williams, *Triple top signal as a probe of charged Higgs in a 2HDM*, *Phys. Lett.* **B780** (2018) 603–607.
- [153] J. Ren, R.-Q. Xiao, M. Zhou, Y. Fang, H.-J. He, and W. Yao, *LHC Search of New Higgs Boson via Resonant Di-Higgs Production with Decays into $4W$* , *JHEP* **06** (2018) 090.
- [154] M. Kakizaki, Y. Ogura, and F. Shima, *Lepton flavor violation in the triplet Higgs model*, *Phys. Lett.* **B566** (2003) 210–216.
- [155] J. Garayoa and T. Schwetz, *Neutrino mass hierarchy and Majorana CP phases within the Higgs triplet model at the LHC*, *JHEP* **03** (2008) 009.
- [156] S. Mantry, M. Trott, and M. B. Wise, *The Higgs decay width in multi-scalar doublet models*, *Phys. Rev.* **D77** (2008) 013006.
- [157] C.-S. Chen, C.-Q. Geng, D. Huang, and L.-H. Tsai, *Many high-charged scalars in LHC searches and Majorana neutrino mass generations*, *Phys. Rev.* **D87** (2013), no. 7 077702.
- [158] F. del Aguila, M. Chala, A. Santamaria, and J. Wudka, *Discriminating between lepton number violating scalars using events with four and three charged leptons at the LHC*, *Phys. Lett.* **B725** (2013) 310–315.
- [159] F. del Águila and M. Chala, *LHC bounds on Lepton Number Violation mediated by doubly and singly-charged scalars*, *JHEP* **03** (2014) 027.
- [160] S. Blunier, G. Cottin, M. A. Díaz, and B. Koch, *Phenomenology of a Higgs triplet model at future e^+e^- colliders*, *Phys. Rev.* **D95** (2017), no. 7 075038.

- [161] E. Boos and I. Volobuev, *Simple Standard Model Extension by Heavy Charged Scalar*, *Phys. Rev.* **D97** (2018), no. 9 095014.
- [162] A. Arhrib, R. Benbrik, M. Chabab, G. Moulataka, M. C. Peyranère, L. Rahili, and J. Ramadan, *Higgs potential in the type ii seesaw model*, *Phys. Rev. D* **84** (Nov, 2011) 095005.
- [163] **Particle Data Group** Collaboration, K. A. Olive *et. al.*, *Review of Particle Physics*, *Chin. Phys.* **C38** (2014) 090001.
- [164] M. D. Campos, D. Cogollo, M. Lindner, T. Melo, F. S. Queiroz, and W. Rodejohann, *Neutrino Masses and Absence of Flavor Changing Interactions in the 2HDM from Gauge Principles*, *JHEP* **08** (2017) 092.
- [165] S. Biswas, E. Gabrielli, M. Heikinheimo, and B. Mele, *Dark-Photon searches via Higgs-boson production at the LHC*, *Phys. Rev.* **D93** (2016), no. 9 093011.
- [166] G. Barello, S. Chang, C. A. Newby, and B. Ostdiek, *Don't be left in the dark: Improving LHC searches for dark photons using lepton-jet substructure*, *Phys. Rev.* **D95** (2017), no. 5 055007.
- [167] **CMS** Collaboration, C. Collaboration, *Search sensitivity for dark photons decaying to displaced muons with CMS at the high-luminosity LHC*, *CERN Document Server* (2018).
- [168] **ATLAS** Collaboration, M. Aaboud *et. al.*, *Combination of searches for heavy resonances decaying into bosonic and leptonic final states using 36 fb^{-1} of proton-proton collision data at $\sqrt{s} = 13\text{ TeV}$ with the ATLAS detector*, *Phys. Rev.* **D98** (2018) 052008.
- [169] J. Alwall, P. Demin, S. de Visscher, R. Frederix, M. Herquet, F. Maltoni, T. Plehn, D. L. Rainwater, and T. Stelzer, *MadGraph/MadEvent v4: The New Web Generation*, *JHEP* **09** (2007) 028.
- [170] J. Alwall, M. Herquet, F. Maltoni, O. Mattelaer, and T. Stelzer, *MadGraph 5 : Going Beyond*, *JHEP* **06** (2011) 128.

- [171] **CMS** Collaboration, C. Collaboration, *A search for doubly-charged Higgs boson production in three and four lepton final states at $\sqrt{s} = 13$ TeV, CERN Document Server* (2017).
- [172] E. da Silva Almeida, A. Alves, N. Rosa Agostinho, O. J. P. Éboli, and M. C. Gonzalez-Garcia, *Electroweak Sector Under Scrutiny: A Combined Analysis of LHC and Electroweak Precision Data, Phys. Rev. D* **99** (2019), no. 3 033001.
- [173] A. Alves, N. Rosa-Agostinho, O. J. P. Éboli, and M. C. Gonzalez-Garcia, *Effect of Fermionic Operators on the Gauge Legacy of the LHC Run I, Phys. Rev. D* **98** (2018), no. 1 013006.
- [174] M. Cepeda *et. al.*, *Report from Working Group 2, CERN Yellow Rep. Monogr.* **7** (2019) 221–584.
- [175] P. Ko, Y. Omura, and C. Yu, *Dark matter and dark force in the type-I inert 2HDM with local $U(1)_H$ gauge symmetry, JHEP* **11** (2014) 054.
- [176] **CMS** Collaboration, A. M. Sirunyan *et. al.*, *Search for electroweak production of charginos and neutralinos in multilepton final states in proton-proton collisions at $\sqrt{s} = 13$ TeV, JHEP* **03** (2018) 166.
- [177] **CMS** Collaboration, C. Collaboration, *Search for production of a Higgs boson and a single top quark in multilepton final states in proton collisions at $\sqrt{s} = 13$ TeV, CERN Document Server* (2017).
- [178] P. Fayet, *Extra $U(1)$ ’s and New Forces, Nucl. Phys.* **B347** (1990) 743–768.
- [179] P. Fayet, *U-boson production in $e^+ e^-$ annihilations, psi and Upsilon decays, and Light Dark Matter, Phys. Rev. D* **75** (2007) 115017.
- [180] G. Arcadi, T. Hugle, and F. S. Queiroz, *The Dark $L_\mu - L_\tau$ Rises via Kinetic Mixing, Phys. Lett. B* **784** (2018) 151–158.
- [181] A. Blondel *et. al.*, *Research Proposal for an Experiment to Search for the Decay $\mu \rightarrow eee$, arXiv:1301.6113* (2013).
- [182] M. Lindner, F. S. Queiroz, W. Rodejohann, and X.-J. Xu, *Neutrino-electron scattering: general constraints on Z' and dark photon models, JHEP* **05** (2018) 098.

- [183] A. Freitas, J. Lykken, S. Kell, and S. Westhoff, *Testing the Muon $g-2$ Anomaly at the LHC*, *JHEP* **05** (2014) 145. [Erratum: JHEP09,155(2014)].
- [184] Y. Kaneta and T. Shimomura, *On the possibility of a search for the $L_\mu - L_\tau$ gauge boson at Belle-II and neutrino beam experiments*, *PTEP* **2017** (2017), no. 5 053B04.
- [185] K. Kowalska and E. M. Sessolo, *Expectations for the muon $g-2$ in simplified models with dark matter*, *JHEP* **09** (2017) 112.
- [186] M. Dutra, M. Lindner, S. Profumo, F. S. Queiroz, W. Rodejohann, and C. Siqueira, *MeV Dark Matter Complementarity and the Dark Photon Portal*, *JCAP* **1803** (2018) 037.
- [187] S. Profumo, F. S. Queiroz, J. Silk, and C. Siqueira, *Searching for Secluded Dark Matter with H.E.S.S., Fermi-LAT, and Planck*, *JCAP* **1803** (2018), no. 03 010.
- [188] E. Ma, *Neutrino mass from triplet and doublet scalars at the TeV scale*, *Phys. Rev.* **D66** (2002) 037301.
- [189] Y. Sui and Y. Zhang, *Prospects of type-II seesaw models at future colliders in light of the DAMPE e^+e^- excess*, *Phys. Rev.* **D97** (2018), no. 9 095002.
- [190] C. Bonilla, J. M. Lamprea, E. Peinado, and J. W. F. Valle, *Flavour-symmetric type-II Dirac neutrino seesaw mechanism*, *Phys. Lett.* **B779** (2018) 257–261.
- [191] A. Biswas and A. Shaw, *Explaining Dark Matter and Neutrino Mass in the light of TYPE-II Seesaw Model*, *JCAP* **1802** (2018), no. 02 029.
- [192] P. S. B. Dev, C. M. Vila, and W. Rodejohann, *Naturalness in testable type II seesaw scenarios*, *Nucl. Phys.* **B921** (2017) 436–453.
- [193] M. M. Ferreira, T. B. de Melo, S. Kovalenko, P. R. D. Pinheiro, and F. S. Queiroz, *Lepton Flavor Violation and Collider Searches in a Type I + II Seesaw Model*, *Eur. Phys. J.* **C79** (2019), no. 11 955.
- [194] A. Geiser, *PseudoDirac neutrinos as a potential complete solution to the neutrino oscillation puzzle*, *Phys. Lett.* **B444** (1999) 358.

- [195] D. Chang and O. C. W. Kong, *Pseudo-Dirac neutrinos*, *Phys. Lett.* **B477** (2000) 416–423.
- [196] J. F. Beacom, N. F. Bell, D. Hooper, J. G. Learned, S. Pakvasa, and T. J. Weiler, *PseudoDirac neutrinos: A Challenge for neutrino telescopes*, *Phys. Rev. Lett.* **92** (2004) 011101.
- [197] M. Safarzadeh, E. Scannapieco, and A. Babul, *A limit on the warm dark matter particle mass from the redshifted 21 cm absorption line*, *Astrophys. J.* **859** (2018), no. 2 L18.
- [198] J. S. Martins, R. Rosenfeld, and F. Sobreira, *Forecasts for Warm Dark Matter from Photometric Galaxy Surveys*, *Mon. Not. Roy. Astron. Soc.* **481** (2018), no. 1 1290–1299.
- [199] P. Villanueva-Domingo, N. Y. Gnedin, and O. Mena, *Warm Dark Matter and Cosmic Reionization*, *Astrophys. J.* **852** (2018), no. 2 139.
- [200] L. Lopez-Honorez, O. Mena, S. Palomares-Ruiz, and P. Villanueva-Domingo, *Warm dark matter and the ionization history of the Universe*, *Phys. Rev.* **D96** (2017), no. 10 103539.
- [201] V. Irsic *et. al.*, *New Constraints on the free-streaming of warm dark matter from intermediate and small scale Lyman- α forest data*, *Phys. Rev.* **D96** (2017), no. 2 023522.
- [202] D. Hooper, F. Ferrer, C. Boehm, J. Silk, J. Paul, N. W. Evans, and M. Casse, *Possible evidence for MeV dark matter in dwarf spheroidals*, *Phys. Rev. Lett.* **93** (2004) 161302.
- [203] Y. Farzan and E. Ma, *Dirac neutrino mass generation from dark matter*, *Phys. Rev.* **D86** (2012) 033007.
- [204] T. Toma and A. Vicente, *Lepton Flavor Violation in the Scotogenic Model*, *JHEP* **01** (2014) 160.
- [205] T. Hugle, M. Platscher, and K. Schmitz, *Low-Scale Leptogenesis in the Scotogenic Neutrino Mass Model*, *Phys. Rev.* **D98** (2018), no. 2 023020.

- [206] D. A. Camargo, A. G. Dias, T. B. de Melo, and F. S. Queiroz, *Neutrino Masses in a Two Higgs Doublet Model with a $U(1)$ Gauge Symmetry*, *JHEP* **04** (2019) 129.
- [207] **ATLAS** Collaboration, G. Aad *et. al.*, *Search for high-mass dilepton resonances using 139 fb^{-1} of pp collision data collected at $\sqrt{s}=13\text{ TeV}$ with the ATLAS detector*, *Phys. Lett.* **B796** (2019) 68–87.
- [208] X. Cid Vidal *et. al.*, *Report from Working Group 3*, *CERN Yellow Rep. Monogr.* **7** (2019) 585–865.